GEAR TECHNOLOGY

The Journal of Gear Manufacturing

JANUARY/FEBRUARY 1989

Fracture Toughness of High-Carbon Martensitic Steels

Fillet Geometry of Ground Gear Teeth

Spur Gear Fundamentals

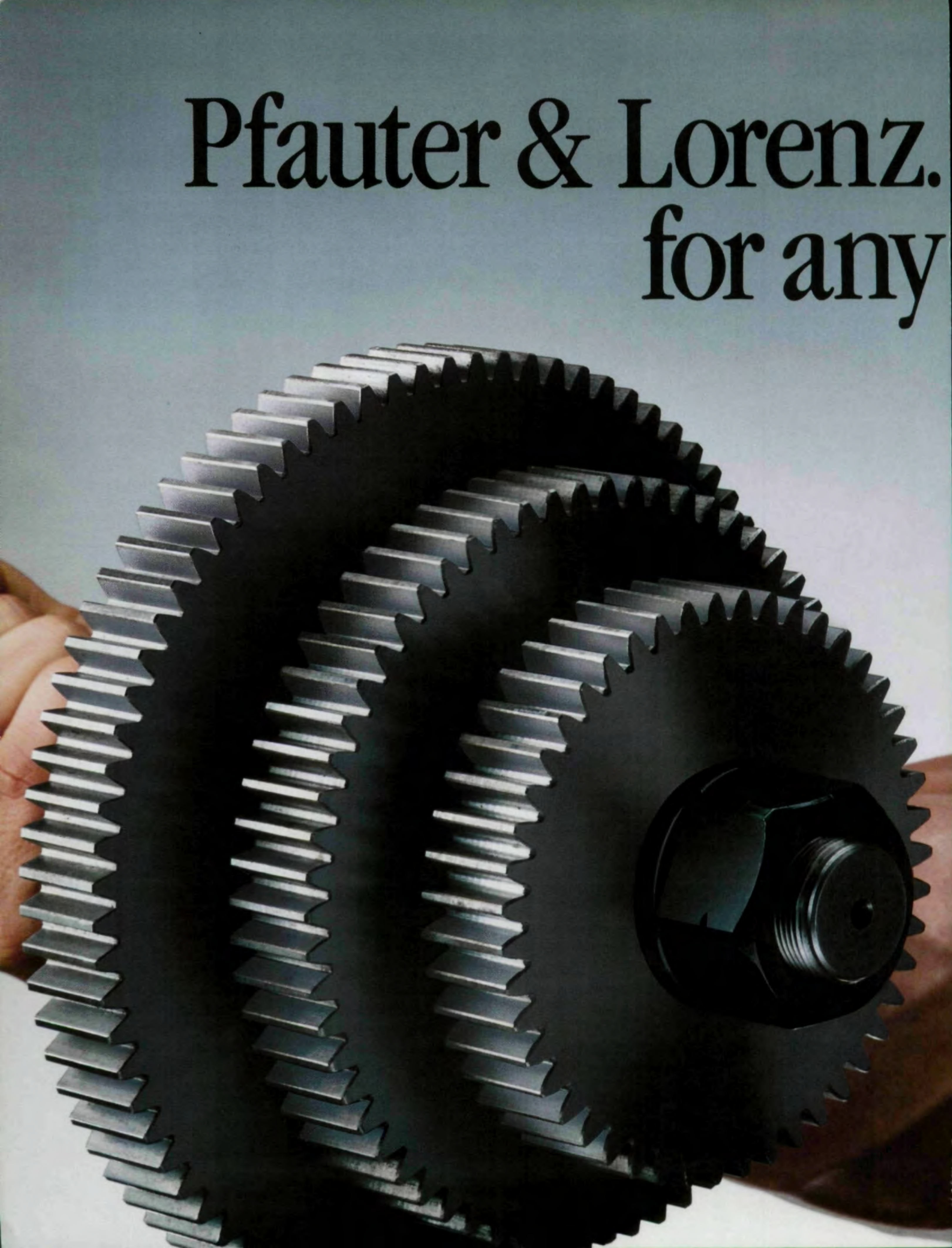
Pfauter & Lorenz.
for any


Powerful flexibility
size job.
Pfauter CNC hobbers and Lorenz CNC shapers are used in more gear manufacturing applications than any other CNC machines. Why? Because of their complete flexibility to handle just about any lot size economically.
• Latest generation CNC controls make program preparation and execution an easy task for a single operator.
• Loading/unloading systems are designed to minimize non-productive time.
• Expandable storage capacity substantially increases unattended operation.
• Simple, quick-change tooling increases efficiency.
CAD/CAM designed and built by American Pfauter, these machines have become the reliable standards in aerospace, automotive, truck and tractor, and job shops of every size.
If you'd like to find out how Pfauter and Lorenz CNC technology can improve your productivity, contact American Pfauter, 925 Estes Ave., Elk Grove Village, IL 60007. Phone (312) 640-7500.
AMERICAN PFAUTER
Building American Productivity
CIRCLE A-1 ON READER REPLY CARD

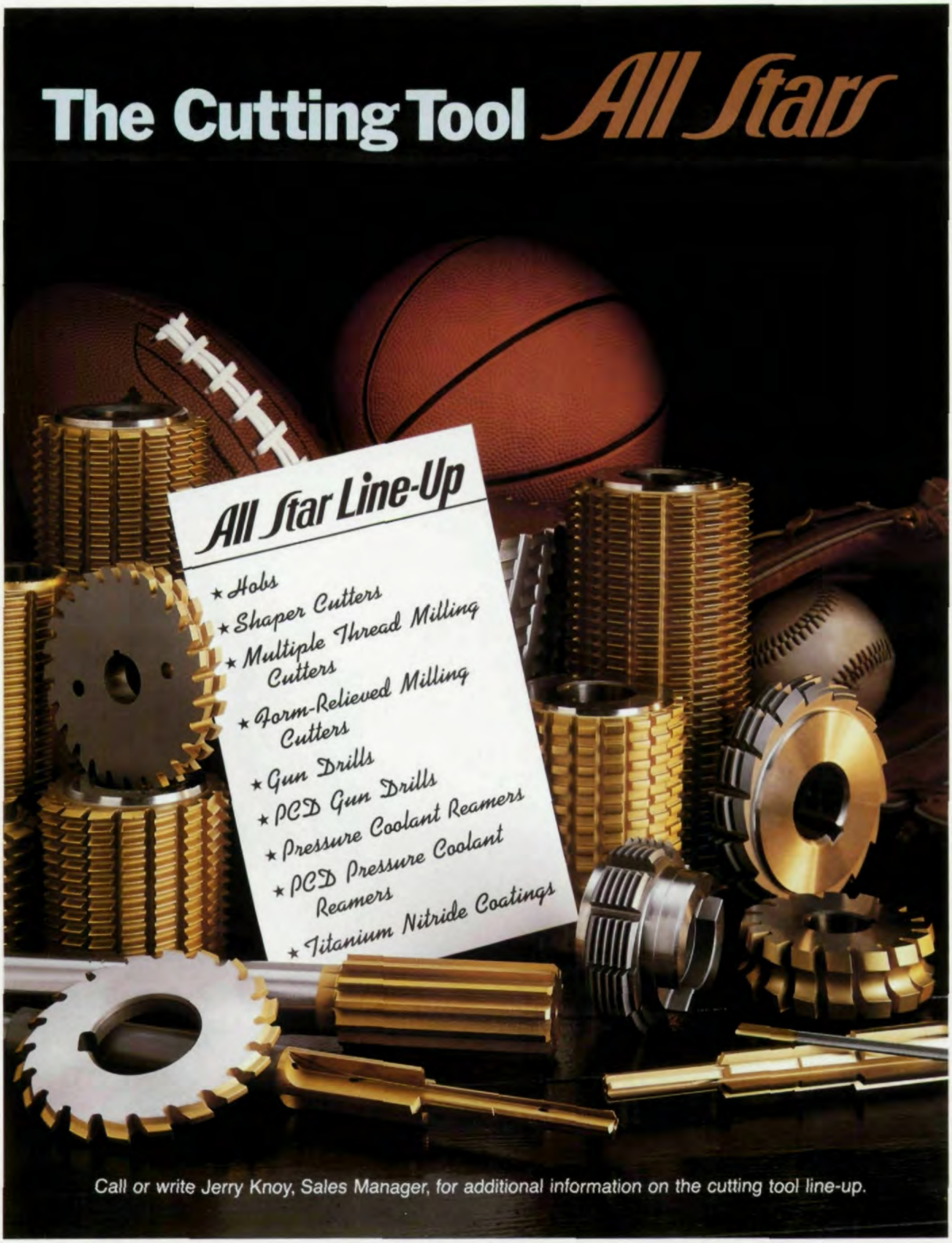
The Cutting Tool All Stars
All Star Line-Up
★ Hobs
★ Shaper Cutters
★ Multiple Thread Milling Cutters
★ Form-Relieved Milling Cutters
★ Gun Drills
★ PCD Gun Drills
★ Pressure Coolant Reamers
★ PCD Pressure Coolant Reamers
★ Titanium Nitride Coatings
Call or write Jerry Knoy, Sales Manager, for additional information on the cutting tool line-up.

RANDALL PUBLISHING
1401 Lunt Avenue
P.O. Box 1426
Elk Grove, IL 60007
(312) 437-6604

The Advanced Technology
of
Leonardo da Vinci
1452-1519

COVER

The only known documented likeness of Leonardo, this self-portrait was done during his last years in Italy. He was around 60 years old at the time the drawing was done. The dimensions of the original are 13 11/12 x 8 5/12, and the medium is red chalk. At the bottom of the drawing is an inscription added by a later hand, "Leonardo da Vinci, portrait of himself as an old man." The original work is in the Biblioteca Real, Turin, Italy.

GEAR TECHNOLOGY

The Journal of Gear Manufacturing

CONTENTS — PAGE NO.

FEATURES

DEPARTMENTS

January/February, 1989 — Vol. 6, No. 1

GEAR TECHNOLOGY, The Journal of Gear Manufacturing (ISSN 0743-6858) is published bimonthly by Randall Publishing Co., Inc., 1425 Lunt Avenue, P. O. Box 1426, Elk Grove Village, IL 60007. GEAR TECHNOLOGY, The Journal of Gear Manufacturing. Subscription rates are: $40.00 in the United States, $50.00 in Canada, $55.00 in all other foreign countries. Second-Class postage paid at Arlington Heights, IL and at additional mailing office.

Postmaster: Send address changes to GEAR TECHNOLOGY, The Journal of Gear Manufacturing, 1425 Lunt Avenue, P. O. Box 1426, Elk Grove Village, IL 60007.

MANUSCRIPTS: We are requesting technical papers with an educational emphasis for anyone having anything to do with the design, manufacture, testing or processing of gears. Subjects sought are solutions to specific problems, explanations of new technology, techniques, designs, processes, and alternative manufacturing methods. These can range from the "How to . . ." of gear cutting (BACK TO BASICS) to the most advanced technology. All manuscripts submitted will be carefully considered. However, the Publisher assumes no responsibility for the safety or return of manuscripts. Manuscripts must be accompanied by a self-addressed, self-stamped envelope, and be sent to GEAR TECHNOLOGY, The Journal of Gear Manufacturing, P.O. Box 1426, Elk Grove, IL 60009, (312) 437-6604.

M&M Precision Systems . . .
the innovators in CNC gear inspection

Smart™ Probe package. LVDT probe and μprocessor-based convertor deliver high-speed data in μinches.

Operator Control Panel for part loading and machine set up.

Keyboard with "Mouse" for one-time entry of part print and tolerance data. "Mouse" permits use of CAD techniques.

Color graphics CRT with touch screen makes operation simple and fast.

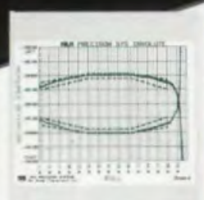

Graphics printer copies CRT.

Plotter delivers multi-color hard copy of graphics and test data.

CNC status monitor provides status and positional display of mechanical system and CNC control functions.

Our Model 3000 QC Gear Analyzer is a third generation CNC gear inspection system incorporating all of the comprehensive analytical tests and evaluation capabilities of previous M & M systems, such as our Model 2000, but with these added capabilities:

- Dramatically improved speed and accuracy through new mechanical system design and advanced CNC control technology.
- Computer hardware and applications software are modular to allow the user to buy only the required capability. This makes the 3000 QC adaptable to laboratory testing or production-line inspection.
- Integrated Statistical Process Control with local data base capability is an optional feature.
- Networking with MAPS compatibility is available.
- Robotic interfacing for totally automatic load/test/unload operation can be incorporated.

For more information or applications assistance, write or call: M & M Precision Systems, 300 Progress Rd., West Carrollton, OH 45449, 513/859-8273, TWX 810/450-2626, FAX 513/859-4452.

M&M PRECISION SYSTEMS

AN ACME-CLEVELAND COMPANY

CIRCLE A-3 ON READER REPLY CARD

EDITORIAL

LEONARDO, THE ENGINEER

"Mechanical science is most noble and useful above all others, for by means of it, all animated bodies in motion perform their operations."

Leonardo da Vinci.

These lines, interestingly enough, are from the notebooks of an artist whose images are part of the basic iconography of Western culture. Even people who have never set foot in a museum and wouldn't know a painting by Corregio from a sculpture by Calder, recognize the Mona Lisa. But Leonardo da Vinci was much more than an artist. He was also a man of science who worked in anatomy, botany, cartography, geology, mathematics, aeronautics, optics, mechanics, astronomy, hydraulics, sonics, civil engineering, weaponry and city planning. There was little in nature that did not interest Leonardo enough to at least make a sketch of it. Much of it became a matter of lifelong study. The breadth of his interests, knowledge, foresight, innovation and imagination is difficult to grasp.

Choosing Leonardo da Vinci, the prototypical Renaissance Man, as a role model for a highly specialized technical magazine may seem a little peculiar. What can Leonardo, the man who seemed to know almost everything and seemed to do it all very, very well, say to us in our highly specialized world of gear design and manufacture?

It is the spirit of Leonardo we at GEAR TECHNOLOGY wish to honor and to emulate — the spirit of excellence and the spirit of curiosity.

Leonardo was never satisfied with the way things were. He never ceased to question, to experiment, to improve his own skills and designs. The 5,000-odd pages of his notebooks that still exist are full of sketches of an infinite variety of natural and mechanical objects. He drew hundreds of sketches of various plans for bridges, weapons, clocks and hydraulic systems; for geared machines for lifting, moving, cutting and drilling; for ornithopters, which he hoped would enable humans to fly, and for parachutes, "horseless carriages" and other devices far ahead of his time. Leonardo's vision frequently outstripped the science of his day, and many of his "inventions" were never put into use at the time simply because there was no practical means to power them.

This capacity for dreaming, questioning, experimenting and tinkering until the optimum design is achieved lies at the root of the science of engineering. We cannot all expect to have the breadth of knowledge and talent that Leonardo had, but we can certainly emulate his attitude — that the natural world is full of wonders that can be known, and, once known, turned into machines that make life better, easier and safer for everyone.

Researching and reading about Leonardo is both an interesting and a fulfilling experience. One is constantly astonished by the scope of his skill; even rough sketches in his notebooks are little works of art. His vision — of nature, science and engineering, as well as art — is awesome. Every staff member at GEAR TECHNOLOGY that has worked on the Leonardo covers has been enriched by the experience.

The Leonardo covers have been one of our most consistently popular features among both our readers and our staff. You may have noticed, however, that on several recent occasions, we did not feature one of his drawings on the cover. The reason for this is simple: We are running out of Leonardo's sketches that feature gearing, and we have little descriptive information for the ones that are left.

Part of the problem is that Leonardo's sketches were never systematically organized. Some of both the charm and the difficulty of the sketchbooks is their spontaniety. Leonardo wrote down or sketched ideas as they came to him, and he rarely went back to edit or categorize his work. It was a project he always intended to undertake . . . Then, after his death, the 5,000 unorganized pages were separated, scattered, in some cases, destroyed. Those portions of the manuscripts remaining are found in a number of museums and libraries throughout the world.

The variety of Leonardo's interests also complicate searching for appropriate sketches. They are apt to show up in books on almost any subject. A hunt for Leonardo's sketches can cover an entire library. The place to start is any good biography of the artist, but from there, the trail can lead almost anywhere.

So we issue you a challenge. Go to your library and spend an afternoon absorbing some of the spirit and wisdom of Leonardo. If you come across in your reading any of his sketches featuring gears or geared mechanisms that have not been featured on our covers, send copies to us, and we will be pleased to share them with the rest of the GEAR TECHNOLOGY audience. We will run these sketches as cover art and credit you and your company as their source.

Eventually, of course, we will completely run out of Leonardo's gear-related sketches. The chances of getting the artist to produce more are slim. However, sketches or no, the spirit of Leonardo will continue to inspire us here at GEAR TECHNOLOGY, and, we hope, will continue to inspire you as well — for inventiveness, intellectual risk taking and simple curiosity are always at the root of success for any engineer.

Michael Goldstein

Michael Goldstein, Editor/Publisher

TECHNICAL CALENDAR

CALL FOR PAPERS. AGMA Fall Technical Meeting, November 8-9, 1989. Papers on gear design, analysis, manufacture and applications of gear drives and related products will be accepted. Deadline for abstracts is **JANUARY 5, 1989.** Contact AGMA headquarters for more information.

MARCH 19-22, 1989. First International Applied Mechanical Systems Design Conference. Convention Center, Nashville, TN. Presentation of papers, tutorials and panel sessions on various design topics. For further information, contact: Dr. Cemil Bagci, Tennessee Technological University, Cookeville, TN 38505. (615) 372-3265.

APRIL 25-27, 1989. ASME 5th Annual Power Transmission & Gearing Conference, Chicago, IL. Presentations on emerging technologies for gears, couplings and other power transmission devices, gear geometry, noise, manufacturing and other gear-related subjects. For more information, contact Donald Borden, P.O. Box 502, Elm Grove, WI 53122.

SEPTEMBER 12-20, 1989. European Machine Tool Show, Hannover, West Germany. Exhibits from 36 countries will show cutting and forming equipment, machine tools, CAD/CAM, robotics, etc. For more information, contact: Hannover Fairs, USA, Inc., 103 Carnegie Center, Princeton, NJ, 08540. (609) 987-1202.

NOVEMBER 6-8, 1989. AGMA Gear Expo '89, David Lawrence Convention Center, Pittsburgh, PA. Exhibition of gear machine tools, supplies, accessories and gear products. For more information, contact: Wendy Peidl, AGMA, 1500 King Street, Suite 201, Alexandria, VA 22314. (703) 684-0211.

AGMA TECHNICAL EDUCATION SEMINARS. AGMA is offering a new series of technical education seminars, each one focusing on a different aspect of gear manufacturing and taught by industry experts.

Jan. 11, Cincinnati, OH. "Specifying and Controlling the Quality of Shot Peening."

March 7/8, Rochester, NY. "Source Inspection of Loose Gears from the Customer's Standpoint."

May 2, Cincinnati, OH. "Gear Math at the Shop Level for the Gear Shop Foreman."

June 6, AGMA Headquarters. "Specifying and Verifying Material Quality per AGMA Material Grades."

For more information, contact: Bill Daniels, AGMA, 1500 King St., Suite 201, Alexandria, VA, 22314. (703) 684-0211.

Factors Influencing Fracture Toughness of High-Carbon Martensitic Steels

V. K. Sharma, Navistar International Transportation Corp., Ft. Wayne, IN
G. H. Walter, J. I. Case, Hinsdale, IL
D. H. Breen, ASME-Gear Research Institute, Naperville, IL

Abstract:

Plane strain fracture toughness of twelve high-carbon steels has been evaluated to study the influence of alloying elements, carbon content and retained austenite. The steels were especially designed to simulate the carburized case microstructure of commonly used automotive type gear steels. Results show that a small variation in carbon can influence the K_{IC} significantly. The beneficial effect of retained austenite depends both on its amount and distribution. The alloy effect, particularly nickel, becomes significant only after the alloy content exceeds a minimum amount. Small amounts of boron also appear beneficial.

Introduction

The issue of toughness of materials used for machine elements remains controversial, although much is understood about the subject. In the past few decades, our quantitative understanding of the subject has increased significantly. Concerned by brittle fractures in World War II liberty ships and, more recently, by rocket motor case failures, engineers have developed a comprehensive understanding of the concepts and test methods of fracture toughness and its measurement. Yet many myths concerning the use of toughness concepts in design persist. It is certainly an acceptable principle that designs must be strong and tough; however, application of strength and toughness concepts in the real world must be done through compromise, especially when fatigue is one of the design criteria.

Increased strength is usually accompanied by decreased toughness. In designs for which steel strengths below approximately 1700 MPa (40 R_C) are acceptable, material systems are available which offer appreciable toughness. However, in carburized applications, such as gears which are case-hardened to obtain a high-hardness, high-carbon martensitic case with a relatively low-hardness, low-carbon core, toughness becomes a specialized area of knowledge. Considerable controversy surrounds the problem of defining and evaluating the toughness required for heavy duty automotive gears.[1]

The present study was undertaken to obtain data useful

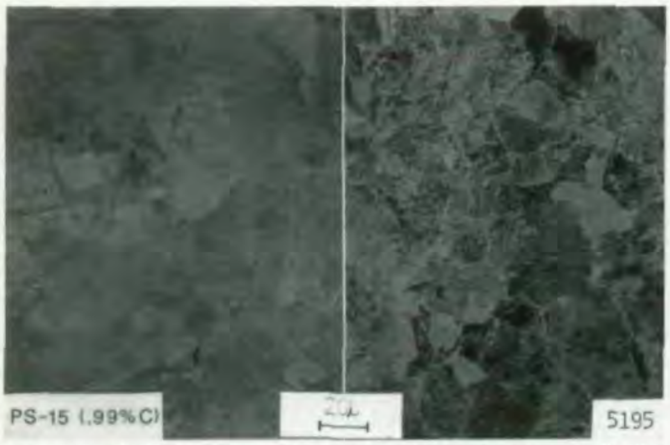

Fig. 1 – As-rolled microstructure in 0.99% C PS-15 and 5195 steels. Similar grain boundary carbide network surrounding pearlitic grains was developed in 8697, IH-50 and ERCH-1.

Table 1 – Chemical Composition

	C	MN	Cr	Ni	Mo	Si	Al	S	P
PS-15	0.99	1.09	0.54	0.03	0.16	0.32	0.05	0.02	0.02
PS-15	0.86	1.19	0.54	0.03	0.16	0.36	0.04	0.02	0.02
PS-15	0.72	1.11	0.51	0.03	0.17	0.28	0.04	0.02	0.02
8697	0.97	0.83	0.52	0.60	0.22	0.31	0.04	0.02	0.01
IH-50	0.97	1.37	0.05	0.03	0.01	0.68	0.05	0.02	0.02
4895	0.95	0.73	0.06	3.44	0.26	0.32	0.04	0.02	0.01
4870	0.70	0.76	0.05	3.50	0.25	0.31	0.04	0.02	0.01
ERCH-1	1.00	1.57	1.25	0.03	0.01	0.70	0.05	0.02	0.02
ER-8	0.95	1.32	0.95	1.57	0.01	0.31	0.03	0.02	0.01
9399	0.99	0.65	1.16	3.22	0.13	0.34	0.04	0.02	0.01
5195	0.95	1.00	0.93	0.03	0.01	0.31	0.04	0.02	0.01
PS15+B*	1.00	1.11	0.56	0.03	0.16	0.35	0.04	0.03	0.02

*PS15+B had 0.0008% B.
B content of all other steel < 0.0005%

in designing and selecting carburizing steels. The effects of alloying elements, carbon content and retained austenite on plane strain fracture toughness properties of high-carbon martensitic steels especially designed to simulate carburized case microstructure of several commonly used automotive steels were examined.

Procedure

Twelve 60 kg, high-carbon steel ingots were poured from air induction melted heats made with fine grain practice using aluminum and silicon. Chemical composition of the steels investigated is given in Table 1. All steels have a high carbon content to simulate the surface of a carburized component. The steels were designed to study the effect of alloying elements, case carbon content and retained austenite. To study the effect of carbon content on K_{IC}, Mn-Cr-Mo PS-15 steel was poured at 0.99%, 0.86% and 0.72% carbon, and Ni-Mo 4800 steel was produced at a carbon content of 0.99% and 0.70%. At equivalent carbon levels, SAE PS-15 steel is a cost-effective replacement steel for Mn-Cr-Ni-Mo 8600 series steel. Mn-Cr-Mo type steels have been used successfully in axles and power train components for over 15 years.

Comparison of the fracture toughness of 0.99% C PS-15 steel (residual nickel) with 8697 (intermediate nickel levels) provides information about the influence of low Ni on K_{IC} of high-carbon steels. IH-50 is a high-manganese, high-silicon steel. This type of steel is generally not used for carburizing applications because it has a relatively low case hardenability. The 4800 series steels, ERCH-1 and ER-8, were included to study the effect of nickel on fracture toughness. ERCH-1 and ER-8 are nickel-free and reduced nickel replacement steels (same case and base hardenability) for 4800 steels. The 4800 steel was poured at carbon contents of 0.95% and 0.70% to determine the effect of carbon content on K_{IC} of high-nickel, high-carbon steels. Other steels include 9300 steel with 0.99% C (9399), 5100 steel with 0.95% C (5195) and PS-15 with boron. The 9399 is a 1.16 Cr-3.22 Ni steel. The 5195 is a Mn-Cr steel with hardenability equivalent to high-carbon PS-15 and 8697 steels. Boron additions in Mn-Cr-Mo (PS-15 with boron) steel were made using commercially available Batts alloy.

The ingots were furnace-cooled and appropriate sections from each ingot were rolled into two 15 cm wide, 1 cm thick plates. Proper care was exercised to prevent cracking and distortion during the processing. Four to six compact tension specimens with width (W) equal to four times thickness (B) were machined from each grade of steel per ASTM E-399. The specimens were prepared in the "L-T" crack plane orien-

AUTHORS:

V.K. SHARMA *is Chief Materials Engineer at Navistar International Transportation Corp., Fort Wayne, IN. Prior to taking this post he worked at Navistar as research engineering manager in the areas of structural metallurgy and metal and lubricants technology. He did his undergraduate work at the Indian Institute of Technology and earned a MS in metallurgical engineering from the University of Michigan and a PhD in materials engineering from Illinois Institute of Technology. He also holds an MBA from the University of Chicago. Dr. Sharma is a member of ASM, SAE, ASTM and AIME.*

G.H. WALTER *is Manager, Materials Technology – Agricultural Equipment and Component Engineering at J.I. Case Co. He has also worked for International Harvester Co. with responsibilities in the area of materials specifications development and metallurgical research. Mr. Walter holds a B.S. in metallurgical engineering from Illinois Institute of Technology. He is a member of SAE and current chairman of SAE Division 8 on Carbon and Alloy Steel Hardenability and a Fellow of the American Society for Metals. He is also a member of Tau Beta Pi engineering honorary fraternity.*

DALE H. BREEN *is Secretary and Director of ASME-Gear Research Institute. Prior to taking this post, he worked for sixteen years for International Harvester Co., managing the corporate metallurgical research laboratories. His technical interests include gear technology, fatigue and fracture of metals, alloy steel and iron technology, tribology and mechanics. Mr. Breen did undergraduate work in mechanical engineering at Bradley University, Peoria, IL. He holds a MS degree in metallurgy from the University of Michigan and a MBA from the University of Chicago. He is the author of numerous books and papers on gears, metallurgy and fatigue and is a member of ASM, ASME, SAE, ASLE and the American Institute of Mining and Metallurgical Engineers.*

tation. Before final machining, 3.75 x 3.75 x 1 cm pieces from the plates were ground to 0.6 cm. A minimum of 0.1 cm material was ground from each surface to remove any decarburized layer. Although all the data in this report were obtained using Standard ASTM E-399 compact tension specimens, tapered double cantilever beam (DCB) and oversized compact tension specimens (W=8B) were also used in the preliminary studies. DCB and oversized CT specimens resulted in 10-20% higher K_{IC} values. (See Table 2.)

Completely machined specimens were austenitized for two hours at 930°C, cooled to 845°C and vertically submerged into an oil quench tank at room temperature and tempered at 190°C for one hour. The surfaces of the specimens were protected from decarburization with a protective "decarb" stop coating. Representative heat treated specimens were checked for residual stresses, distortion and quench cracks. Quench cracks were not detected, and all specimens were within the dimensional tolerances permitted by ASTM E-399. Average residual stresses measured on the surfaces of two tapered DCB specimens were found to be +1.3 MPa. Considering the size and geometry of the compact tension specimen, it is assumed that the K_{IC} values reported herein are independent of macroresidual stresses.

The specimens were fatigue precracked, loaded to fracture in tension, and fracture toughness values were calculated from the autographic plot of load versus displacement in accordance with standard ASTM procedure. The K_{IC} values reported herein are averages of at least three replicate tests.

Since the specimens were heavily textured, the amount of retained austenite could not be determined by routine x-ray analysis. The volume fraction of retained austenite was measured by x-ray diffraction using a tilting and rotating stage.[2] The use of a rotating and tilting stage averages the x-ray peak intensity for a set of planes from a maximum number of possible crystallographic orientations.

Fractographic features on several selected compact tension specimens were studied using a scanning electron microscope. In addition, several compact tension specimens were sectioned and evaluated metallographically.

Results and Discussion

As-Rolled Microstructure.

The cleanliness level of all steels met typical JKT cleanliness requirements for commercial quality steels. The sulphides were pancake-shaped, having no abnormal size or distribution. Although each steel experienced a similar heating, rolling and cooling cycle, as-rolled microstructure of the plates varied significantly depending on the chemistry. (See Table 3.) Lower carbon, 0.72% C and 0.86% C, PS-15 steels developed a fully pearlitic microstructure. A proeutectoid grain boundary carbide network formed in 0.99% C PS-15, 8697, IH-50, ERCH-1 and 5195 steels. Typical as-rolled microstructures for 0.99% C PS-15 and 5195 steels are shown in Fig. 1. The as-rolled grain size in 0.99% C PS-15 steel was significantly coarser (ASTM grain size 1-2 as compared to 4-5) than all other steels showing proeutectoid carbides. The ER-8 steel had a primarily spheroid microstructure with small amounts of grain boundary carbides. High carbon 4895 steel developed a bainitic microstructure with patches of martensite. (See Fig. 2.) Fig. 2 also shows as-rolled microstructure for 9399 steel. Because of its high hardenability, 9399 steel developed a completely martensitic matrix with proeutectoid carbides in the grain boundaries.

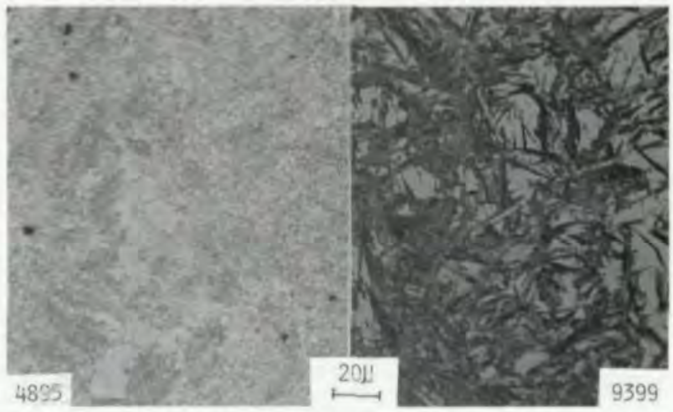

Fig. 2—As-rolled microstructures of 4895 and 9399 steels. Photomicrograph for 4895 steels shows essentially bainitic microstructure with patches of martensite. The 9399 steel developed proeutectoid carbides in a completely martensitic matrix.

As-rolled microstructure can influence subsequent heat treated mechanical properties of high-carbon, martensitic steels.[3],[4] Nakazawa and Krauss[4] evaluated the effect of proeutectoid carbides on the fracture toughness of quenched and tempered 52100 steel. Two series of specimens—one with grain boundary proeutectoid carbides in pearlitic matrix (Series A), and the other with well-distributed, fine spherical

Table 2 — Specimen Geometry Effect (High Carbon IH-50 Steel)

Hardness Rc	Fracture Toughness MPa.m$^{1/2}$ ASTM STD CT W=4B	Compact Tension W=8B	Tapered DCB
59.5	17.6	21.0	24.2
60.0	18.0	17.9	23.3
60.0	17.5	18.0	23.3
59.5	17.9	21.7	—
Average	**17.7**	**19.6**	**23.2**

Table 3 — As-Rolled Microstructures

Steel	Microstructure
PS-15 (.72% C, .86% C)	Fully Pearlitic
PS-15 (0.99% C)	Pearlitic With GB Carbides ASTM 1-2 GS
8697, IH-50, ERCH-1, 5195	Pearlitic With GB Carbides ASTM 4-5 GS
ER-8	Spheroidized With Small Amounts of GB Carbides
4895	Bainitic With Patches Of Martensite
9399	Martensitic With Proeutectoid Carbides

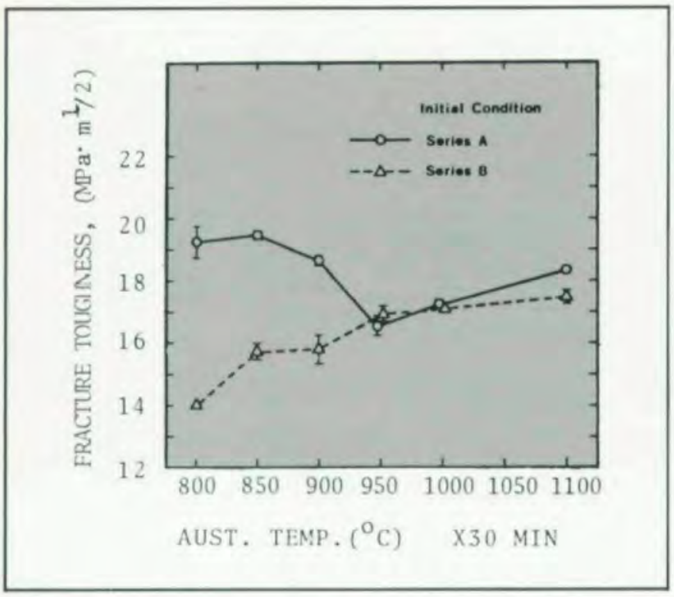

Fig. 3 – Influence of starting microstructure on K_{IC} of 52100 steel. Series A had proeutectoid carbides. Series B contained only fine carbides.[4]

carbides in a spheroidized matrix (Series B) – were produced, and their fracture toughness was determined as a function of the austenitizing temperature. The results are reproduced in Fig. 3. When austenitized below 950°C, martensitic specimens with proeutectoid carbides in the starting microstructure (Series A) are significantly tougher than Series B, which contained only fine spherical carbides. Above

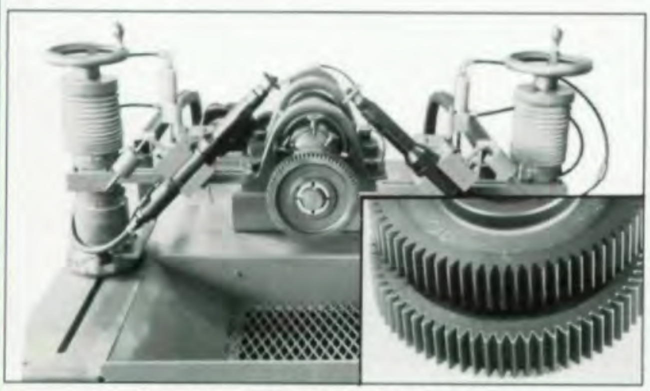

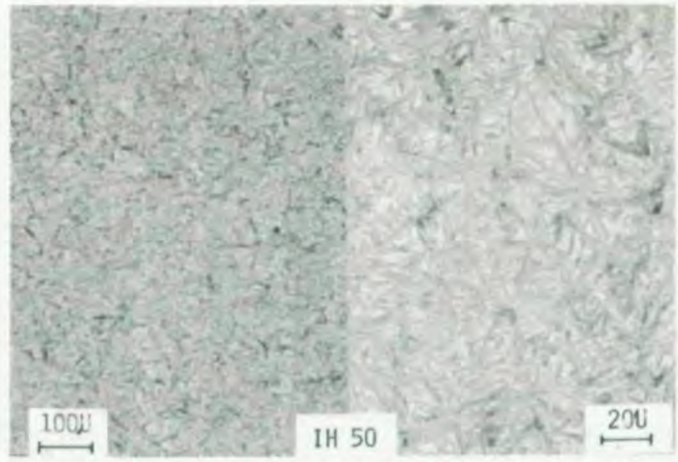

Fig. 4 – Microstructure of high carbon IH-50 steel. The microstructure shows a uniform, lightly tempered, high-carbon martensite and retained austenite with no carbides or microcracks.

950°C, where all carbides dissolve to form a homogenous austenite, both series have about the same toughness. Nakazawa and Krauss explained the increased toughness of Series A on the basis of higher toughness of carbide-free, transgranular areas present between the proeutectoid carbides. Below 950°C, specimens containing only fine spheroid particles have low toughness because of the very fine microvoid coalescence (small ligaments of tough carbide-free areas) associated with the closely spaced carbides. In the present studies, all specimens were austenitized at 930°C, where essentially all proeutectoid carbides were dissolved. Therefore, variations in as-rolled microstructure are expected to have little or no influence on the K_{IC} values.

Heat Treated Microstructure.

Typical microstructures for various steels after the heat treatment (austenitized at 930°C for two hours, quenched in oil from 845°C and tempered at 190°C for one hour) are shown in Figs. 4-7. As shown in Fig. 4, IH-50 developed a uniform microstructure containing lightly tempered, high-carbon martensite and retained austenite with no carbides or microcracks. This is the type of surface microstructure which is most desirable in carburized parts. However, as indicated previously, IH-50 (high-manganese, high-silicon) is not a suitable steel for most automotive gearing and shaft applications because it does not have sufficient case hardenability.

With the exception of IH-50 steel, all other steels exhibited non-uniform, banded microstructures. The severity of carbon and alloy segregation varied depending upon the type

Table 4 – Undissolved Carbides QIA 720 Measurements

Steel	% Carbides
PS-15 (.99% C)	1.0%
8697	1.0%
ERCH-1	9.0%
ER-8	1.5%
9399	8.5%
5195	1.0%
PS-15 + B	1.0%

.72% C PS-15, .86% C PS-15, 4870 and 4895 contained no undissolved carbides.

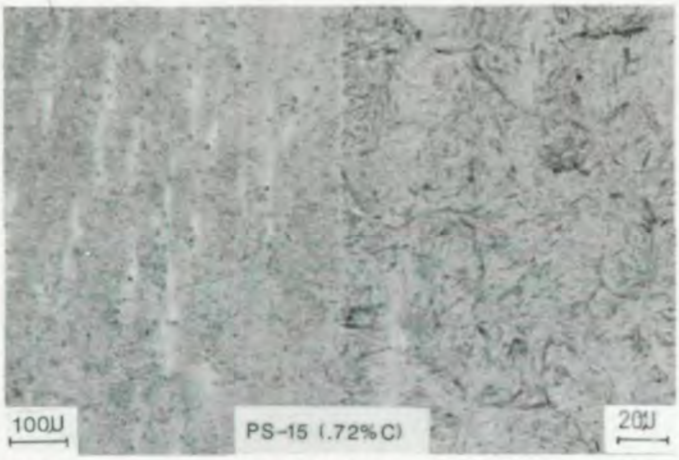

Fig. 5 – Microstructure of 0.72% C PS-15 steel. The white etching bands are higher carbon areas which are relatively soft and contain higher amounts of retained austenite. No carbides or microcracks are visible.

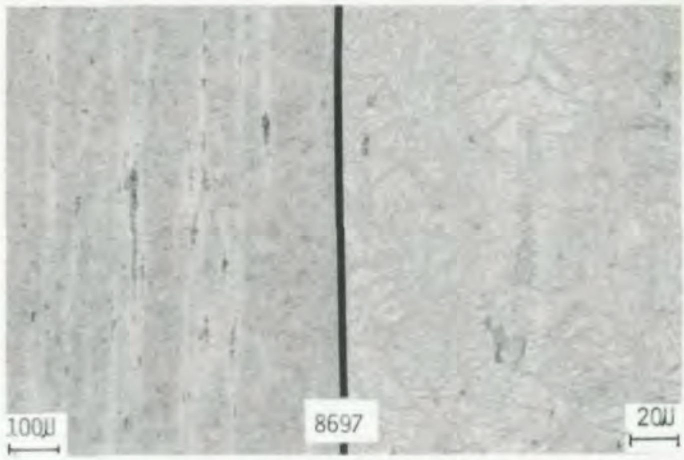

Fig. 6 – Microstructure of 8697 steel. PS-15 with 0.99% C also showed a similar microstructure. In addition to the microcracks, the white etching bands contained undissolved carbides.

and amount of alloying elements. PS-15 steels with 0.72% and 0.86% carbon, when examined at 100X, showed numerous white etching bands (Fig. 5). The white etching bands were relatively soft (HRC 62 vs 65) and contained a higher volume fraction of retained austenite as compared to the surrounding matrix. Carbides or microcracks were not observed in the 0.72% C PS-15 steel. The 0.86% C PS-15 steel also did not have carbides, but occasionally microcracks were observed. Microstructures of high-nickel 4870 and 4895 steels were similar to the 0.72% PS-15 steel. High-nickel steels also showed non-uniform microstructure with no carbides or microcracks. The frequency of white etching bands, however, was low. The martensitic plate size in the nickel steels was somewhat coarser.

The 8697 and 0.99% C PS-15 steels had similar microstructures. In addition to microcracks, the white etching bands contained numerous undissolved carbides. A typical microstructure for heat treated 8697 is shown in Fig. 6. The worst situation with respect to carbides and banding was observed in ERCH-1, a nickel-free substitute steel for the 4800 grade of steel (Fig. 7). The microstructure of 9399 steel was very similar to ERCH-1.

The amount of undissolved carbides was determined using a quantitative image analyzing system. As illustrated in Table 4, 0.99% C PS-15, 8697, 5195 and PS-15+B steels have less than 1% carbides. ER-8, a substitute steel for 4800 steel with reduced nickel content, had 1.5% undissolved carbides. The highest amount of carbides, 8.5 and 9%, were present in 9399 and ERCH-1 steel, respectively.

The influence of carbides on K_{IC} was investigated by determining the fracture toughness of ERCH-1 steel after austenitizing it at 930°C for two, four and seven hours. Samples of carbide free 0.86% C PS-15 steel were also included in the study for comparison. Increasing the austenitization time from two to seven hours did not change fracture toughness of either steel significantly (Table 5). The influence of massive carbides on fracture toughness of austenitic and martensitic white cast iron has been studied by Gahr and Scholz.[5] On the basis of the results shown in Fig. 8 from that study, the authors concluded that increasing the volume of carbides from 7% to 30% had no significant influence on K_{IC}. Only when the volume of carbide increases beyond 30%, did the fracture toughness start decreasing. The matrix of martensitic white cast iron is essentially the same as the high carbon steel. None of the steels included in the present investigation contained more than 9% undissolved carbides. In fact,

Table 5 – Effect of Austenitizing Time at 930°C

	K_{IC} MPa.m$^{1/2}$		
Steel	2 Hours	4 Hours	7 Hours
PS-15 (.87% C)	22.4	23.8	21.8
ERCH-1	20.7	21.1	20.0

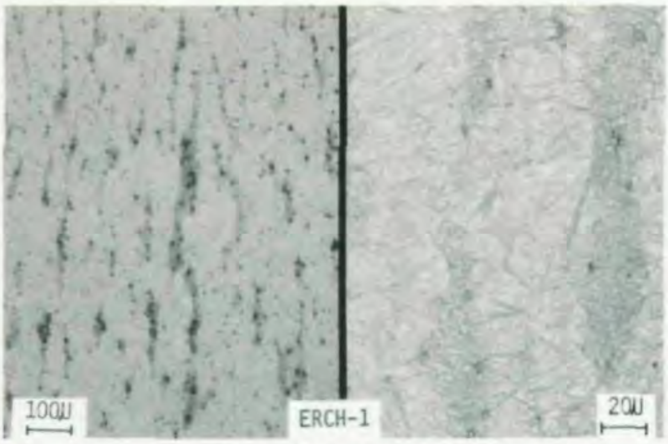

Fig. 7—Microstructure of ERCH-1 steel. ERCH-1 steel showed maximum banding with greatest amount of undissoved carbides.

as given in Table 4, the majority of steels have less than 2% undissolved carbides. It is, therefore, reasonable to assume that the fracture toughness values reported herein have not

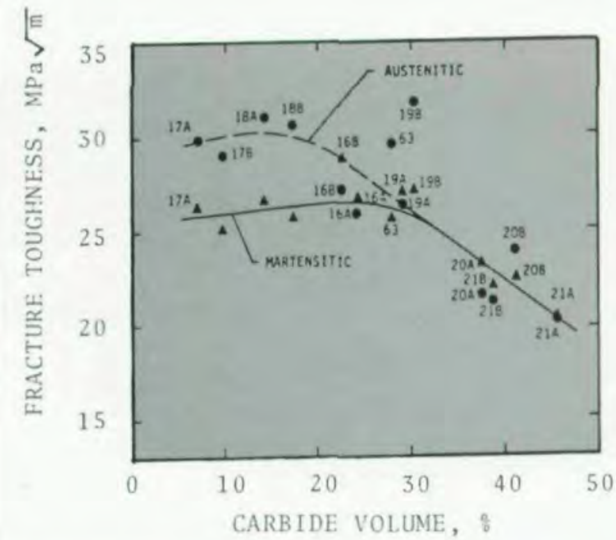

Fig. 8—Influence of carbides on fracture toughness of martensitic and austenitic white cast irons.[5]

been influenced by the presence of carbides. Since more than 90% of the fracture propagates through a martensite-austenitic matrix, fracture toughness values should be dominated by the matrix properties rather than the carbides.

Influence of Retained Austenite.

The presence of retained austenite, particularly as a continuous thin film surrounding martensitic plates rather than as a discreet blocky phase, is considered to enhance fracture toughness of martensitic steels. Thomas[6] has emphasized the importance of mechanical and thermal stability of retained austenite. Retained austenite has been proposed to improve crack propagation resistance and, thereby, increase fracture toughness by crack branching or blunting,[7] by strain or stress induced transformation resulting in the development of compressive stresses in front of the advancing crack,[8] by preventing the formation of brittle boundary carbides, and by breaking the continuity of the cleavage planes across various martensitic plates.[9]

The influence of retained austenite on fracture toughness of high carbon steels was studied by varying the amount of retained austenite in 4895 steel by deep freezing at −84°C and −207°C. The results in Table 6 show that a decrease in the austenite from 40% to 18.5%, caused by deep freezing, quenched and tempered 4895 steel at −84°C, decreased fracture toughness from 24.5 MPa.m$^{1/2}$ to 14.6 MPa.m$^{1/2}$. Further deep freezing at −207°C reduced retained austenite to 15.5% causing an additional decrease in the toughness to 12.5 MPa.m$^{1/2}$. The amount of retained austenite, therefore, has a significant effect on the K_{IC} of high-carbon, martensitic steels. The microstructure of 4895 steel after the subzero treatments is shown in Fig. 9. Deep freezing transforms retained austenite to martensite. A careful examination of the microstructure revealed that additional microcracks were generated as a result of the transformation. A 50% decrease in the K_{IC} value, however, cannot be explained on the basis of an increase in the density of microcracks. This decrease is primarily related to the reduction of retained austenite. Suf-

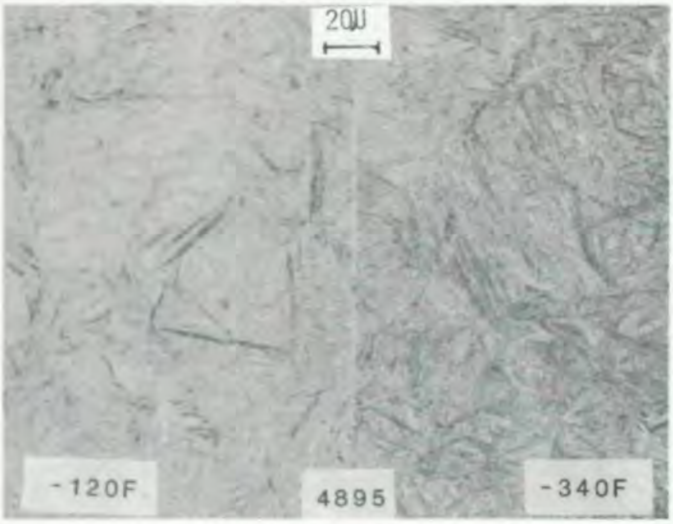

Fig. 9 – Microstructure of 4895 steel austenitized at 930° C, quenched in oil, tempered at 190° C for 1 hour and deep frozen at −84° C and −207° C for two hours.

ficient data were not generated to determine the minimum level of retained austenite necessary to increase toughness significantly. The beneficial effect of retained austenite depends on its nature and distribution. Retained austenite is most effective when present as continuous films surrounding martensite rather than a discontinuous blocky phase.[9] Heat treatment and alloying elements could be selected to maximize the influence of retained austenite at lowest levels necessary so that the toughness can be improved without detrimentally affecting the hardness and other related properties.

Effect of Carbon Content.

Increased strengthening caused by carbide precipitation or interstitial solid solution strengthening by carbon is usually accompanied by decreased toughness. In designs for which steel strength below 1700 MPa (40 HRC) are acceptable, material systems are available offering appreciable toughness. In high-hardness, carburized applications, (2000 MPa (57 HRC) and above) such as gears, toughness becomes a specialized area of knowledge. Earlier work in this area was done by Schwartzbart and Sheehan.[10] Results of some of their work, replotted, are shown in Fig. 10. This work was done with Charpy V-notch specimens. The same hardness at different carbon levels was obtained by tempering.

In the present investigation, the effect of carbon on K_{IC} of high-carbon, martensitic steel was studied by testing PS-15 steel at 0.99%, 0.86% and 0.72% carbon. Also, the fracture toughness of 4800 steel was determined at 0.95% and 0.70% carbon. The results are shown in Table 7. Lowering carbon enhances fracture toughness. The effect of carbon, however,

Table 6 — Effect of Retained Austenite 4895 Steel

Heat Treatment	Rc	RA	K_{IC}MPa.m$^{1/2}$
190°C Temper	55.5	40.0%	24.5
Deep Frozen -84°C	64.0	18.5%	14.6
Deep Frozen -207°C	65.0	15.5%	12.5

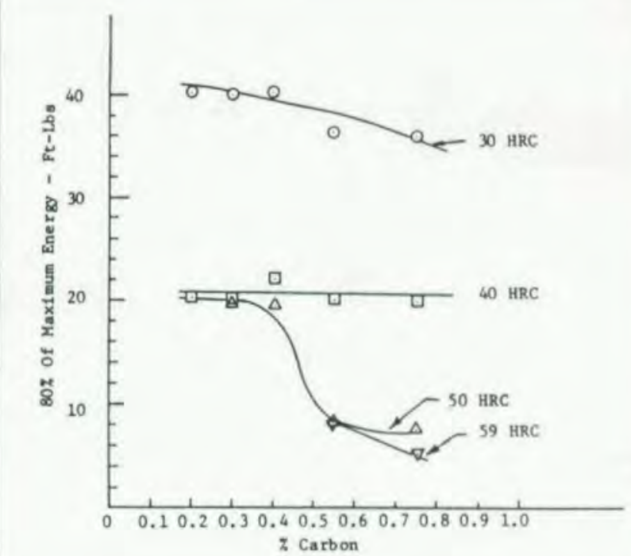

Fig. 10 – Isohardness relation of carbon and toughness. Toughness determined by Charpy V-notch.[10]

must be considered in conjunction with retained austenite. In general, the amount of retained austenite decreases with decreasing carbon. In the case of PS-15 steels, a change in the carbon from 0.99% to 0.86% decreased retained austenite from 39% to 23%. Discounting other effects, this

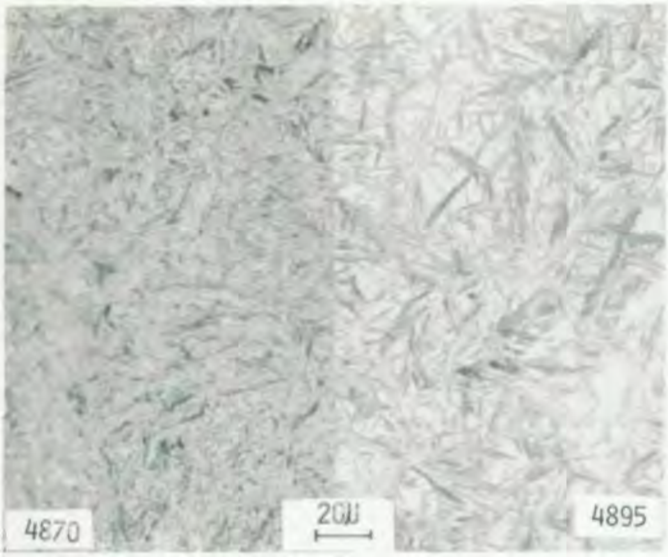

Fig. 11 – Microstructure of 4870 and 4895 steels.

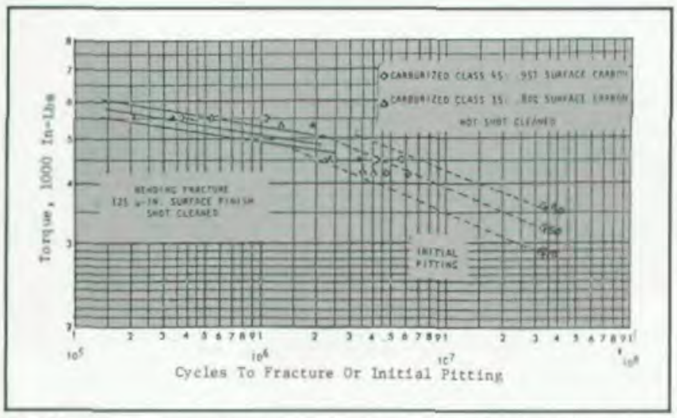

Fig. 12 – Comparison of bending and contact fatigue life durability of carburized Mn-Cr steel with G10, G50, and G90 (solid and dotted lines) bands for carburized 8622 steel.

reduction should have lowered the toughness. However, the toughness increased, indicating the importance of carbon. K_{IC} decreased slightly when the carbon content was reduced from 0.86% to 0.72% C. Improved toughness resulting from lowering the carbon in this case is more than offset by a decrease in the toughness caused by a change in the retained austenite from 23% to 16%.

The effect of carbon on fracture toughness of high-carbon steels becomes more evident in the case of high-nickel 4800 series steels. A decrease in the carbon from 0.95% to 0.70% increased K_{IC} from 24.5 MPa.m$^{1/2}$ to 34.5 MPa.m$^{1/2}$. Nickel promotes the stablization of retained austenite. Therefore, even at 0.70% C, 4870 steel containing 3.50% nickel retained 21% austenite. The highest fracture toughness was recorded

Table 7 – Effect of Carbon Content on K_{IC}

Steel	%C	Rc	RA	K_{IC}MPa.m$^{1/2}$
PS-15	0.99	60.0	39%	16.6
PS-15	0.86	60.5	23%	22.4
PS-15	0.72	60.5	16%	21.7
4895	0.95	55.5	40%	24.5
4870	0.70	57.0	21%	34.5

for this steel. Notice that the fracture toughness improved in spite of an increase in the hardness by nearly 2 Rc.

Lower carbon martensites are inherently more ductile. It is well known that the morphology of martensite changes from dislocated laths to twinned plates with increasing solute content. Carbon has the strongest effect in promoting twinning. Alloy composition and martensitic transformation temperature influence the transition of martensite from lath to plate martensite. The dislocated laths are composed of bundles of slightly misoriented grains having high density of tangled dislocations. The fine structure of plate martensite consists of fine transformation twins.[11] Lower carbon dislocated lath martensites are relatively less brittle, because under stress, dislocations can move, resulting in deformation by slip. Higher-carbon martensite, which consists primarily of plate martensite with internal twins, is brittle. Twinned martensites have extremely low fracture toughness. A reduction in the percentage of twinned martensite, resulting from lowering carbon content, can be expected to improve K_{IC} significantly. It has been shown that plane strain fracture toughness of AISI 4130 (medium-carbon low-hardenability steel) can be improved two-fold by a high temperature and step-cooling austenitizing treatment, which virtually eliminates twinned martensite plates.[12]

The microstructures of 4895 and 4870 steels are shown in Fig. 11. Photomicrographs show a difference in the martensitic plate size and the amount of retained austenite. The 4870 has finer plate size and less retained austenite. It is also likely that the 4870 steel contains lower amounts of plate martensite, although the structure for both steels is mostly plate type.

Alloy Effects.

Our past experience indicates that in automotive gear steels, small amounts of nickel and molybdenum can be replaced with other alloying elements. A basic assumption in the development of cost-effective carburizing steel is that engineering performance of a component made from low alloy steel is dictated by the base and case carbon content, microstructure and residual stresses. As long as the steel selected meets these requirements, equivalent engineering performance can be expected. The microstructure and residual stresses are governed by the carbon content, hardenability and martensite start and finish transformation temperatures. The major reason for alloying these steels is to influence hardenability and transformation temperatures. Sufficient hardenability, coupled with adequate and uniform quenching, provides microstructure optimization and control. The dependence of performance/strength on microstructure is basic.

Considerable laboratory test and field history data exist to support these basic assumptions. SAE PS-16 (Mn-Cr-Mo) steel, which is a nickel-free, cost-effective replacement steel for standard AISI 8622 (Mn-Cr-Mo-Ni) steel, has been used successfully in the production of heavy duty truck rear axle ring gears and in tractor and combine power trains for over 15 years. SAE PS-59, a cost-effective, Mn-Cr replacement steel, has also been used to substitute for PS-16 and 8622 steel for the last five years. Fig. 12 shows torque-life gear data from PS-59 steel at two carbon levels, superimposed on the G10, G50 and G90 bands for 8600 type steel. The bending and contact fatigue durability data were obtained by testing carburized and hardened six-pitch test pinions in a power circulating rig. The results show that the Mn-Cr steel and Mn-Cr-Mo-Ni (8622) steel have equivalent fatigue properties.

The data in Fig. 12 indicates that in low alloy gearing steels, small amounts of nickel and molybdenum can be replaced with other more cost-effective alloying elements. Nonetheless, the effect of alloying elements on the performance of gears is quite controversial. Using a modified Brugger test, Diesburg[13] studied the influence of carbon, alloy and residual stress on fracture stress and very low cycle fatigue life. Carbon and residual stress were shown to be very important. Alloy content was also found to be important, but the amount of alloy appeared more important than the specific alloy. DePaul,[14] Shea[15] and Love and Campbell,[16] among others, provide a technology base concerning the effect of major alloys on properties of carburized steel. Most of this relatively small amount of work on alloy effects has been related only to gear tooth bending fatigue strength, not gear tooth flank durability (pitting fatigue). Krauss[17] concluded, based on roller specimens, that the alloying elements alone had no effect on flank durability. Allsopp, Weare and Love [18] also were not able to detect an alloy influence in tests using gears. None of the above programs, however, were designed specifically to systematically study alloy effects.

Effect of Nickel at Intermediate Levels.

Fracture toughness K_{IC} for 0.99% C PS-15 steel, Mn-Cr-Ni-Mo steel 8697 and 5195 steels are given in Table 8. At equivalent carbon levels, K_{IC} for PS-15 and 8600 series steels are exactly the same; i.e., 16.6 $MPa.m^{1/2}$. The 8695 steel has a slightly lower retained austenite. However, the amount of austenite is sufficient to provide its maximum contribution to toughness. Fracture toughness of 5195 Cr-Mn steel is superior to both the high carbon PS-15 and 8699 steels. This improved toughness is thought to be related to a lower matrix carbon concentration in 5195 steel caused by the formation of chromium carbides. The data in Table 8 show that small amounts of nickel, molybdenum and other alloying elements do not influence the fracture toughness of high carbon steels significantly.

Table 8 — Fracture Toughness of High Carbon PS-15, 8600 and 5100 Steels

Steel	C	Mn	Cr	Ni	Mo	HRC	% RA	$K_{IC} MPa.m^{1/2}$
PS-15	0.99	1.09	0.54	0.03	0.16	60	39	16.6
8697	0.97	0.83	0.52	0.60	0.22	60	33	16.6
5195	0.95	1.00	0.93	0.03	0.01	60	34	20.8

Effect of Nickel at Higher Levels.

Table 9 shows the effect of nickel on fracture toughness of high-carbon martensitic steels. A comparison of K_{IC} for 4895, ER-8 and ERCH-1 reveals that fracture toughness increases with increasing nickel content. ER-8 and ERCH-1 are reduced nickel and nickel-free replacement steels for 4800 steel. K_{IC} of ER-8, in which half of the nickel in 4800 steel is replaced with other alloying elements, has approximately 10% lower fracture toughness as compared to the 4895 steel. ERCH-1, which contains no nickel, has the lowest toughness. The effect of nickel can also be seen by comparing the K_{IC} of 0.72% C PS-15 steel with 4870 and 9399 steel with 5195. Although some of the improvement in toughness may be explained on the basis of higher amounts of retained austenite and lower hardness of 4870 and 5195 steels, a nominal 3.5% nickel in these steels seems to promote improved toughness.

Effect of Boron.

Limited data obtained on testing a steel containing boron reveals that small additions of boron can enhance fracture toughness of high-carbon martensitic steels significantly. (See Table 10.) The addition of 0.0008% boron to 0.99% C PS-15 steel improved fracture toughness from 16.6 $MPa.m^{1/2}$ to 21.2 $MPa.m^{1/2}$. Boron is known to be a potent contributor to hardenability in the low and medium carbon range, but has very little influence on the hardenability of high-carbon steels. This non-hardenability related improvement in the

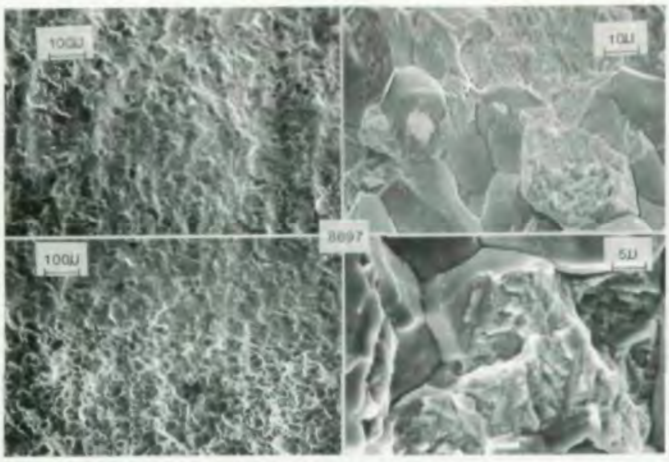

Fig. 13 – Photomicrographs showing fracture modes in fatigue precrack and single overload regions of 8697 steel. (A) Fatigue precrack area, (B) and (C) fatigue crack/single overload interface, and (D) transgranular area in single overload.

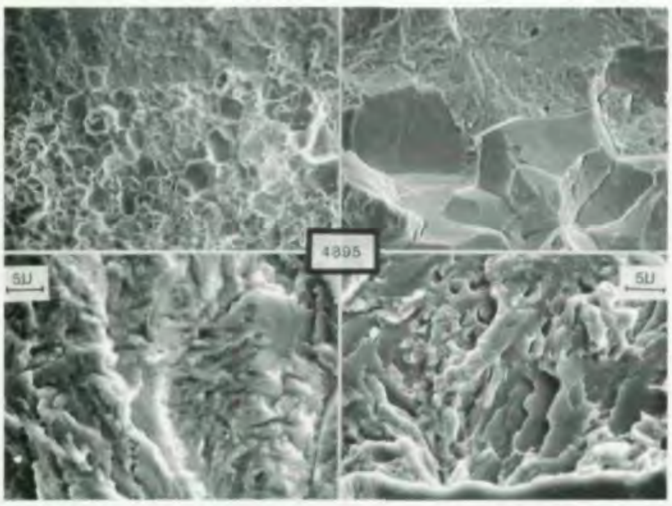

Fig. 14 – Photomicrographs showing fracture modes, fatigue precrack and single overload regions of 4895 steel. (A) and (C) fatigue precrack/single overload interface, (B) transgranular area in fatigue precrack area, and (D) transgranular area in the overload region.

Table 9 – Effect of Nickel Content On K_{IC}

Steel	%C	% Ni	Rc	RA	K_{IC}MPa.m$^{1/2}$
4895	.95	3.44	55.5	40%	24.5
ER-8	.95	1.57	60.5	47%	22.4
ERCH-1	1.00	0.08	58.5	42%	20.7
PS-15	.72	0.03	60.5	16%	21.7
4870	.78	3.50	57.0	21%	34.5
9399	.99	3.22	53.0	49%	27.1
5195	.95	0.08	60.0	34%	20.8

Table 10 – Effect of Boron On K_{IC}

Steel	%C	Rc	RA	K_{IC}MPa.m$^{1/2}$
PS-15	0.99	60	39%	16.6
PS-15 + B*	1.00	60	31%	21.2

*Added as Fe-Al-B (BATTS #2) Alloy.

Table 11 – Critical Crack Size and Load Carrying Capability of Various Steels

STEEL (%C)	K_{IC}(MPa.m$^{1/2}$)	Ac (mm)	σc (MPa)(1)	R(2)
PS-15 (.99)	16.6	0.363	690	1.00
PS-15 (.86)	22.4	0.660	930	1.35
PS-15 (.72)	21.7	0.615	900	1.30
8697 (.97)	16.6	0.363	690	1.00
IH-50 (.97)	20.3	0.543	840	1.22
4895 (.95)	24.5	0.787	1015	1.47
4870 (.70)	34.5	1.520	1410	2.04
ERCH-1 (1.00)	20.7	0.566	860	1.25
ER-8 (.95)	22.4	0.660	930	1.35
9399 (.99)	27.1	0.965	1125	1.63
5195 (.95)	20.8	0.571	870	1.26
PS-15 + B (1.00)	21.2	0.589	885	1.28

(1) Critical applied stress for a crack size of 0.363 mm.
(2) R = $\sigma c/\sigma$ for PS-15.

fracture toughness of high-carbon boron steel may depend on how boron additions are made. Unlike the domestic practice of alloying with "protected" boron by simultaneously adding titanium, zirconium and aluminum, the German practice is to alloy with ferroboron. The German practice is an inefficient way to use boron for hardenability enhancement, but the practice is said to improve the distortion, toughness and low and high cycle fatigue characteristics of carburized steel.[19] According to the German practice, when added as a ferroboron, boron acts as a nitrogen fixer during both the steel making process and subsequent carburizing treatment. After combining with nitrogen during the steel making process, enough boron remains in the soluble form to combine with nitrogen picked up in carburizing and, thus, high carbon martensite-austenite surface is low in soluble nitrogen and has enhanced properties.[20] Additional research is required to fully assess non-hardenability related beneficial effects of boron-containing carburized steels.

Significance of Fracture Toughness in Design.

Small differences in the K_{IC} resulting from carbon content, retained austenite or alloy effects can have a significant influence on the critical size (A_c) and load carrying capability (σ_c) of high-carbon steels. The data in Table 11 were calculated using basic fracture mechanics concepts involving relationships between stress intensity factor, applied stress and crack length. The critical size (A_c) was calculated for an elliptical surface crack with a geometry A/2c of 0.5, assuming applied stress of 690 MPa and applied stress-to-yield strength ratio of 0.33. The results show that a change in the K_{IC} of high-carbon steel from 16.6 to 22.4 MPa.m$^{1/2}$ nearly doubles the size of the crack that the material can sustain before an unstable crack growth occurs. Similarly, for a given crack size, the load carrying ability of the steel improves by 35%.

Fractography.

The fatigue precrack and single overload regions of several samples were examined using SEM. Typical fractographs are shown in Figs. 13-15. Stable fatigue crack growth in the precrack area was characterized by both transgranular and intergranular fracture modes. In all samples, fracture topography at low stress-intensity range was smooth and primarily transgranular. As the stress-intensity range in-

FAST.

The CNC controlled HNC-35 Worm and Thread Grinder

Klingelnberg introduces the fastest . . . most accurate complex worm and thread grinder available . . . anywhere in the world! The CNC controlled HNC-35 stores data for up to 960 complex shapes, reducing set-up to 10-15 minutes . . . a fraction of the time required with mechanically controlled grinders.

The HNC-35 is versatile too. It performs creep-feed grinding from the solid, eliminating the need for preliminary milling of worms, threads and rotors. It's two machines in one . . . with the high degree of accuracy you'd expect from Klingelnberg.

The HNC-35 is available with a mechanical dresser or an optional CNC dresser, for special forms and flanks. Whether you produce small quantities or long production runs, the FAST set-up . . . FAST cycling . . . HNC-35 will improve your worm and thread productivity.

For additional information and a copy of our catalog, contact: Klingelnberg Corporation, 15200 Foltz Industrial Parkway, Cleveland, OH 44136. Or, phone (216) 572-2100 for an extra FAST response.

KLINGELNBERG

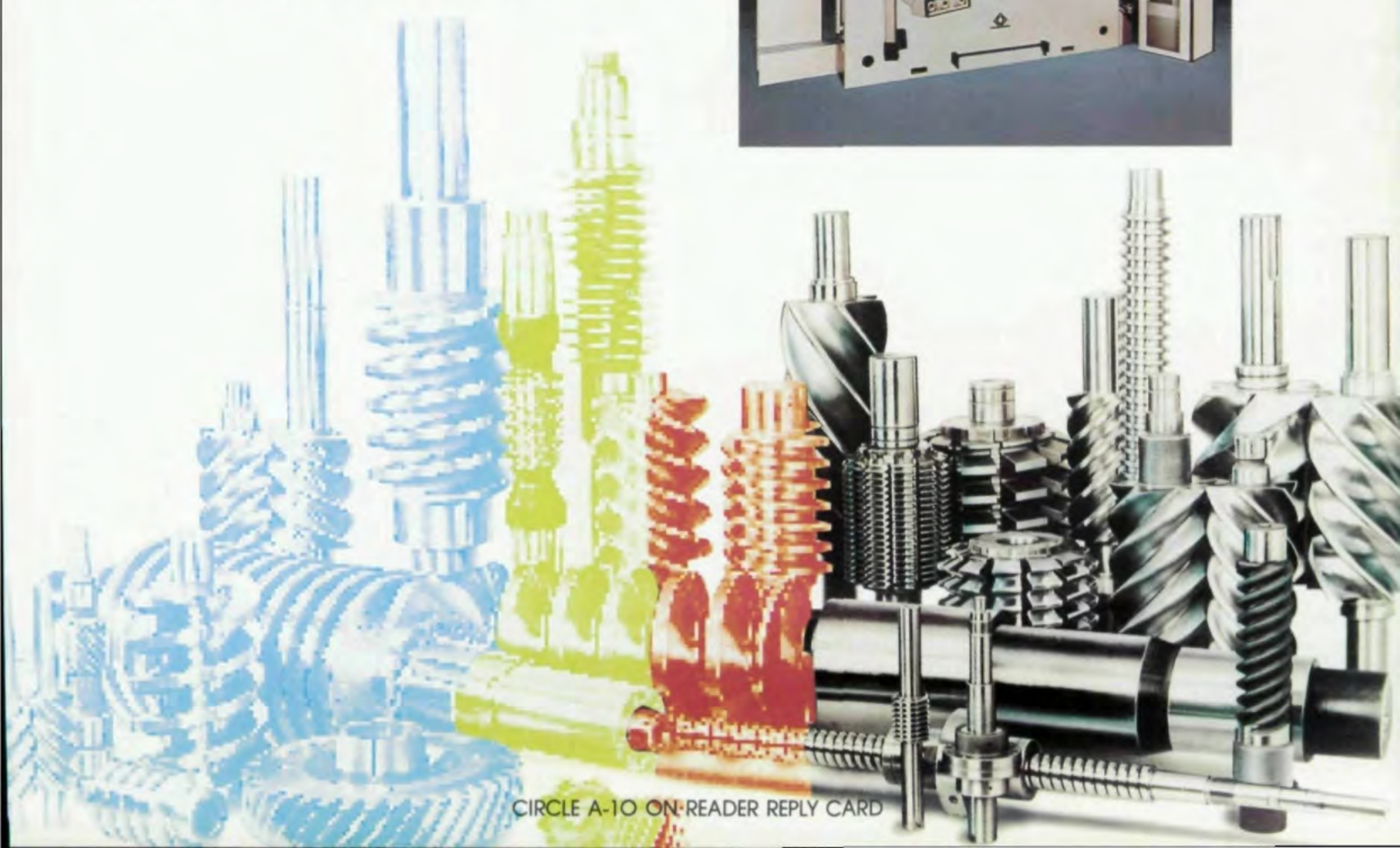

CIRCLE A-10 ON READER REPLY CARD

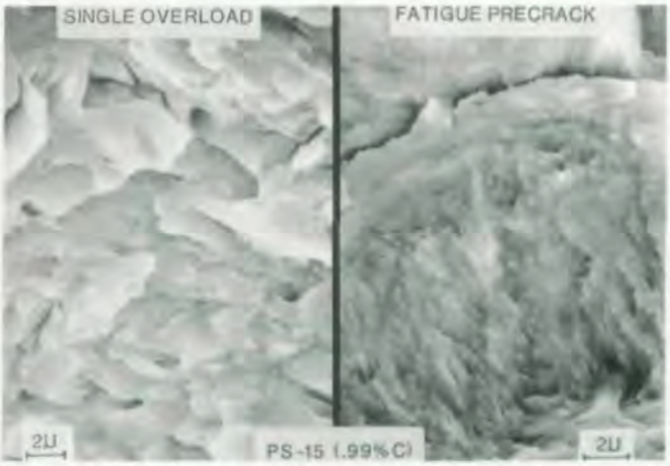

Fig. 15 – Fractographs showing differences in the topography of transgranular fractures in the single overload and fatigue precrack regions.

creased, the fracture surface generally became coarser, and the percentage of transgranular areas decreased, while the amount of intergranular fracture mode increased. Further examination of the transgranular area at higher magnification revealed topography typically associated with crack propagation in high-hardness steels. The fracture surfaces were flat and mottled, but occasionally fatigue striation could be resolved.

The single overload region was primarily intergranular with some transgranular areas present. These transgranular areas were distinctively different from the topography observed in the transgranular fatigue precrack areas. (See Fig. 15.) These transgranular areas were characterized by cleavage and flat dimples.

Conclusion

The results show that a complex interdependency existing between the carbon content, retained austenite and various alloying elements makes interpretation of the data difficult. Experimental steels must be designed carefully to isolate the effect of each of these variables.

A small variation in the carbon can influence the fracture toughness of high-carbon steels significantly. Lowering carbon increases toughness. The effect of carbon, however, must be considered in conjunction with retained austenite, which increases with the increasing carbon content. Higher retained austenite is usually beneficial, but the beneficial effect is dependent on its nature and distribution.

The alloy effect becomes significant only after the alloy exceeds a minimum amount. Results show that small amounts of nickel ($\sim$0.5%), molybdenum ($\sim$0.2%) and other alloying elements do not have significant effect on the plane strain fracture toughness properties of high-carbon steels. Higher nickel promotes toughness. K_{IC} of high-carbon steels containing a nominal 1.5% and 3.5% nickel improved significantly. Small amounts (0.0008%) of boron also appear beneficial. This non-hardenability related improvement may depend on how boron additions are made.

References:

1. RAZIM, C. and STRENG, H. "Properties of Case-Hardened Components – Basic Considerations Concerning the Definition and Evaluation of Toughness," *Proceedings, Case-Hardened Steels: Microstructural and Residual Stress Effects*, D.E. Diesburgh, Ed. AIME, 1983, p. 1-15.
2. SHIN, S.W. and SHARMA, V. K. "Application of a Tilting and Rotating Specimen Stage to X-Ray Retained Austenite Measurements in Textured and Coarse Grained Steels," SAE Paper #800428, *SAE Transactions*, 1980.
3. STICKELS, C.A. "Plastic Deformation of Quenched and Tempered 52100 Steels Under Compression," *Metallurgical Transactions A*, 1977, Vol. 8A, pp. 63-70.
4. NAKAZAWA, K. and KRAUSS, G., "Microstructure and Fracture of 52100 Steel," *Metallurgical Transactions A*, Vol. 9A, 1978, pp. 681-689.
5. GAHR ZUM, K.H., and SCHOLZ, W.G. "Fracture Toughness of White Cast Irons," *Journal of Metals*, October, 1980, p. 38.
6. THOMAS, G. "Retained Austenite and Tempered Martensite Embrittlement," *Metallurgical Transactions A*, Vol. 9A, March, 1978, p. 439.
7. WEBSTER, D."Development of a High Strength Stainless Steel with Improved Toughness and Ductility," *Metallurgical Transactions* Vol. 2, 1971, p. 2097.
8. GERBERICH, W.W., et al. *Fracture 1969*, Proc. of 2nd. International Conference on Fracture, Brighton, U.K. Chapman and Hall, Ltd., 1969, p. 288.
9. KOO, J., RAO, B.V.N., and THOMAS, G. "Designing High Performanace Steels with Dual Phase Structures," *Metal Progress*, September, 1979, p. 67.
10. SCHWARTZBART, H. and SHEEHAN, J. "Impact Properties of Quenched and Tempered Alloy Steel," *Final Report ONR Contract N60NR244T.O.I.*, September, 1955, Research conducted at IIT, Chicago.
11. KRAUSS, G. and MARDER, A.R. "The Morphology of Martensite in Iron Alloys," *Metallurgical Transactions*, Vol. 2, September, 1971, p. 2343.
12. ZACKAY, V. F., "Fundamental Consideration in the Design of Ferrous Alloys," *Alloy Design for Fatigue and Fracture Resistance, AGARD-CP-185*. NATO, January, 1976.
13. DIESBURG, D.E. and SMITH, Y.E. "Fracture Resistance in Carburized Steels, PE II: Impact Fracture," *Metal Progress*, 115 (6), June, 1979, pp. 35-39.
14. DEPAUL, R.A. Impact Fatigue Resistance of Commonly Used Gear Steels, SAE paper 710277, 1971.
15. SHEA, M.M. Impact Properties of Selected Gear Steels, SAE Paper 780772, 1978.
16. LOVE, R.A. and CAMPBELL, J.G. "Bending Strength of Gear Teeth," Report 1925/5, Motor Industry Research Association of U.K., December, 1952.
17. KRAUSS, G. "Influential Factors in the Fatigue Behavior of Case Hardened Steels Subjected to Rolling-Sliding Loads," Lecture to the Union of German Engineers, 3/22/72.
18. ALLSOPP, H.C., WEARE, A.T., and LOVE, R.J. "Resistance to Pitting of Gear Teeth, Re," Report 1959/2, Motor Industry Research Association of U.K., June, 1957.
19. LLEWELLYN, D.T. and COOK, W.T. "Metallurgy of Boron-Treated Low Alloy Steels," *Metals Technology*, December, 1974, p. 517.
20. GERMAN PATENT 1608732, "Procedure for Producing Tough Boron Treated Steels," September, 1969.

Acknowledgement: *Reprinted with permission of the American Gear Manufacturers Association. The opinions, statements and conclusions presented in this paper are those of the authors and in no way represent the position or opinion of the AMERICAN GEAR MANUFACTURERS ASSOCIATION.*

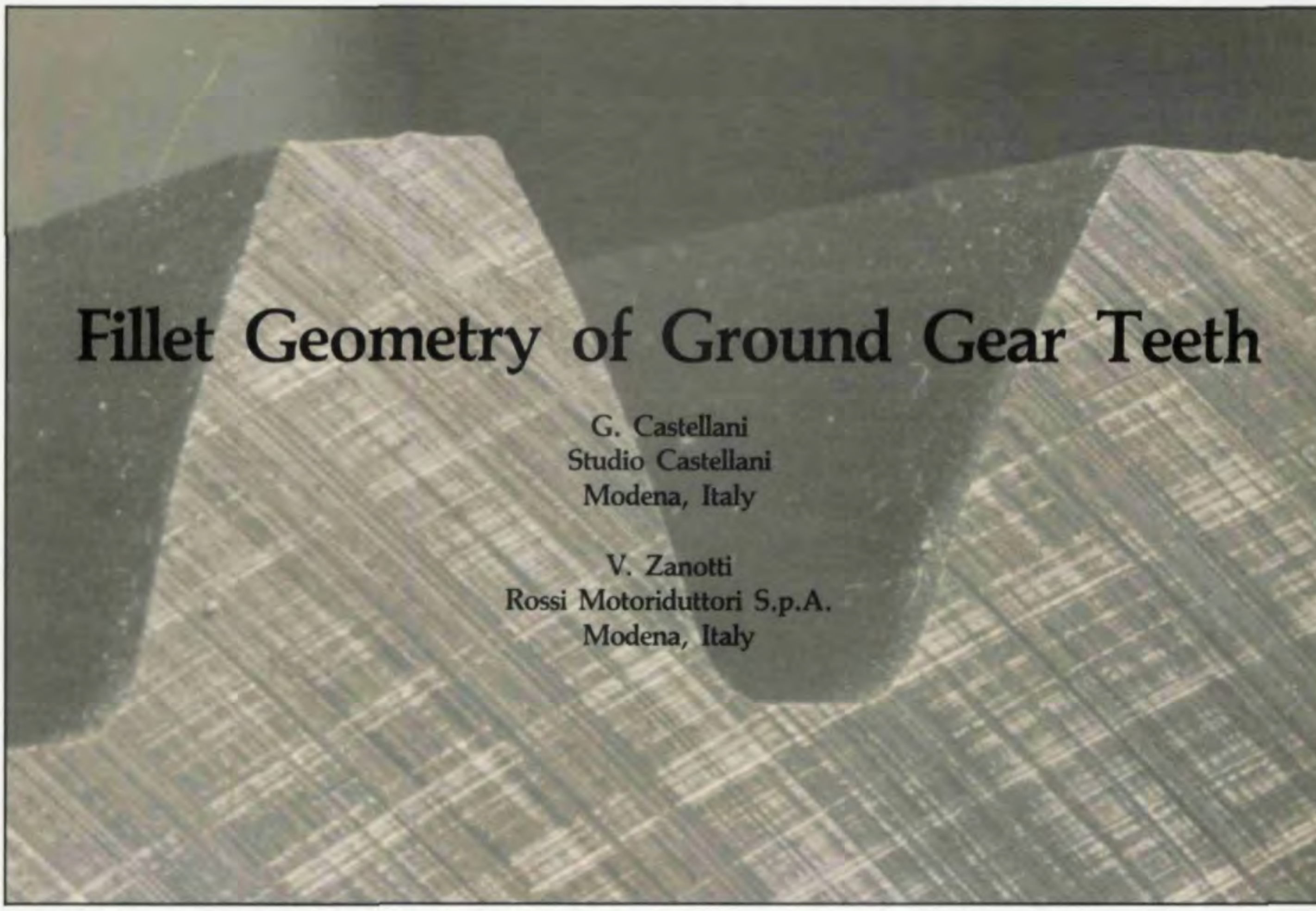

Fillet Geometry of Ground Gear Teeth

G. Castellani
Studio Castellani
Modena, Italy

V. Zanotti
Rossi Motoriduttori S.p.A.
Modena, Italy

Abstract

This article investigates fillet features consequent to tooth grinding by generating methods. Fillets resulting from tooth cutting and tooth grinding at different pressure angles and with different positions of the grinding wheel are compared. Ways to improve the final fillet of the ground teeth with regard to tooth strength and noise, as well as the grinding conditions, are shown. "Undergrinding" is defined and special designs for noiseless gears are described.

Introduction

Tooth fillets of involute gears often are more important than the involute itself in determining manufacturing cost, precision and gear pair operating success. The purpose of this study is to illustrate features of tooth fillets as they affect manufacturing conditions on grinding machines and as they pertain to gear strength and noise in gear operation.

Tooth generating methods are considered. The computations extend the procedure in Reference 1 to helical gears, using the criterion of Salamoun and Suchy[2] and are applied to both tooth cutting and grinding. (See Appendix A.) A rigorous approach for helical fillets should consider the conjugation of either tools or grinding wheels with the generated teeth in the space, but an approximation of the adopted procedure is more than sufficient for the engineer's investigations, as it does not concern the mating flanks of the gears of a pair, but only fillet forms.

AUTHORS:

DR. ENG.GIOVANNI CASTELLANI *is a gear consultant to private industry specializing in the relationship of gear design to manufacturing problems. Prior to entering the private consulting field, Dr. Castellani was a professor of mechanics at the State Technical Insitute. He has published two books on gear design as well as numerous articles and papers for technical conferences all over the world. Dr. Castellani is a member of AIPI (Associaztione Italiana Progettisti Industriali), chief of the technical committee of ASSIOT (Associazione Italiana Costruttori Organi di Trasmissione e Ingranaggi), a member of the ISO and the IFToMM Gearing Committee.*

MR. VITTORIANO ZANOTTI *is in charge of the Calculation and Applications Department of ROSSI MOTORIDUTTORI S.p.A. an Italian manufacturer of speed reducers, geared motors and motor-variators. He is a member of the company's working group for UNI (The Italian Standardization Board) and a member of ASSIOT. Mr. Zanotti earned his bachelor's degree in mechanical engineering from the University of Bologna in 1974.*

The computation is extended for helical gears to a "normal coordinate," whose abscissa is the half-ellipse chord normal for the local helix according to Castellani[3]. This criterion is preferable to that of actual spur gears because the computed limit between involute and fillet remains exactly the same as for the transverse section, and is also the same for tooth undercutting or undergrinding. Nevertheless, we checked that no appreciable difference exists between the plottings based on "normal coordinates" and plottings of actual teeth as far as the assessment of the fillet quality is concerned.

Plotted and manufactured examples of typical grindings of hobbed or rack-cut industrial gears are given and a generalization is made. The effects of different grinding methods and criteria are compared. Special attention is given to an uncommon grinding method adopting an increased pressure angle, whose mathematical basis is the same as for the contrary method used in older machines for 15° grinding of teeth cut by a 20° pressure angle.[4]

Regarding gear strength, neither AGMA 218.01[5] nor ISO 6337[6] give any indications of the effect of grinding steps at the tooth root of gears that are cut without a protuberance or with an insufficient one. Entwürf DIN 3990/1980[7] does, but, in our opinion, its experimental basis[8] should be widened. On the other hand, the number of possibilities is infinite. Computer analysis can serve not only to avoid dangerous "notches in the notch" in specific cases, but also to identify the grinding methods and parameters which are more likely to improve strength. In the future, tests might be restricted to convenient cases.

Fillet analysis has two effects on gear noise. It helps avoid false contacts for industrial gears and enables special gear designs to be adopted for special cases.

Grinding Tooth Fillets of Gears for a Speed Reducer

Let us consider a gear pair, A/B, designed for a nominal gear ratio of 3.55 and a center distance of 125 mm. The main data are given in Fig. 1a for the pinion and in Fig.2 for the gear. The teeth are hobbed without protuberances and ground by a wheel that has no facility for rounding the tip edge, $\varrho_{aG} = 0$, but permits any pressure angle.

Pinion A. Fig. 1b is the complete drawing of a tooth and Fig. 1c is the detail of the tooth fillet, both ground by a 24° grinding wheel. Figs. 1d, e, and f show fillets obtained by a 20° grinding wheel in various radial positions. An arc, cf, indicates the limit of the contact with the mating gear. The arcs, pf0 and pfG, relate to the involute limits obtained by hobbing and by grinding respectively. The point lG is the lower limit of the ground fillet.

In Fig. 1d, we consider the same grinding limit $r_{pfG} = 25.36$ as in Fig. 1c. In Fig. 1e the limits of the involutes obtained by hobbing and by grinding coincide. In Fig. 1f the

Nomenclature

(Note: symbols in parentheses relate to computer outputs.)

a' (A')	operating center distance
d_{al} (Dal)	tip diameter at the outer contact end
d_{cf} (Dcf)	root diameter at the inner contact end
d_f (Df)	root diameter
d_{pf0} (Dpf0)	diameter at the inner limit of the involute generated by cutting
h_{ar} (Har)	addendum of the reference rack
h_{a0} (Ha0)	addendum of the generating rack, either hob or rack-cutter
i_{bn} (Ibn)	final reduction of normal base thickness of a tooth with regard to the nominal one
I_{bn0} (Ibn0)	"reduction" of the normal base thickness after cutting: It is usually negative if the tooth must be ground.
k_{sl} (Ksl)	tooth shortening coefficient for the outer contact end
m_n (Mn)	reference normal module
m_{nG} (MnG)	reference normal module at grinding
r_{al} (Ral)	radius of the diameter d_{al}
r_{cf} (Rcf)	radius of the diameter d_{cf}
r_f (Rf)	root radius
r_{fG} (RfG)	radius of the fictitious root circle generated by the center of the tip edge arc of the grinding wheel
r_{fG0} (RfG0)	radius of the fictitious root circle generated by the grinding wheel
r_{lG} (RlG)	radius at the inner end of grinding
r_{pf0} (Rpf0)	radius of the diameter d_{pf0}
r_{pfG} (RpfG)	radius at the inner limit of the ground involute
$\bar{s}_{aN}$ (S-aN)	ellipse chord normal to tip helices; i.e., normal tip thickness
u_0 (U0)	protuberance amount
u_s (Us)	grinding stock
x (X)	nominal coefficient of addendum modification
z (Z)	tooth number
α_n (αn)	normal reference pressure angle
α_{nG} (αnG)	normal reference pressure angle at grinding
β (β)	reference helix angle
β_G (βG)	reference helix angle at grinding
ϱ_{a0} (roa0)	radius of the tip edge rounding of the tool
ϱ_{aG} (roaG)	radius of the tip edge rounding of the grinding wheel

We shall call "grinding step" the variation in the slope of the tooth profile where a ground zone connects with a cut one.

Further nomenclature is given in Appendix A.

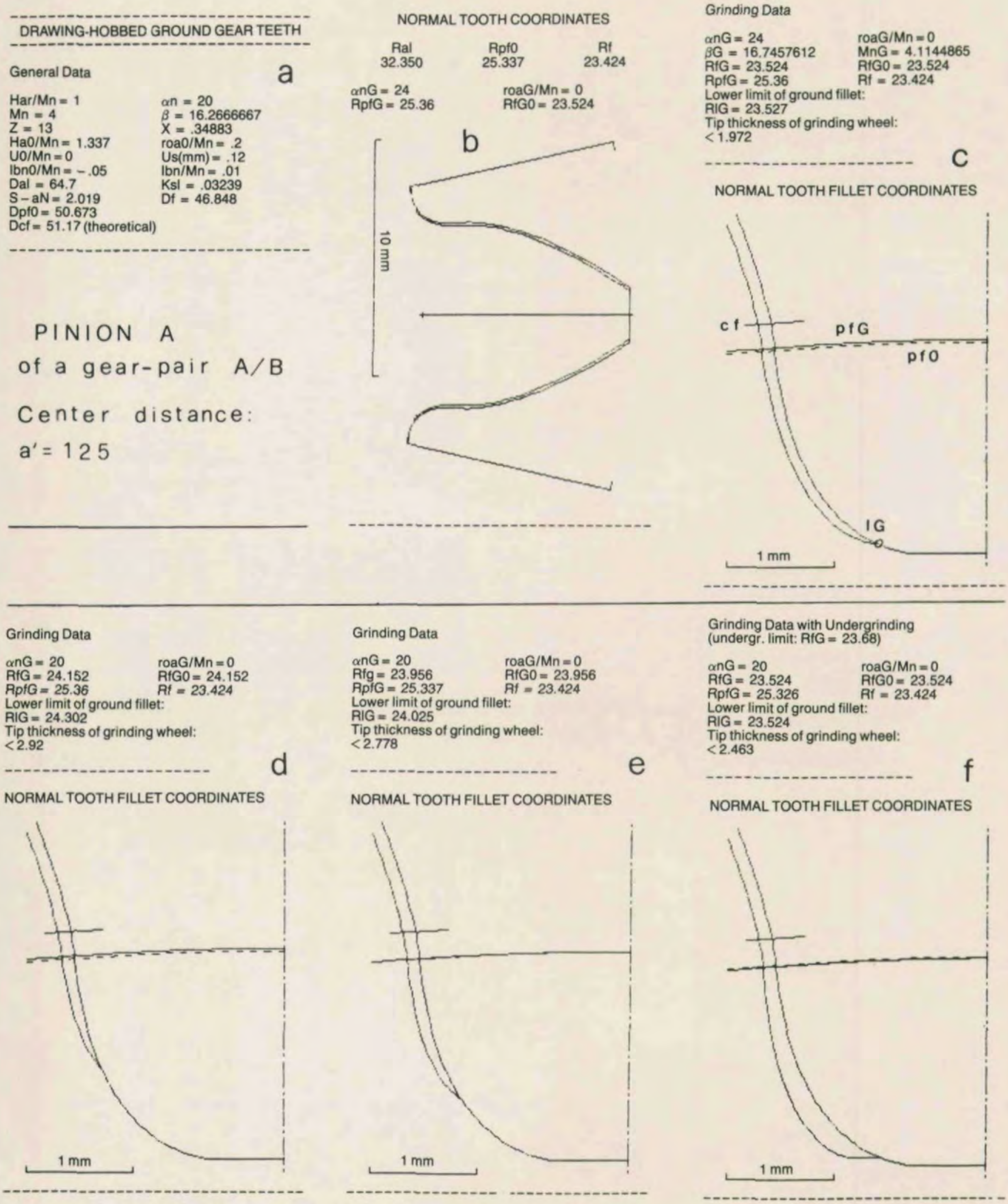

Fig. 1—Data (a), drawing of a tooth (b) and various fillet grindings (c,d,e,f) of a pinion A.

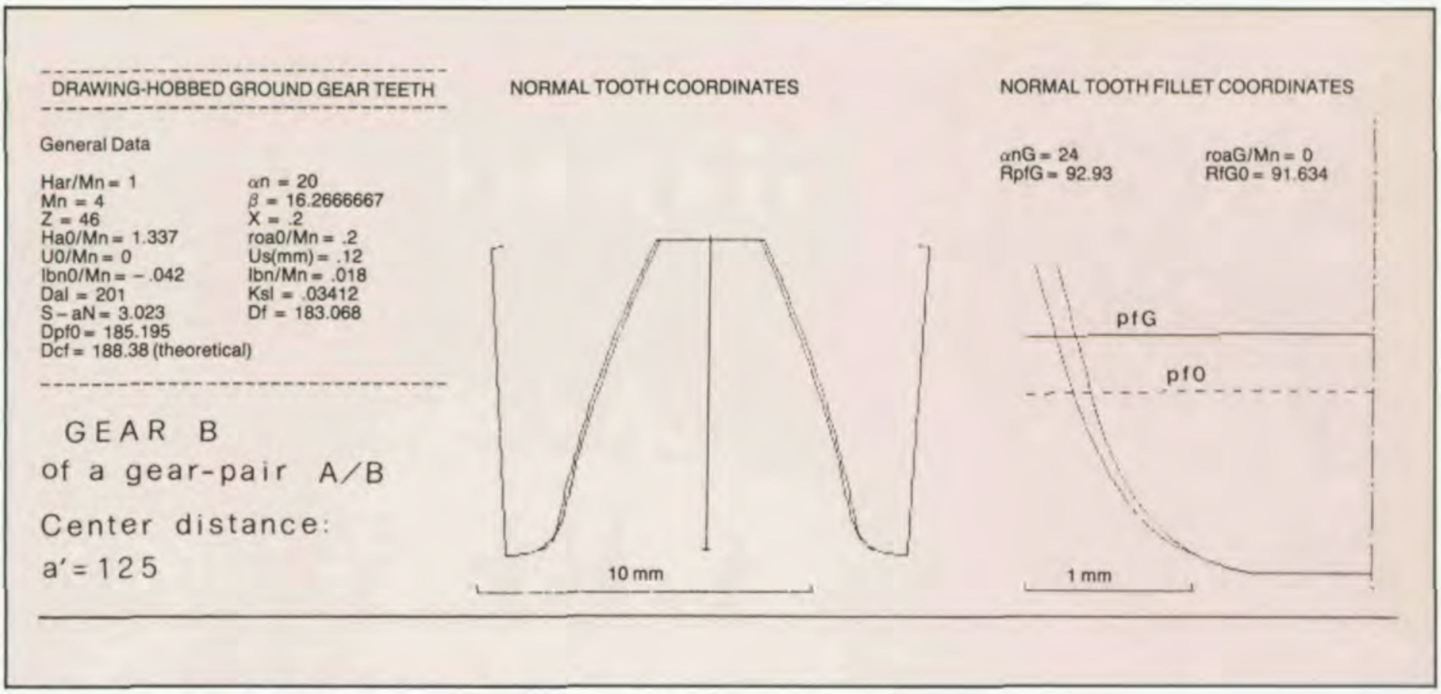

Fig. 2—Data, tooth and fillet of a Gear B, ground by 24° pressure angle.

radial position of the grinding wheel is the same as in Fig. 1c. Its tip is 0.1 mm from the tooth root, and the fictitious root circle generated by grinding has a radius $r_{fG0} = 23.524$, while the actual root radius obtained by hobbing is $r_f = 23.424$ mm.

Theoretical and practical false contact. The contact limit radius, r_{cf}, must be greater than the calculated involute limit, r_{pfG}, to avoid *theoretical false contacts.* A good margin between the two circles is needed, especially if the grinding machine has no apparatus for sharpening the grinding wheel periodically. In fact, the tip of the grinding wheel wears more rapidly than the internal zone of its profile. Thus, a prominent error can arise in the generated involute in the extreme region towards the tooth root, so that we would get a *practical false contact,* even if not a theoretical one, as well as noise and dynamic overloads.

(Tip reliefs of the mating gear may somehow compensate for the effects of a fillet contact or of an involute error, but this compensation is unpredictable, and it is not the intended purpose of the elastic deformation of the teeth already in mesh.)

In our case, the grinding machine is equipped with automatic sharpening apparatus and the margin between r_{cf} and r_{pfG} is sufficient. We observe that it varies very little according to the methods and the positions of the grinding wheel. (See Fig. 1.)

Observations on the ground fillets of the Pinion A. Grinding operators very often bring the grinding wheel very close to the root of the tooth space for two main reasons. First, if they are conscious of the risk of false contacts, they wish to achieve the maximum margin against it. On the other hand, if they are not, they prefer that no grinding step be too visible. Such indiscriminate practice usually removes a large amount of metal at the tooth root when grinding with the same pressure angle as in cutting. (See Fig. 1f.) This has two disadvantages: The carburized layer of case-hardened gears is reduced, and the grinding wheel needs frequent sharpenings. Furthermore, the grind operation is heavy, which can badly affect the precision grade of the teeth. If there is any vibration, the heavy operation will worsen it.

On the other hand, if we content ourselves with shorter ground fillets like those in Figs. 1d or 1e, then the grinding step is not too bad. In our case, it is much worse for high tooth numbers, high helix angles and high addendum modifications. However, such a step seriously impairs gear strength because it is not very far from the point of maximum stress of the decisive cut profile.[8] In any case, the plottings enable a compromise choice.

But we have a better option. If we grind the tooth with an increased pressure angle, we obtain a gradual diminution of the ground metal amount and a lighter operation. We can also expect improved gear strength because the ground fillet has a smaller curvature and covers the zone of maximum local stress[9] where it is advantageous to have low surface roughness. Both influences are taken into account by the general ISO and DIN ratings.[6,7] See the example of Fig. 1c in the case of Pinion A.

Plotting enables us to optimize the combination of pressure angle and grinding wheel position, as it is not always practical to bring the grinding wheel close to the tooth root.

Gear B. In Fig. 2 we give data and plottings for Gear B as ground with a 24° pressure angle. The contact limit is out of the field of the plotted fillet. This is usual for the bigger gear of a pair. There is a good margin between contact and involute limits.

We performed two manufacturing tests of this gear by grinding it close to the tooth root with 24° and 20° pressure angles. (See Figs. 3a and 3b.) The fillets are plotted in the transverse section in Figs. 4a and 4b to compare them with the photos. Note that the operator brought the grinding wheel


We're proud to serv
GREAT
AMERICAN
GEARMAKERS

Great American Gearmakers demand maximum production, highest quality, minimum downtime and fast payback from their equipment suppliers. That's exactly what CIMA-USA delivers...with global technology and state-of-the-art controls on each and every gear hobber.

From stand alone units...to semi-automatics...to fully automatic hobbers (for FMS Cells), CIMA-USA brings World Class hobbing machine designs to the gear industry with operator-friendly, easily maintainable componentry and controls.

Built tough to withstand rigorous gear making conditions, CIMA-USA hobbers employ double ribbed wall meehanite construction for maximum stiffness and resistance to torsional and bending stresses. The worktable is composed of case hardened and tempered steel for maximum durability. All moving and stationary components are designed with one thing in mind...years and years of optimum performance.

CIMA 220

CIMA 350

CIMA 160

CIMA-USA offers an abundance of standard features like: 6 axis operation, full thermal compensation, air-conditioned cabinetry, 4 synchronized software control options, and semi-automatic hob changing. With options for differential feeding, fully automatic hob changing, automatic fixture change and a host of loading configurations, CIMA-USA can custom-build a machine to match your exact specifications.

Product innovation constitutes the future at CIMA-USA. To keep Great American Gearmakers competitive in a rapidly changing marketplace, CIMA-USA recently introduced the Model 160, a compact, 6 axis hobber featuring higher table and hob head speeds. New models, soon to be introduced include a larger diameter hobber and a highly specialized grinder for cost-effective production of "ground quality" gearing.

CIMA-USA is proud to serve Great American Gearmakers with equipment that REDUCES CYCLE TIMES, IMPROVES or MONITORS QUALITY and INCREASES SHOP PROFITABILITY. And, we support equipment with unparalleled spare parts & service capability...if it's ever required.

Ask our sales representative for further details or contact CIMA-USA, Division of GDPM Inc., 501 Southlake Blvd., Richmond, VA 23236. Phone (804) 794-9764, FAX (804) 794-6187, Telex 6844252.

CIMA USA

Global Technology with a U.S. Base

CIRCLE A-12 ON READER REPLY CARD

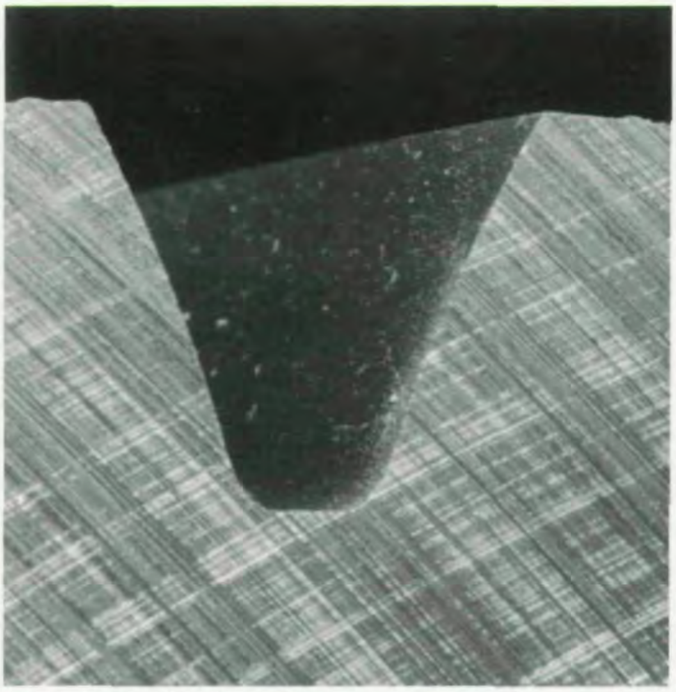

Fig. 3a – Teeth of Gear B ground by 24° pressure angle.

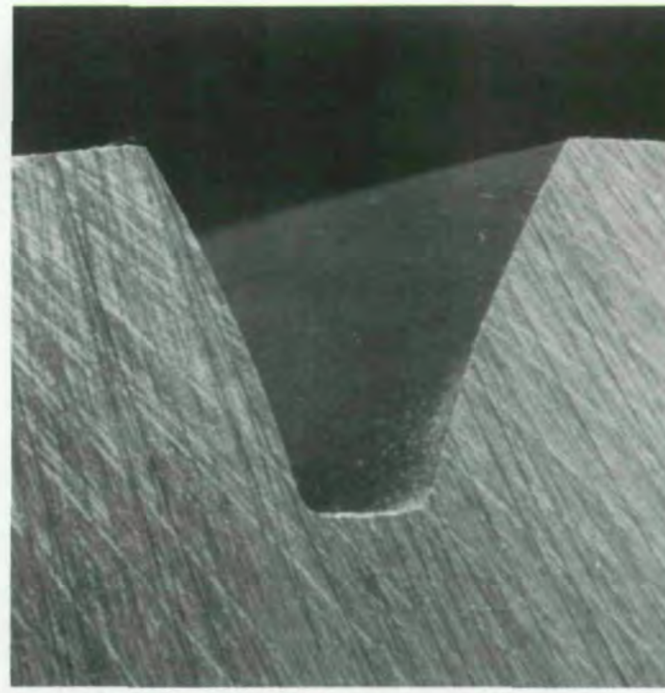

Fig. 3b – Teeth of Gear B ground by 20° pressure angle.

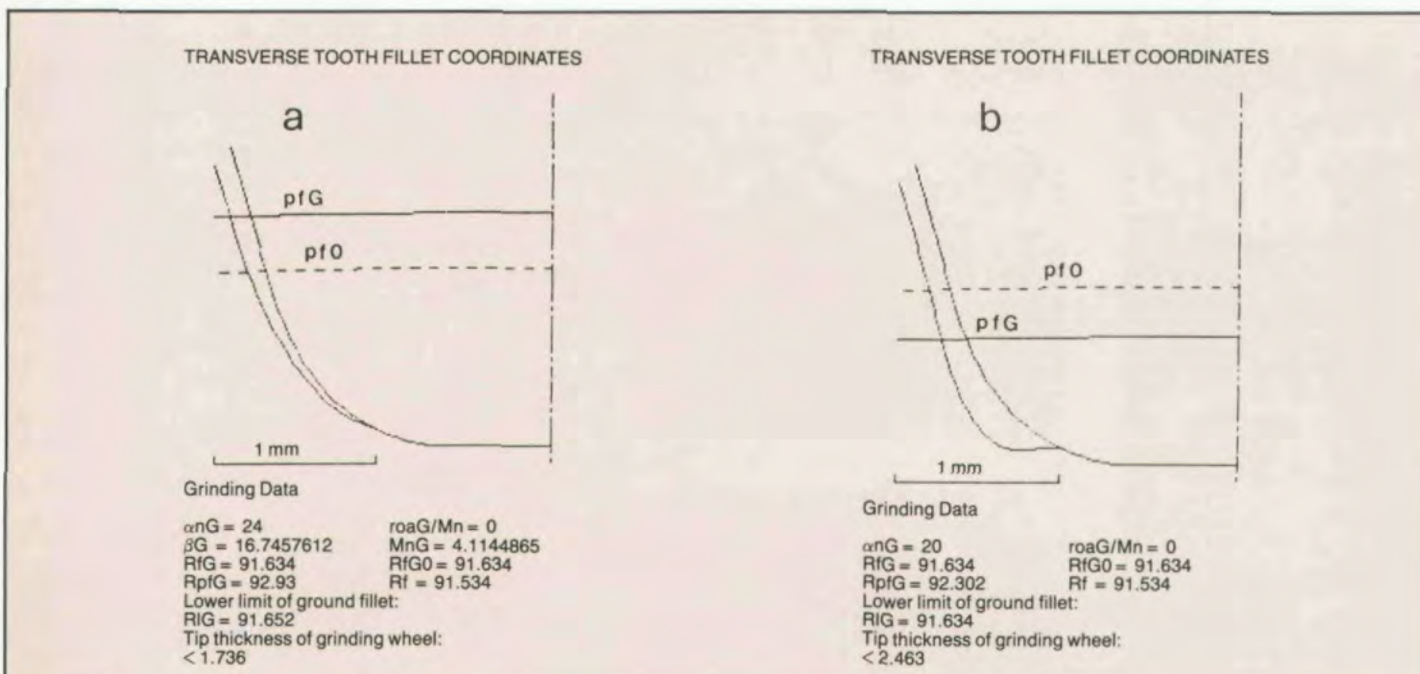

Fig. 4 – Tooth fillets of Fig. 3 plotted in the transverse section.

a little closer to the tooth root in these areas. Similar observations can be made for Pinion A. (See above.)

Gear Hobbed with an Insufficient Protuberance

Fig. 5 gives data and plottings of a gear specially designed for hobbing with a non-standard hob with protuberance and increased tooth height. The gear works as the driving element of a speed increaser, which motivates the relatively high addendum modification.

The grinding was planned for the 0° method.[10] This method gives no ground fillets out of the basis circle. The ground involute should connect with the hobbed fillet without any step or with a very slight one. But for the examined gear, case-hardening caused distortions and general size increases, so that the data given in Fig. 5 correspond to the actual situation after heat treatment, and the grinding stock to be removed was too large for the protuberance. (See Appendix A.) Therefore, it was impossible to avoid grinding steps such as presented in Fig. 6.

In such cases, plotting of hobbed fillets helps us to choose the grinding limit and minimize steps, as in Fig. 6a. Other-

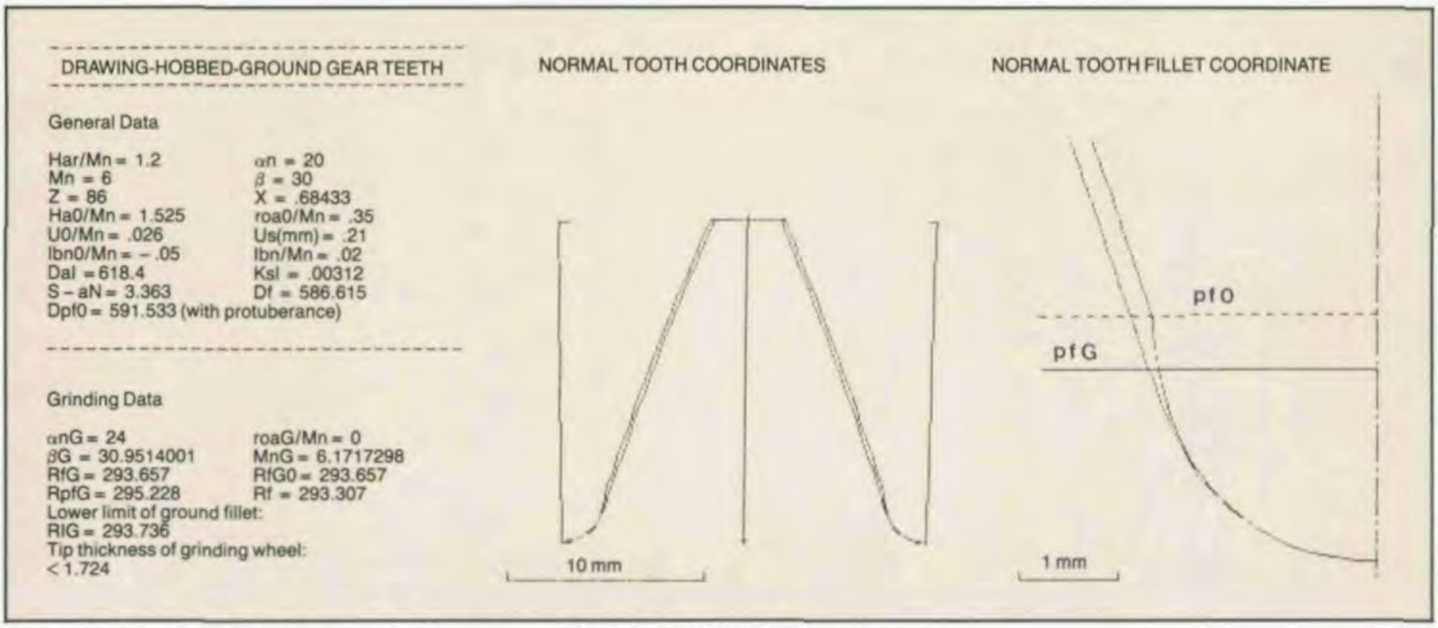

Fig. 5 – Tooth involute and fillet grinding by 24° pressure angle of a gear hobbed with protuberance.

wise, worse steps can occur, and, in fact, they are frequent in industrial practice, even close to the tooth root. (See Figs. 6b and c.) Of course, this does not invalidate the 0° method; it just indicates that a greater protuberance is needed, but it also raises the problem of saving a costly gear.

Common 20° grinding (Figs. 7a and 7b) makes the step less sharp, apparently by creating some ground fillets, but these are extremely short with a high curvature due to higher tooth number, higher addendum modification and higher helix angle than the teeth in Figs. 1 and 2. A completely satisfactory connection between cut and ground fillets by 20° grinding can only be obtained if the grinding wheel can have its tip edge rounded. (See Fig. 7c where a rounding radius, $\varrho_{aG} = 0.24$, has been adopted.)

A similar good connection and an even better curvature radius of the ground fillet can be achieved by using a 24° grinding as in Fig. 5 without any rounding of the tip edge of the grinding wheel. (Note that not all grinding machines permit such pressure angles, but they do not enable tip edge rounding either. In general, in available machines the pressure angle is obtained by means of sharpening rather than by the inclination of the grinding wheel.) In all cases, plotting is necessary to optimize either the tip edge rounding or the pressure angle of the grinding wheel, as well as its radial position.

Undergrinding

Let us compare "undergrinding" to "undercutting": a tooth is underground when the generation of the fillet removes a portion of the generated involute, so that the radius at the inner limit of the ground involute is greater than the base radius with a step. The computer signals undergrinding in Fig. 1f because the tip of the grinding wheel should be at a radius of $r_{fG} = 23.68$ mm instead of 23.524 to avoid the problem.

Deliberate Undergrinding of a Pinion Tooth

Like undercutting,[11] undergrinding does not always mean poor design criteria. On the contrary, it can improve reliability against false contacts to such an extent that the theoretical involute limit can coincide with the contact limit without drawbacks. There are two reasons for this: The slight step between the involute and the ground fillet, and the fact that the involute limit is ground, not by the tip edge of the grinding wheel, but by a point a little away from the edge.

This possibility contributes to obtaining higher contact ratios, together with low pressure angles and/or greater tooth heights. Theoretical investigations [12] show that spur gears with contact ratios greater than 2 have less tendency to dynamic overloads, and industrial experience with some of Castellani's designs confirms that gears (both spur and helical) with such contact ratios can be satisfactorily noiseless. This conclusion is supported by some published industrial results.[13]

Undergrinding in itself does not diminish gear strength. The strength diminution due to a lower module and unfavorable tooth form can be compensated for in part by good curvature radius and low roughness of the fillet zone. Such compensation requires careful determination of the fillet features so that grinding covers the zone of maximum stress, and the trend of the ground fillet is correct. The choice of the pressure angle and of the grinding wheel position greatly affect the fillet features.

As an example, let us propose the problem of designing a spur gear pair for a low noise level, with the same center distance and about the same gear ratio as the gear part A/B. (See Figs. 1 and 2.) We want to employ a readily available European hob which has a 15° pressure angle.

The main data for the pinion are reported in Fig. 8. The gear has 98 teeth and a tip diameter of 197.7 mm, which relates to the contact limit of the pinion $d_{cf} = 54.092$, coinciding in turn with the base diameter. Following the choice of the grinding data with an 18° pressure angle, we obtain a good ground fillet with a moderate undergrinding. We position the grinding wheel at a fictitious radius $r_{fG0} = 25.485$; whereas, $r_{fG0} = r_{fG} = 25.722$ mm would avoid undergrind-

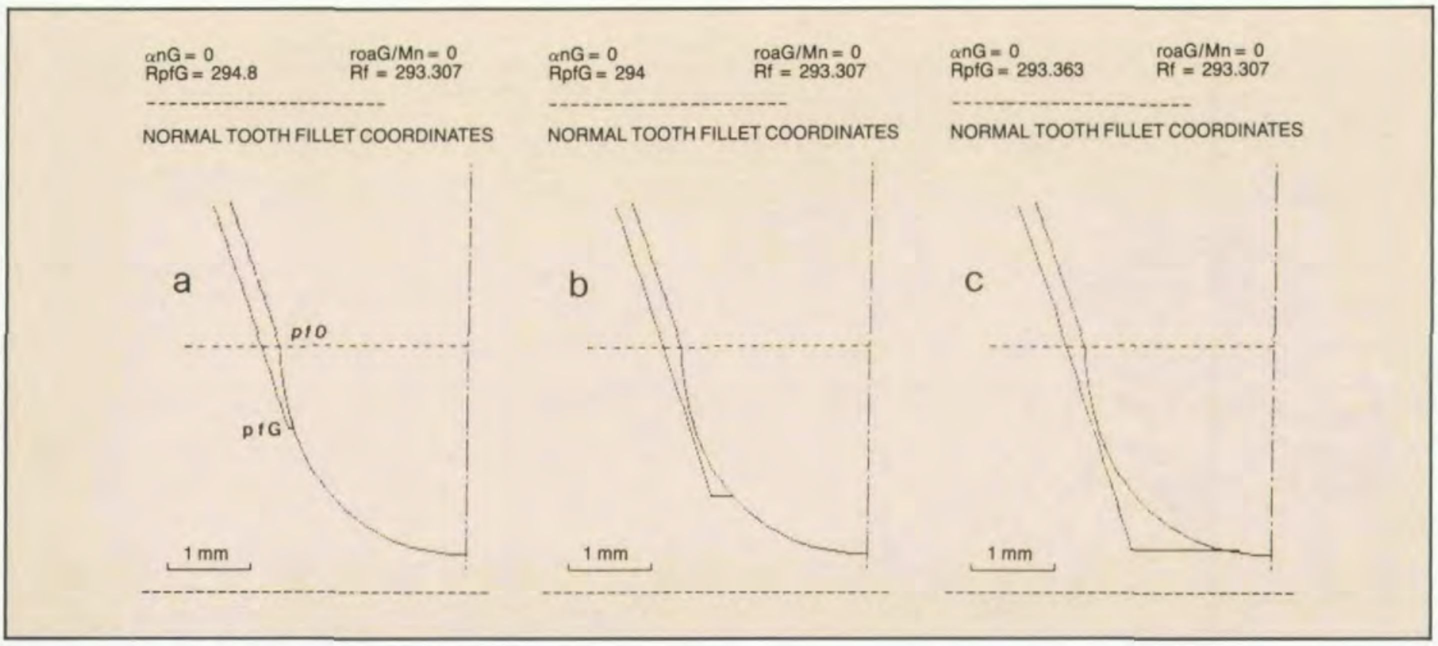

Fig. 6—0° grinding of the gear in Fig. 5.

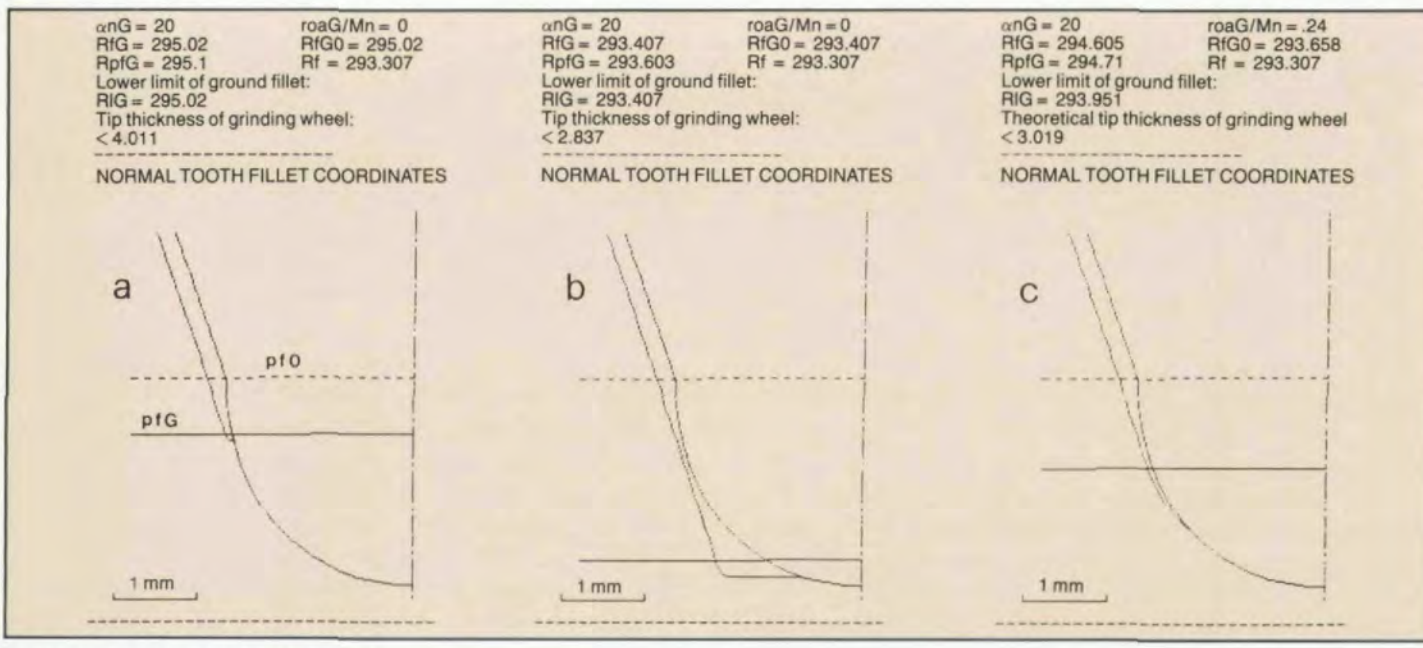

Fig. 7—20° grinding of the gear in Fig. 5.

ing. The difference is small, but sufficient to ensure that no practical false contact will arise. The involute limit, r_{pfG} = 27.048 mm, is just a little greater than the base radius and does not hinder the achievement of a 2.21 contact ratio, as r_{cf} and r_{pfG} are practically equal.

Summary

In the previous paragraphs we have seen typical examples of fillets generated by both common and less usual procedures. Now we want to classify fillets by some other well-known features.

Influencing parameters. The features of the fillet as well as the trend and the amount of metal to be removed depend on the following:

- the grinding pressure angle α_{nG};
- the radius of the tip edge rounding of the grinding wheel, ϱ_{aG}, which is often zero;
- the radial position of the grinding wheel, expressed by the difference, r_{pG0} - r_f, between the root radius generated by grinding, usually fictitious for industrial gears, and the radius generated by cutting, usually real.

As for the influence of the parameters of the gear itself, higher normal pressure angle, higher helix angle, higher tooth number and higher addendum modification create shorter fillets, both cut and ground. (For 0° grinding, see below.)

0° grinding. There is no ground fillet except for undergrinding. A proper choice of protuberance ensures a good connection between involute and fillet. Sharp grinding steps are

Matrix CNC Thread Grinders...

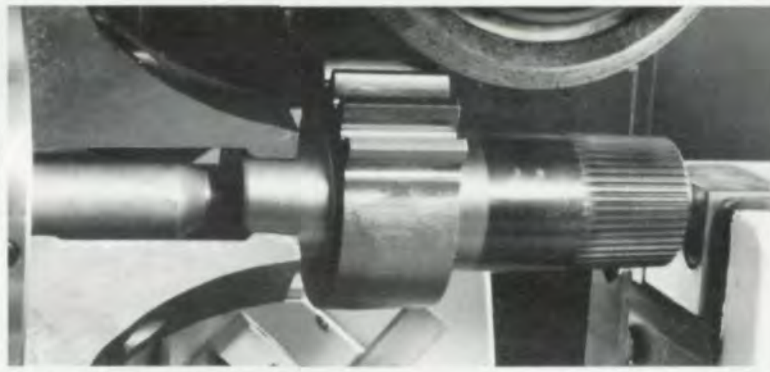

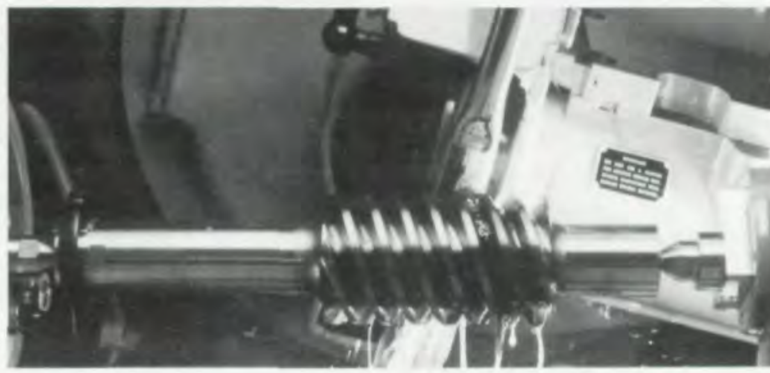

...Dramatically Slash Production Time!

CNC Thread Grinders from Matrix can drastically reduce your production time. Programmable control of infeed and auto-grind cycle, plunge grinding cycles and dressing, combined with the largest family of thread grinders in the world, make Matrix the logical choice to solve your grinding problems regardless of material or application.

Appropriate to a multitude of applications, Matrix CNC Thread Grinders are ideal for ball screw production, internal and external A. P. I. grinding, worm grinding, micrometer and surgical screw production, grinding the tracks in recirculating ball nuts, and many more. These Matrix machines can handle almost any aspect of precision grinding.

	1600 Series	4750 Series	5750 Series	6900 Internal	7000 Lg. Capacity
Swing over table ways	8"	15"-75"	15"-75"	19"	15.5"
Distance between centers	18"	49"	90"	-	197"
Maximum ground length	8"	41"	78"	118"	161"
Maximum ground diameter	8"	12.5"	12.5"	10"	10"
Grinding wheel diameter	14"	-	20"	1" to 5"	20"
HP of wheelhead drive	5 and 7½	10, 20 or 25	10, 20 or 25	5	10, 20 or 25
Helix of wheel, LH & RH	20°	45°	45°	10°	24°
Workhead thru bore	1.5"	3.97"	3.97"	N/A	6⅛"

Internal or external threads of virtually any form, single or multi-start, right or left hand, parallel or tapered can be easily ground with or without relief. It only takes the right Matrix CNC Thread Grinder for the Job.

Choices of wheel dressing units are available in conventional template or dresser arm style, diamond roll, crush roll plus a versatile CNC Dress Unit.

Several of the more popular Matrix thread grinding models are shown in the table at left. Details on other models available can be obtained by writing or calling Matrix-Churchill Corporation, 5903 Harper Road, Solon, Ohio 44139 or 216/248-7950. FAX 216-248-7981.

MATRIX-CHURCHILL

CIRCLE A-13 ON READER REPLY CARD

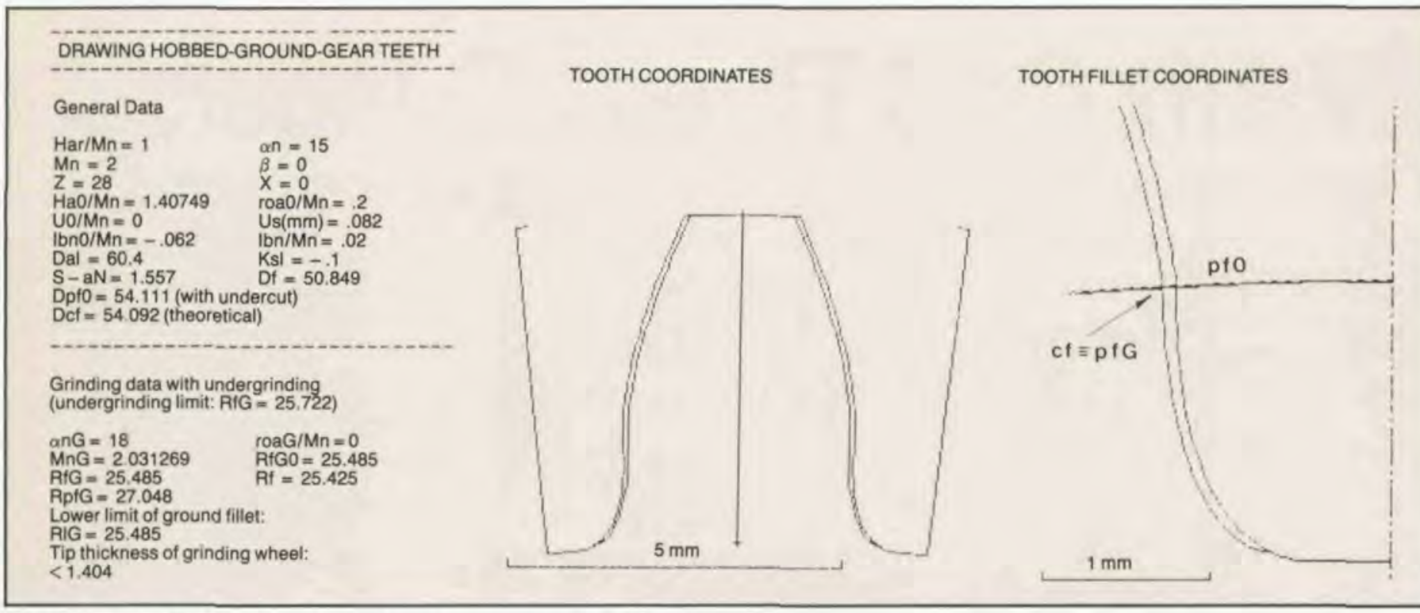

Fig. 8—Pinion hobbed by 15° and ground by 18° pressure angles with undergrinding.

unavoidable for gears cut without protuberance or with insufficient protuberance. (See Fig. 6.)

$\alpha_{nG} = \alpha_n$, $\varrho_{aG} = 0$. With sufficient protuberance—no ground fillet except for ground fillet stretches following incorrect positioning of the grinding wheel.

Without protuberance—ground fillet stretch of widely different form and extent and various steps with the cut profile. (See Figs. 1d, e, f, 4b, 7a, b.)

$\alpha_{nG} = \alpha_n$, $\varrho_{aG} > 0$ *or* $\alpha_{nG} > \alpha_n$, $\varrho_{aG} = 0$. Both methods are applicable for pressure angles obtained by dressing rather than by inclination of the grinding wheel. The first one requires special dressing facilities. Both methods enable smaller steps and lower fillet curvature, provided the grinding parameters are well chosen. (See Fig. 7c for the first case and Figs. 1c, 2, 4a, 5 and 8 for the second use.)

$\alpha_{nG} < \alpha_n$. Some grinding machines do not permit operation beyond a given pressure angle. For instance, let us suppose that we cut at 25°, but must grind at 20°. Then the opposite tendencies must be expected, because of an increase of the pressure angle: Wider margins between contact and involute limits at pinion root, but worse fillet features for gears cut without protuberance.

Undergrinding. Undergrinding can occur when using the 0° method following incorrect choice of grinding parameters, and in this case it should be considered an anomaly, as it can accompany pronounced (even if not sharp) steps, bad curvature and excess metal removal. See, for instance, the "Prüfradvariante Nr. 20" [8] that showed a loss of nearly 70% in fatigue resistance as compared to similar teeth free from grinding steps.

If the teeth are ground by a proper choice of the pressure angle, then undergrinding can help achieve a high contact ratio. It enables extension of the contact as far as the theoretical limit of the involute toward the pinion root without any risk of practical false contact. This may be essential to achieve noiseless working of the gear pair.

Limitations. When deciding the grinding specifications, two limitations cannot be disregarded: Theoretical false contact and inadequate tip thickness of the grinding wheel when the pressure angle is obtained by means of dressing.

It is always necessary to obtain an involute limit radius, r_{pfG}, less than the contact limit radius, r_{cf}, to accomplish the first condition. A further margin is necessary to guard against practical false contacts due to involute errors, or due to the frequency of grinding wheel dressings, except in undergrinding. For sharp and deep grinding steps, it may be necessary to ascertain that the intersection point of the ground zone with the cut fillet does not interfere with the tip edge of the mating gear.[10]

The second condition is bound up with the necessity of grinding one tooth flank at a time and is related to the material of the grinding wheel and the amount of metal to be removed.

Both conditions are more restrictive for grinding with a rounded tip edge of the grinding wheel or by an increased pressure angle. On the other hand, tip thickness of the grinding wheel usually is not a problem for industrial grindings that do not affect the root circle. As for the false contacts, this is never a problem for the greater gear of a gear pair. For the pinion, it just means that proper investigation must be made.

Strength and Strength Rating. Fillet features greatly affect fatigue strength and, to lesser extent, static strength of the tooth root. Even for case-hardened gears, Winter and Wirth [8] state that problems in reducing the case-hardened layer by grinding and in altering the residual compressive stresses are less important than the geometrical form of the fillet. Then fillet curvature, grinding extension and depth, and localization of the intersection point between grinding and cut fillet are decisive.

If a ground fillet covers the zone of maximum stress, then the general ISO or DIN rating of the stress correction factors can be provisionally applied by taking into account both fillet curvature and surface roughness.[6,7]

Of course, specific tests would be welcome in the future, and the comparison between gradually ground fillets and fillets free from grinding as cut by protuberance tools would be interesting. But in any case, there is no doubt that either solution is far better than continuing to create fillets affected by dangerous steps that are still so frequent in industrial gearing. Such fillets are not likely to be justified in the future because improved computation will enable us to avoid them.

Noise. Fillet features affect gear noise in two ways: Negatively if false contacts, either theoretical or practical, arise, and positively by ensuring extension of the contact and increase of the contact ratio when desired by means of undergrinding.

Manufacturing Conditions on Grinding Machines. For gears cut without protuberance, fillets ground gradually without excessive metal removal make operation easier, reduce the risk of vibrations and improve tooth precision. If we compare teeth ground to near the root by different methods, the rounding of the tip of the grinding wheel improves fillets, but increases costs. But an increased grinding pressure angle (with a sharp tip edge of the grinding wheel) lowers costs of the machining in itself, as less frequent sharpening of the grinding wheel is needed. The cost of the first sharpening of the grinding wheel does not practically increase general costs if a constant pressure angle, α_{nG}, is adopted for a given kind of gear design, or if it is not important when proper grinding of a large gear is involved. Cutting with wide protuberances lowers grinding costs, but increases the cost of the hob cutters, especially if specific protuberances are adopted for specific gears.

General Observations. The analyses of some of these examples may seem to imply that the problem of setting up the grinding wheel is critical, especially for big case-hardened gears, which can grow and distort in irregular ways because of heat treatment. However, computer analyses enable us to identify the kind of procedure that affords the widest protection against every possible drawback.

Let us consider the gear in Figs. 5, 6, and 7. The gear was planned for a grinding stock of 0.12 mm and was hobbed with a hob addendum, $h_{a0} = 1.5\ m_n$. (The value reported in Fig. 5 is fictitious according to Appendix A, "Fillet Analysis After Heat Treatment.") Let us suppose that in some tooth zone it did not grow and distort at all, whereas, in some other zone it grew and distorted much worse than in Fig. 5; that is, it reached a root diameter of $d_f = 586.95$ mm and required a grinding stock, $u_s = 0.294$ mm to be removed. If we then set up the grinding wheel as in Fig. 7b, we would obtain the fillets of Fig. 9a, where there is an unground fillet stretch and a bad notch at the tooth root, or 9b, where a full grinding of the tooth root is shown. This last condition is unusual for industrial gears and dangerous in this case, because of the great variation of the grinding stock. But if we set up a 24° grinding wheel exactly as in Fig. 5, we obtain the fillets of Fig. 10, both more than acceptable. Thus the plotting after heat treatment enables us to choose the grinding parameters more likely to avoid trouble. It must be stressed that the grinding problems of the cited gear were due to a manufacturing error: a greater protuberance should have been adopted. On the other hand, it is well known that

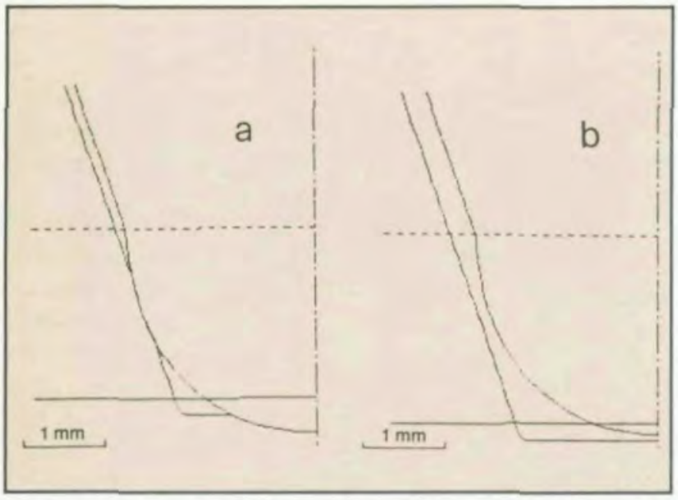

Fig. 9 – 20° grinding of a gear similar to Fig. 7b: (a) undeformed; (b) badly deformed after heat treatment.

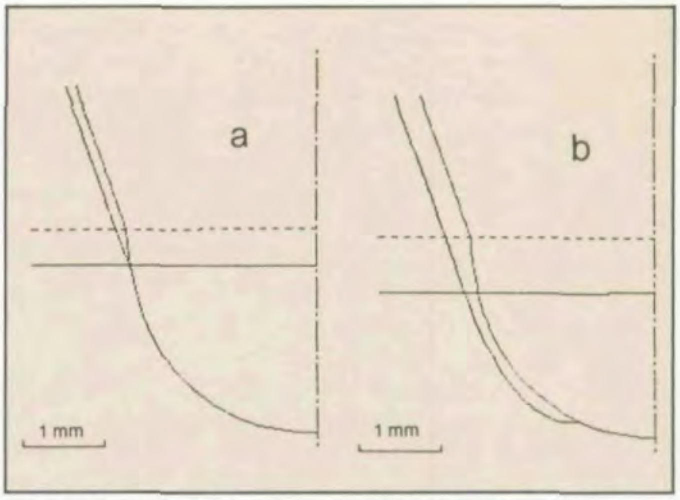

Fig. 10 – 24° grinding of a gear similar to Fig. 5: (a) undeformed; (b) badly deformed after heat treatment.

growth and distortions, especially of the largest case-hardened gears, are so unpredictable that a costly preliminary heat treatment with the sole aim of ascertaining the trend of a particular gear to deform has been suggested.[14] If the planned 0° grinding is to be maintained for the gear, either a very ample protuberance must be adopted or the risk of a situation similar to that of Fig. 6 arises.

In the authors' opinion, grinding steps like those of Fig. 6 should be avoided, although some gears, even with steps like those in Fig. 6c, have been known to work for years without failures. But in other gears, breakages did occur. Of course, higher safety factors would be needed to avoid such failures, but, even then, the strength is aleatory because, besides the bad notch, the grinding may burn the tooth root and cause crackings.

If grinding facilities and computer analyses do enable us to obtain a regular fillet, then even a full grinding of the tooth root may be obtained, like those usually adopted in special fields to improve reliability, as in the case of certain gears ground for use in helicopters. Nevertheless, this increases costs, and we do not think it feasible for common industrial practice.

Conclusions

Mathematical methods are supplied in Appendix A to compute cut or ground fillets of both spur and helical gears. Typical fillet features resulting from different methods of generating grindings and from various choices of the influencing parameters are examined. A final classification is made.

Special attention is given to an uncommon grinding method, namely, grinding at a pressure angle greater than that of the cutting tool, which permits fillet features and lighter manufacturing without protuberance tools or special sharpening apparatus for the grinding wheels.

False contacts of the operating gear pairs at the pinion tooth root are either "theoretical" or "practical" ones.

"Undergrinding" is defined and its contributions to the manufacture of noiseless gears by excluding false contacts and increasing contact ratios is discussed.

A proper choice of grinding method and of grinding parameters enables one to obtain gradual fillets covering the zone of maximum stress with low fillet curvature and low surface roughness, thus improving the fatigue strength of the tooth root and making the general strength ratings applicable to ground teeth while awaiting specific tests.

References

1. CASTELLANI, G., and PARENTI CASTELLI, V. "Rating Gear Strength", *J. of Mech. Design, Trans. ASME*, Vol. 103, April, 1981, pp. 516-527.
2. SALAMOUN, C., and SUCHY, M. "Computation of Helical and Spur Fillets", Proc. of the Int. Symp. ASME/AGMA/IFToMM, San Francisco, Oct., 1972, Paper RM4.
3. CASTELLANI, G., "Calcolo Dello Spessore di Controllo per Dentature Esterne a Evolvente", *Rassegna Internazionale di Meccanica*, n.5/6, Maggio-Giugno, 1968.
4. HENRIOT, G. *Traité Théorique et Pratique des Engrenages*, Tome II, Paris, Dunod, 1961, and other edit.
5. "AGMA Standard for Rating The Pitting Resistance and Bending Strength of Spur and Helical Involute Gear Teeth", AGMA 218.01, Dec., 1982.
6. "Deuxième avant-projet ISO/DP 6336/III, Calcul des Tensions au Pied de Dent", ISO/TC60 424F, 1981.
7. "Grundlagen für die Tragfähigkeitsberechnung von Gerad- und Schrägstirnrädern, Berechnung der Zahnfusstragfähigkeit", Entwurf DIN 3990, Teil 3, März, 1980.
8. WINTER, H., and WIRTH, X. "Einfluss von Schleifkerben auf die Zahnfussdauertragfähigkeit oberflächengehärteter Zahnräder", *Antriebstechnik* 17 (1978) Nr. 1-2, pp. 37-41.
9. WINTER, H., and HIRT, M. "The Measurement of Actual Strains at Gear Teeth, Influence of Fillet Radius on Stresses and Tooth Strength", *Jr. of Eng. for Industry, Trans. ASME*, Feb. 1974, pp. 33-40.
10. "Underlying Theory for the Maag 0° Grinding Method," Maag Zahnräder A.G., Zürich, 956.801/00.01.
11. COLBOURNE, J.R. "The Design of Undercut Involute Gears", Proc. of the Int'l. Power Transm. & Gearing Conf., San Francisco, 1980, ASME Paper No. 80-C2/DET-67.
12. KASUBA, R., and EVANS, J.W. "An Extended Model for Determining Dynamic Loads in Spur Gearing", *Jr. of Mech. Design, Trans. ASME*, Vol. 103, Apr, 1981, pp. 398-409.
13. MURRELL, P.W. "Developments in High Powered Marine Epicyclic Gearing, 30,000 S.H.P. – Prototype Trials Results", Proc. of the Int. Symp. on Gearing and Power Transm., Tokyo, 1981.
14. BLOCH, P., "Deformazioni da Trattamento Termico", Proc. of the 3ª Giornata dell'Ingranaggio, Milan, 1978.
15. CASTELLANI, G., "Il Calcolo Delle Ruote Dentate", Ediz. Rivista di Meccanica, Milan, 1962.

Appendix A – Fillet Coordinates

Nomenclature

This nomenclature is an addition to the general one.

h_{aG}	addendum of the grinding wheel
O	actual gear center
r	reference radius
r_b	base radius
r_{ys}	radius at a tooth chord
s_t	reference arc thickness in the transverse section
$\bar{s}_{ty}$	transverse chordal thickness
$\bar{s}_{yN}$	tooth thickness normal to local helices (ellipse chord)
u, w	coordinates of the center of the tip edge radius of the generating rack
u', w'	coordinates of a point of the tip edge arc of the generating rack
x_{g0}	actual coefficient of the addendum modification at cutting
x_g	actual coefficient of the final addendum modification, here for ground gears
α_t	transverse reference pressure angle
β_b	base helix angle
δ	angle between a fillet tangent and the tooth axis in the transverse section, or in general $\delta = \nu_t - \mu$
μ	rotation angle
ν	angle between the radius vector of a fillet point and the generating line of tool or grinding wheel

Subscripts

G referring to grinding
n normal to generating rack
t transverse
y referring to a generic cylinder

Tooth data referred to grinding. A given pressure angle, $\alpha_{nG} \neq \alpha_n$, can be adopted when grinding, provided that the basic geometric parameters of the tooth flank, r_b and β_b, remain the same and that we obtain the desired tooth thickness. The reference tooth parameters become r_G, β_G, m_{nG}, α_{tG} and the usual gear formulae apply. As in Reference 15

$$\cos\alpha_t/\cos\beta = \cos\alpha_n/\cos\beta_b \tag{1}$$

We have similarly

$$\cos\alpha_{tG}/\cos\beta_G = \cos\alpha_{nG}/\cos\beta_b \tag{2}$$

and we deduce that the normal module relating to grinding depends solely on the given pressure angle:

$$m_{nG} = m_n \cos\alpha_n/\cos\alpha_{nG} \tag{3}$$

As for the helix angle itself, from Reference (15) we deduce

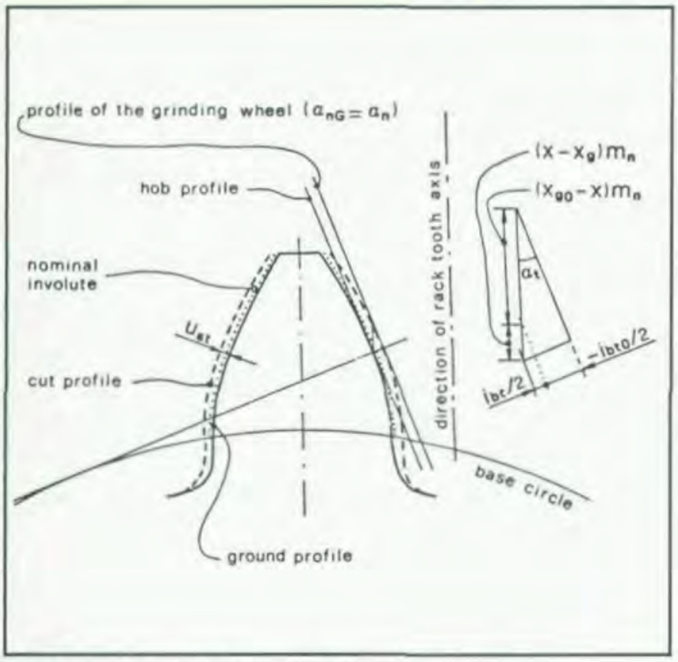

Fig. 11 – Thickness "reductions" in the transverse section.

for a generic cylinder:

$$\sin\beta_b = \sin\beta_y \cos\alpha_{ny} \tag{4}$$

Hence,

$$\beta_G = \arcsin(\sin\beta \cos\alpha_n / \cos\alpha_{nG}) \tag{5}$$

$$r_G = z\, m_{nG}/(2 \cos\beta_G) \tag{6}$$

Coefficients of the addendum modification. The so-called "addendum modification" is the distance between reference and generating lines of the generating rack and is positive if the reference line is external with respect to the generating line. This may seem a simple concept, but when entering the details of cut and ground profiles we must distinguish not less than four values of the addendum modification (none of which is the true modification of the addendum, except for particular cases).

The nominal addendum modifications $x\ m_n$ refer to nominal gear pairs without tooth backlash; i.e., to the dotted involute in Fig. 11.

(Note that it is just a convention to refer the addendum modification coefficient to the normal module; thus, we can maintain it when considering the transverse gear section.)

A reduction i_{bt} of the transverse base thickness is usually adopted to contribute to the tooth backlash for the operating gear pair. Then the final generating addendum modification is

$$x_g\, m_n = x\, m_n - i_{bt}/(2 \sin\alpha_t) \tag{7}$$

Let us assume for the moment that $\alpha_{nG} = \alpha_n$. If the grinding wheel is inclined by β, the tangents to the base cylinder, normal to the tooth flank, are inclined by β_b with respect to the gear axis. Then,

$$i_{bn} = i_{bt} \cos\beta_b \tag{8}$$

and

$$x_g = x - (i_{bn}/m_n)/(2 \sin\alpha_n) \tag{9}$$

as in Reference (15).

$$\sin\alpha_t = \sin\alpha_n / \cos\beta_b \tag{10}$$

Tooth cutting must leave a grinding stock

$$u_s = (i_{bn} - i_{bn0})/2 \tag{11}$$

which defines the value of i_{bn0}, usually negative, because it is defined as a "reduction" of normal base thickness for purposes of generalization. Thus a formula similar to Equation 9 applies for a coefficient relating to cutting:

$$x_{g0} = x - (i_{bn0}/m_n)/(2 \sin\alpha_n) \tag{12}$$

If we grind the teeth by a pressure angle $\alpha_{nG} \neq \alpha_n$, the total addendum modification is $x_{gG}\ m_{nG} \neq x_g\ m_n$ as it refers to $r_G \neq r$. The condition that the transverse reference tooth thickness remains the same can be applied to calculate x_{gG}. Since $s_{tG} = s_t$,

$$s_t = (\pi/2 + 2\, x_g \tan\alpha_n)\, m_n/\cos\beta \tag{13}$$

and

$$x_{gG} = (s_t \cos\beta_G/m_{nG} - \pi/2)/(2 \tan\alpha_{nG}) \tag{14}$$

Thus, the formulae regarding addendum modifications also extend to the grinding conditions.

Note that the tip diameter remains dependent on the nominal x:

$$d_{al} = m_n\, z/\cos\beta + 2\, m_n\, (h_{ar}/m_n + x - k_{sl}) \tag{15}$$

where d_{al} is meant for the contact limit towards the tooth tip that may be affected by "semitopping," and d_{al} is somewhat arbitrary because it depends on our choice of a tooth shortening coefficient, k_{sl}.

Positioning of the grinding wheel. Unlike the tip radius, the root radius depends on the actual generating conditions. Tooth roots usually are not completely ground in industrial gears so that

$$r_f = m_n\, z\, (2 \cos\beta) - h_{a0} + x_{g0}\, m_n \tag{16}$$

whereas, the tip of the grinding wheel generates a "root circle" entirely or partly fictitious:

$$r_{fG0} = m_{nG}\, z/(2 \cos\beta_G) - h_{aG} + x_{gG}\, m_{nG} \tag{17}$$

The addendum of the grinding wheel, h_{aG}, is defined similarly to the tool addendum, h_{a0}, if the grinding wheel operates on both flanks at the same time. More often it grinds one flank at a time. Then we assume r_{fG0} directly by positioning the grinding wheel at a distance, $r_{fG0} - r_f$, from the tooth root. Then h_{aG} becomes fictitious and is defined inversely by Equation 17.

Generation of the tooth fillets. The coordinates of point S in the normal section of a hob or of a rack cutter, Fig. 12, are given by Equation 31 and Equation 17 of Reference (1).

By using the present symbols, with $m_n \neq 1$:

$$\begin{cases} u_n = \dfrac{\pi m_n}{4} + h_{a0} \tan\alpha_n + \delta_{a0} \tan \dfrac{\pi/2 - \alpha_n}{2} - \dfrac{u_0}{\cos\alpha_n} & (18) \\[2ex] w = h_{a0} - x_{g0}\, m_n - \delta_{a0} & (19) \end{cases}$$

Let F be a contact point of the fillet with the generating rack. Its position is defined in the transverse section of the generated gear by the angle ν_t that we assume as an independent parameter. (Fig. 13.) The fillet field is defined by

$$\nu_t \lim \leqslant \nu_t \leqslant \pi/2 \tag{20}$$

where $\pi/2$ means the limit point between root circle and fillet, and ν_t lim corresponds to the limit between fillet and involute. For non-undercut teeth, $\nu_t \lim = \alpha_t$, whereas for undercut ones, the intersecting between fillet and involute must be determined by iteration. If the tool has protuberance, the tooth is always undercut. Otherwise undercut arises if x_{g0} is less than the limit value.

$$x_{g0\ \lim} = \frac{h_{a0} - \delta_{a0}\,(1 - \sin\alpha_n)}{m_n} - \frac{z \sin^2\alpha_t}{2 \cos\beta} \tag{21}$$

Such a condition assumes that the limit point of the straight profile of the rack generates the involute, beginning exactly from the base circle.

An angle such that

$$\begin{cases} \nu_n = \arctan\,(\tan\nu_t \cos\beta) & \text{if } \nu_t < \pi/2 \\ \nu_n = \pi/2 & \text{if } \nu_t = \pi/2 \end{cases} \tag{22}$$

corresponds to ν_t in the normal section of the rack in Fig. 12, and defines the coordinates of point F in the axis set of the rack.

$$\begin{cases} u'_n = u_n - \delta_{a0} \cos\nu_n & (23) \\ w' = w + \delta_{a0} \sin\nu_n & (24) \end{cases}$$

Now we come back to the transverse section of both gear and generating rack, inclined by β with respect to the normal section of the rack, and we have

$$u'_t = u'_n/\cos\beta \tag{25}$$

In Fig. 13, $u'_t = \overline{JK}$, $\widehat{GC_0} = \overline{JC_0}$ and we obtain the rotation angle of the tooth

$$\mu = (u'_t + w' \cot\nu_t)/r \tag{26}$$

By assuming

$$\delta = \nu_t - \mu \tag{27}$$

the coordinates of the point, F, in the axis set of the gear tooth, are

$$\begin{cases} \bar{s}_{ty}/2 = r \sin\mu - \dfrac{w'}{\sin\nu_t} \cos\delta & (28) \\ r_{ys} = r \cos\mu - \dfrac{w'}{\sin\nu_t} \sin\delta & (29) \end{cases}$$

In the case of a grinding wheel (Fig. 14) the coordinates of the point S are

$$\begin{cases} u_{nG} = \pi m_{nG}/4 + h_{aG} \tan\alpha_{nG} + \varrho_{aG} \tan \dfrac{\pi/2 - \alpha_{nG}}{2} & (30) \\ w_G = h_{aG} - x_{gG}\, m_{nG} - \varrho_{aG} & (31) \end{cases}$$

(continued on page 47)

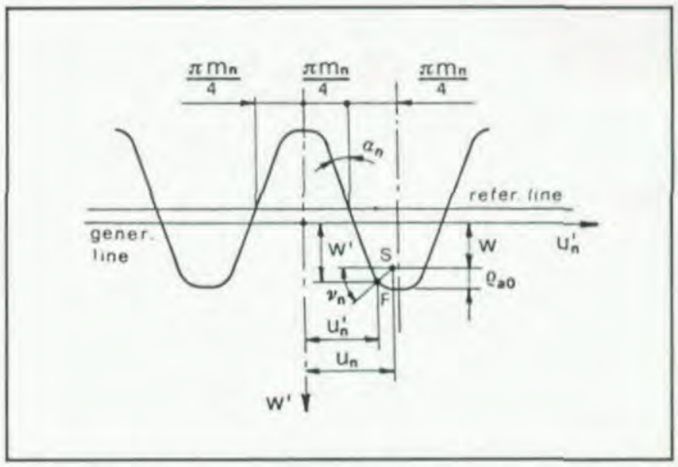

Fig. 12—Data of the generating point F on the rack in the normal section.

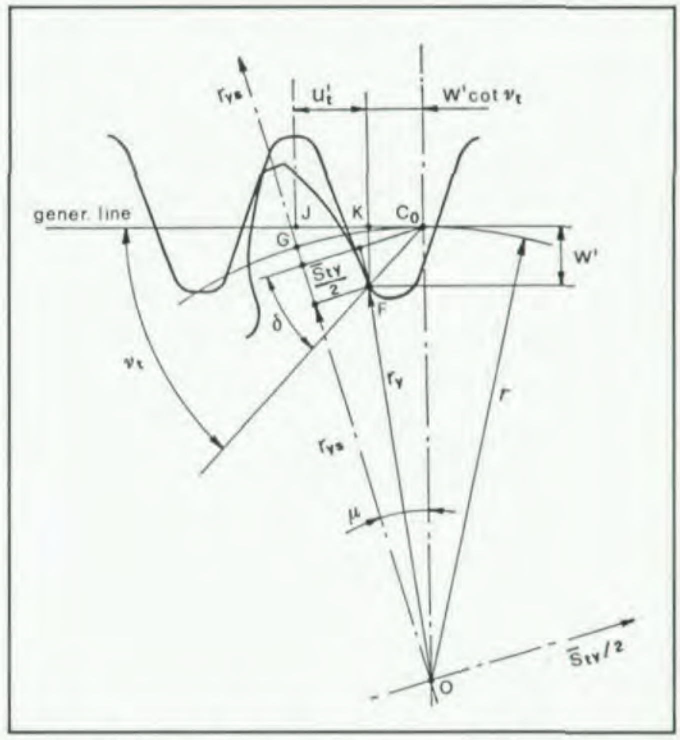

Fig. 13—Calculation of the coordinates of a Point F of the tooth fillet in a transverse section.

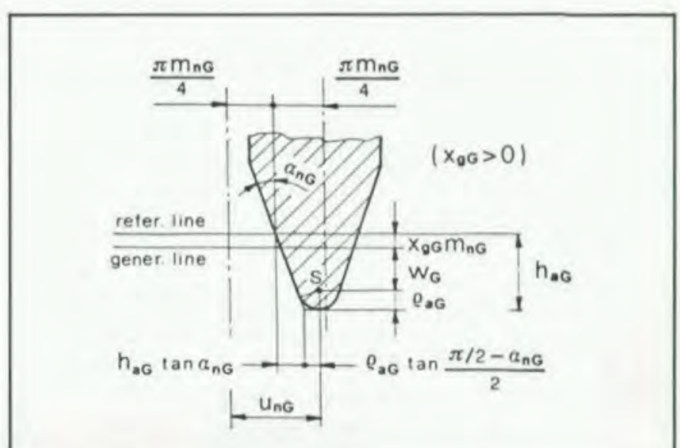

Fig. 14—Data of a rack-like grinding wheel.

BACK TO BASICS...

Spur Gear Fundamentals

Uffe Hindhede
Black Hawk College
Moline, IL

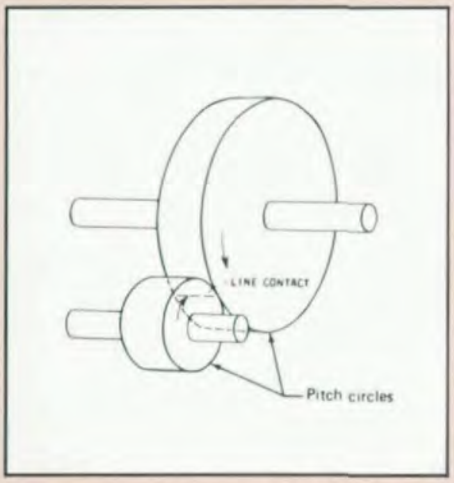

Fig. 1 – Friction wheels on parallel shafts. (Courtesy Mobil Oil Corporation.)

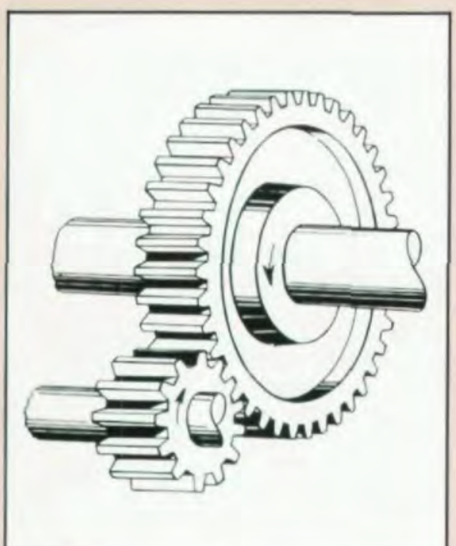

Fig. 2 – Spur gears. The teeth of these gears are developed from blank cylinders. (Courtesy Mobil Oil Corporation.)

Gears are toothed wheels used primarily to transmit motion and power between rotating shafts. Gearing is an assembly of two or more gears. The most durable of all mechanical drives, gearing can transmit high power at efficiencies approaching 0.99 and with long service life. As precision machine elements gears must be designed, manufactured and installed with great care if they are to function properly.

Relative shaft position – parallel, intersecting or skew – accounts for three basic types of gearing, each of which can be studied by observing a single pair. This article will discuss the fundamentals, kinematics and strength of gears in terms of spur gears (parallel shafts), which are the easiest type to comprehend. Spur gears compose the largest group of gears, and many of their fundamental principles apply to the other gear types.

Function and Design

Probably the earliest method of transmitting motion from one revolving shaft to another was by contact from unlubricated friction wheels (Fig. 1). Because they allow no control over slippage, friction drives cannot be used successfully where machine parts must maintain contact and constant angular velocity. To transmit power without slippage, a positive drive is required, a condition that can be fulfilled by properly designed teeth. Gears are thus a logical extension of the friction wheel concept (Fig.2).

Gears are spinning levers capable of performing three important functions. They can provide a positive displacement coupling between shafts, increase, decrease or maintain the speed of rotation with accompanying change in torque, and change the direction of rotation and/or shaft arrangement (orientation).

To function properly, gears assume various shapes to accommodate shaft orientation. If the shafts are parallel, the basic friction wheels and gears developed from them assume the shape of cylinders (Fig. 3a). When the shafts are intersecting, the wheels become frustrums of cones, and gears developed on these conical surfaces are called bevel gears (Fig. 3b). When the shafts cross (skew, one above the other), the friction wheels may be cylindrical or of hyperbolic cross section (Fig. 3c). In addition, a gear is sometimes meshed with a toothed bar called a rack (Fig. 3a), which produces linear motion. Besides shaft position and tooth form, gears may be classified according to:

System of Measurement. Pitch (EU) or module (*SI*).
Pitch. Coarse or fine.
Quality. Commerical, precision and ultraprecision or tolerance classifications per AGMA 390.03.

Law of Gearing

Gears are provided with teeth shaped so that motion is transmitted in the manner of smooth curves rolling together without slipping. The rolling curves are called pitch curves because on them the pitch or tooth spacing is the same for both engaging gears. The pitch curves are usually circles or straight lines, and the motion transmitted is either rotation or straight-line translation at a constant velocity.

Mating tooth profiles, as shown in Fig. 4, are essentially a pair of cams in contact (back to back). For one cam to drive another cam with a constant angular displacement ratio, the common normal at the point of contact must at all times intersect the line of centers at the pitch point. This fixed point is the point of tangency of the pitch circles. To ensure continuous contact and the existence of one and only one normal at each point of contact, the camlike tooth profiles must be continuous differentiable curves.

AUTHOR:

UFFE HINDHEDE *is an Associate Professor in the Engineering Related Technology Department at Black Hawk College, Moline, Illinois. He is a graduate of the Technical University of Denmark and the University of Illinois. Hindhede has authored several technical papers and articles and he is the principal author of* Machine Design Fundamentals.

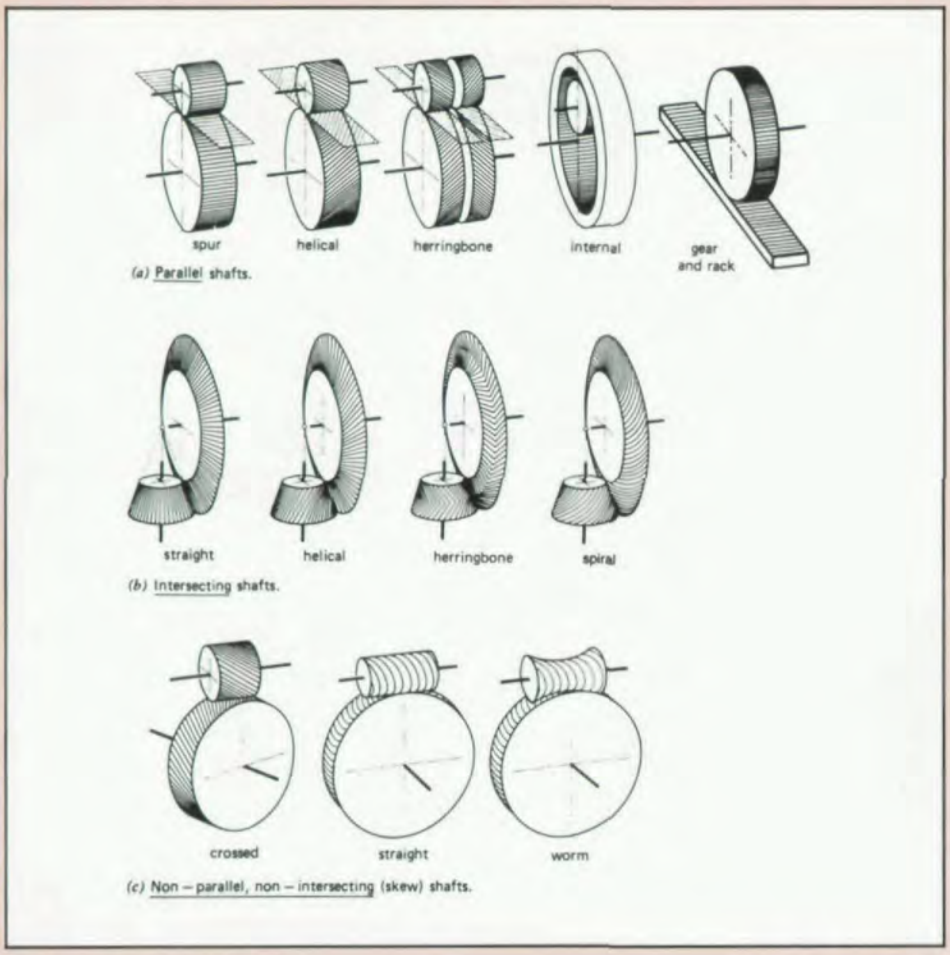

Fig. 3 – Important types of gears.

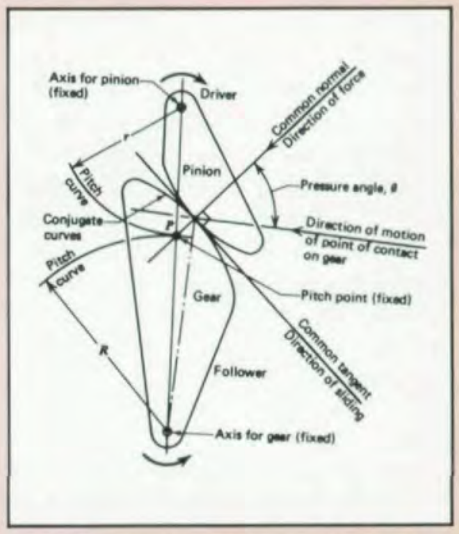

Fig. 4 – Two cams showing the law of gearing. The common normal must, for all useful positions, go through the fixed point P.

Mating cam profiles that yield a constant angular displacement ratio are termed conjugate. Although an infinite number of profile curves will satisfy the law of gearing, only the cycloid and the involute have been standardized. The involute has several advantages; the most important is its ease of manufacture and the fact that the center distance between two involute gears may vary without changing the velocity ratio.

Nomenclature

- a = addendum
- b = dedendum
- B = backlash, linear measure along pitch circle
- C = center distance
- C_v = velocity factor
- D = pitch diameter of gear
- d = pitch diameter of pinion
- D_b = base diameter of gear
- d_b = base diameter of pinion
- D_o = outside diameter of gear
- d_o = outside diameter of pinion
- D_r = root diameter of gear
- d_r = root diameter of pinion
- F = face width
- h = effective height (parabolic tooth)
- h_t = whole depth (tooth height)
- L = lead (advance of helical gear tooth in 1 revolution)
- $L_p(L_G)$ = lead of pinion (gear) in helical gears
- M = measurement over pins
- m = module
- m_f = face contact ratio
- m_G = gear or speed ratio ($m_G = N_G/N_p$)
- m_n = normal module
- m_p = profile contact ratio
- m_t = total contact ratio
- $N_p(N_G)$ = number of teeth in pinion (gear)
- N_c = critical number of teeth for no undercutting
- $n_p(n_G)$ = speed of pinion (gear)
- p_a = axial pitch
- p_b = base pitch (equals normal pitch for helical gears)
- p_c = circular pitch
- P_d = diametral pitch
- P_n = normal diametral pitch of helical gear
- p_n = normal circular pitch of helical gear
- R = pitch radius gear
- r = pitch radius pinion
- $r_b(R_b)$ = base radius of pinion (gear)
- $r_o(R_o)$ = outside radius of pinion (gear)
- S_e = endurance limit
- t_c = circular tooth thickness (theoretical)
- t = tooth thickness at root
- v = pitch line velocity
- W = tooth load, total
- W_a = axial load
- W_r = radial load
- W_t = tangential load
- y = tooth form factor
- Z = length of action
- $\emptyset$ = pressure angle
- $\emptyset_n$ = pressure angle in normal plane
- ψ = helix angle

Involute Gear Principles*

An involute curve is generated by a point moving in a definite relationship to a circle, called the base circle. Two principles are used in mechanical involute generation. Figs. 5a and 5b show the principle of the fixed base circle. In this method the base circle and the drawing plane in which the involutes are traced remain fixed. This is the underlying principle of involute compasses and involute dressers (where the motion of a diamond tool gives an involute profile to grinding wheels).

The second principle, that of the revolving base circle, is used in generating involute teeth by hobbing, shaping, shaving and other finishing processes (Fig. 5c). This method is employed primarily where the generating tool and the gear blank are intended to work with each other like two gears in mesh for purposes of gear manufacturing.

Cord Method. In using this method the involute path is traced by a taut, inextensible cord as it unwinds from the circumference of the fixed base circle (Fig. 6). The radius of curvature starts at zero length on the base circle and increases steadily as the cord unwinds. After one revolution, the radius of curvature equals the circumference of the base circle (πD_b). *It is significant that the radius of curvature to any point is always tangent to the base circle and normal to one and only one tangent on the involute.*

From Fig. 6 it can be seen that the full involute curve is a spiral beginning at the base circle and having an infinite number of equidistant coils (distance πD_b). However, only a small part of the innermost cord is used in gearing. The character of the involute near the base reveals the existence of a cusp at point 0 and a second branch of the involute going in the opposite direction (shown as a dash-dot curve). The second branch serves, as we will see later, to form the back side of the gear tooth after a space is left for a meshing tooth.

Properties of the Involute. The following properties can be seen in Fig. 6.

1. Any tangent to the base circle is always normal to the involute.
2. The length of such a tangent is the radius of curvature of the involute at that point. The center is always located on the base circle.
3. For any involute there is only *one* base circle.
4. For any base circle there is a family of equivalent involutes, infinite in number, each with a different starting point.
5. All involutes to the same base circle are similar (congruent) and equidistant; for example, the distance of any two of such involutes in normal direction is constant πD_b (Fig. 6).
6. Involutes to different base circles are geometrically similar (Fig. 7). That is, corresponding angles are equal, while corresponding lines, curves or circular sections are in the ratio of the base circle radii. Thus, when the radius of the base circle approaches infinity, the involute becomes a straight line. Geometric similarity explains why the teeth of a large gear can mesh properly with those of a small gear.

Involutes in Contact. Mathematically, the involute is a continuous, differentiable curve; that is, it has only one tangent and only one normal at each point. Thus, two involutes in contact (back to back) have one common tangent and one common normal (Fig. 8). This common normal, furthermore, is a common tangent to the base circles. Since this normal for all positions intersects the centerline at a fixed point, conjugate motion is assured. Thus conjugate motion is the term used to describe this important characteristic of involute gear action.

The action portrayed is that of two oversize gear teeth in contact. The oversized teeth are the result of using too large a center distance. This situation is presented only for reasons of clarity.

When two involute gear teeth move in contact, there is a positive drive imparted to the two shafts passing through the base circle centers, thus ensuring shaft speeds proportional to the base circle diameters. This is equivalent to a positive drive imparted by an inextensible connecting cord as it winds onto one base circle and unwinds from the other. It is analogous to a pulley with a crossed belt arrangement. Note that the surfaces of both involutes at the point of contact are moving in the same direction.

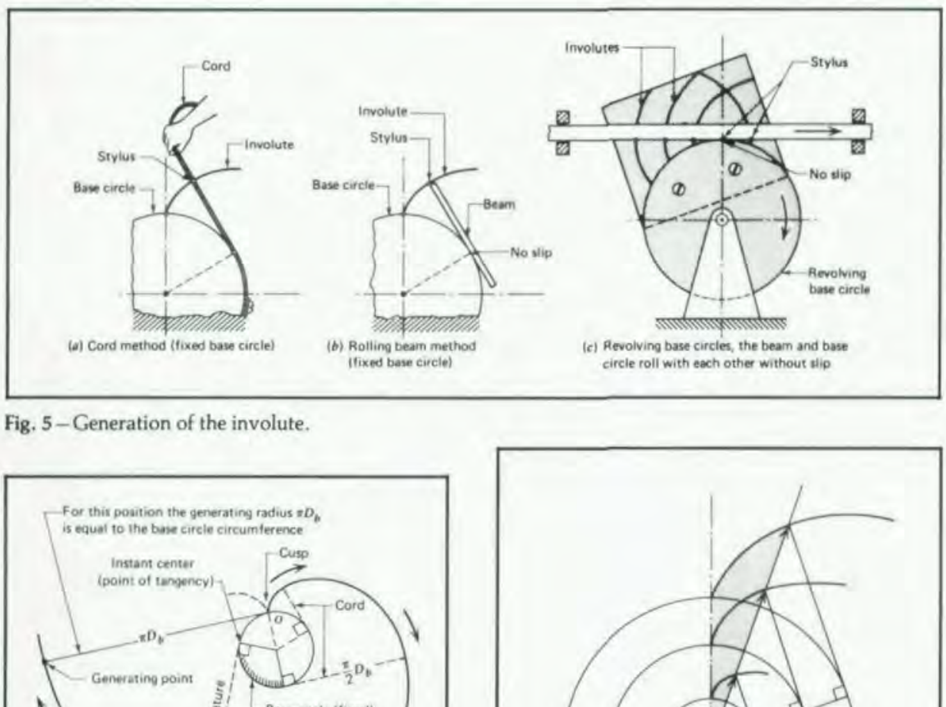

Fig. 5 – Generation of the involute.

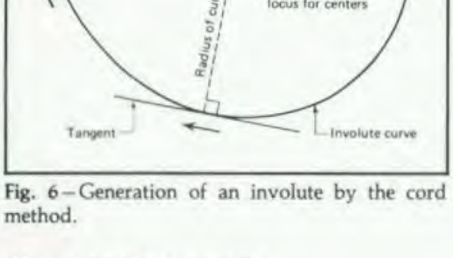

Fig. 6 – Generation of an involute by the cord method.

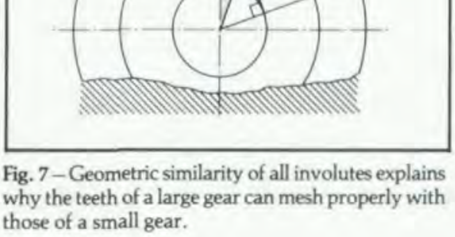

Fig. 7 – Geometric similarity of all involutes explains why the teeth of a large gear can mesh properly with those of a small gear.

*The material in the following three sections was in part extracted from a gear manual formerly used at International Harvester, Farmall Works, courtesy Robert Custer and Frederick Brooks.

A rack is a gear with its center at infinity. It is a simplified gear in which all circles concentric with the base circle and all involutes have become straight lines. A rack therefore has a baseline and a linear tooth profile.

Relationship of Pitch and Base Circles. Referring to Fig. 8, we find that triangles QC_1O_1 and QC_2O_2 are similar. Therefore

$$\cos \emptyset = \frac{r_b}{r} = \frac{R_b}{R} \qquad (1)$$

where

r_b, R_b = base circle radius of pinion and gear, respectively; mm, in.
r, R = pitch circle radius of pinion and gear, respectively; mm, in.

Also,

$$\cos \emptyset = \frac{d_b}{d} = \frac{D_b}{D} \qquad (2)$$

where

d_b, D_b = base diameters of pinion and gear, resepectively; mm, in.
d, D = pitch diameters of pinion and gear, respectively; mm, in.

Fig. 9 shows the smaller of the two gears in Fig. 8 meshing with a rack (obtained by moving the center of the larger gear to infinity). The rack is represented by a single tooth that can move horizontally, as shown. If the involute is turned counterclockwise the "rack" will move to the right because of a horizontal force component. The motion of rack and pinion is conjugate because the pitch point has not changed and the normal to the rack tooth goes through this point.

The Mechanics of Involute Teeth

Effect of Changing Center Distance. Fig. 10 shows the same two involutes as in Fig 8 brought into contact through appropriate rotation on a reduced center distance (2"). Consequently:

- A new pitch point was established.
- The pressure angle was reduced from 70 to 50° (still large by normal standards).
- The line of action was shortened.
- The pitch diameters were reduced (halved), but their ratio remained unchanged (similar triangles).

The speed ratios are not affected by altering center distance because they are functions of base radii only. The two triangles (crosshatched) remain similar, regardless of center distance alterations. Furthermore, two corresponding sides, the base radii, do not change; hence, the ratio of pitch radii *cannot* change.

Rolling and Sliding Action Between Contacting Involutes. Fig. 11a returns the two involutes from Fig. 8 to their former, larger center distance (4"), but in a different relative position — the only position for which corresponding arc lengths are equal (arc 12 = arc 12'). By the belt analogy, an equal length of cord has been exchanged between the smaller base cylinder of the pi-

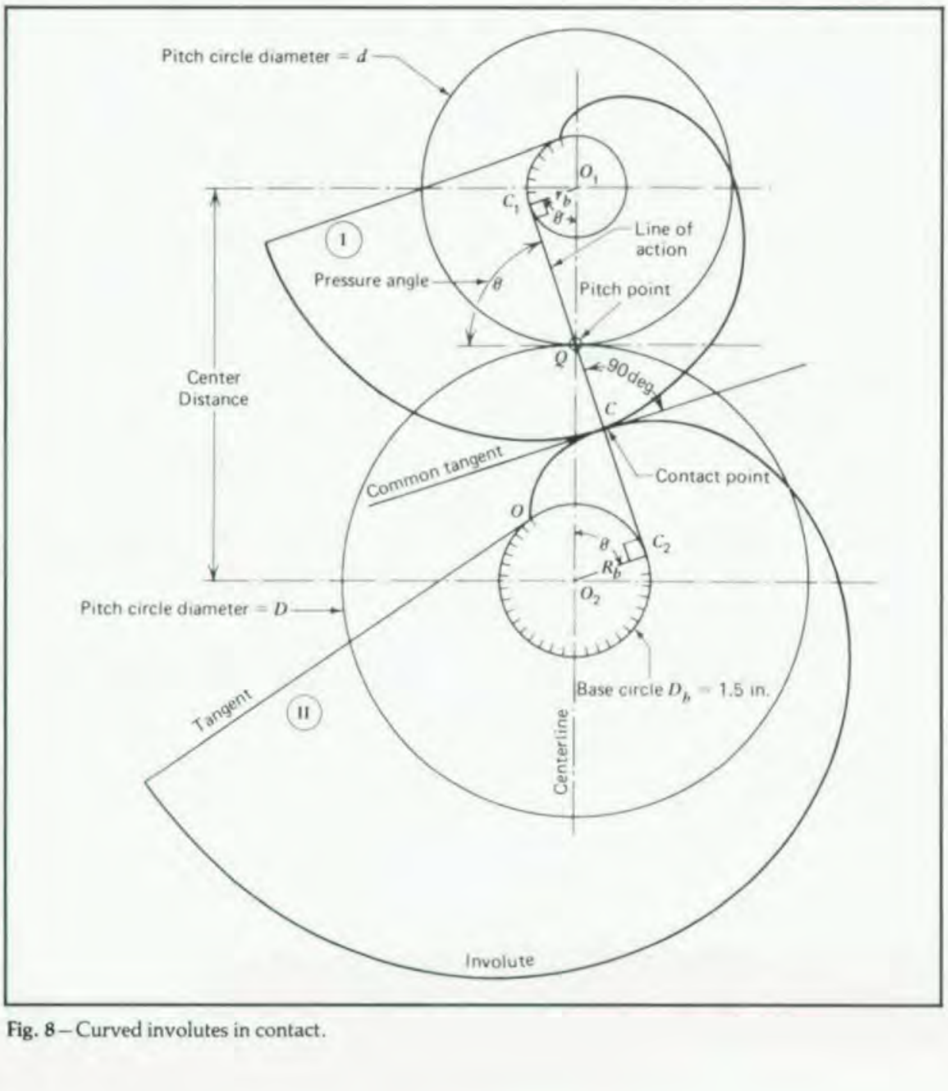

Fig. 8 — Curved involutes in contact.

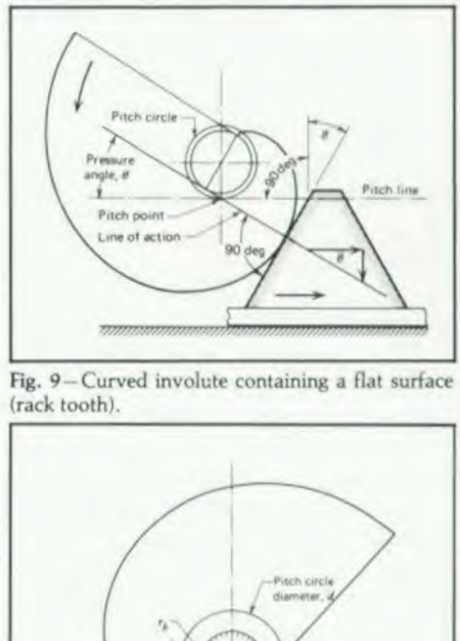

Fig. 9 — Curved involute containing a flat surface (rack tooth).

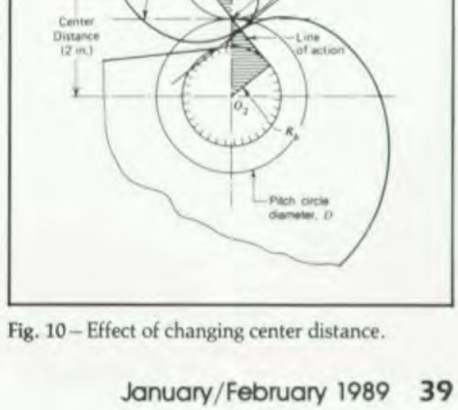

Fig. 10 — Effect of changing center distance.

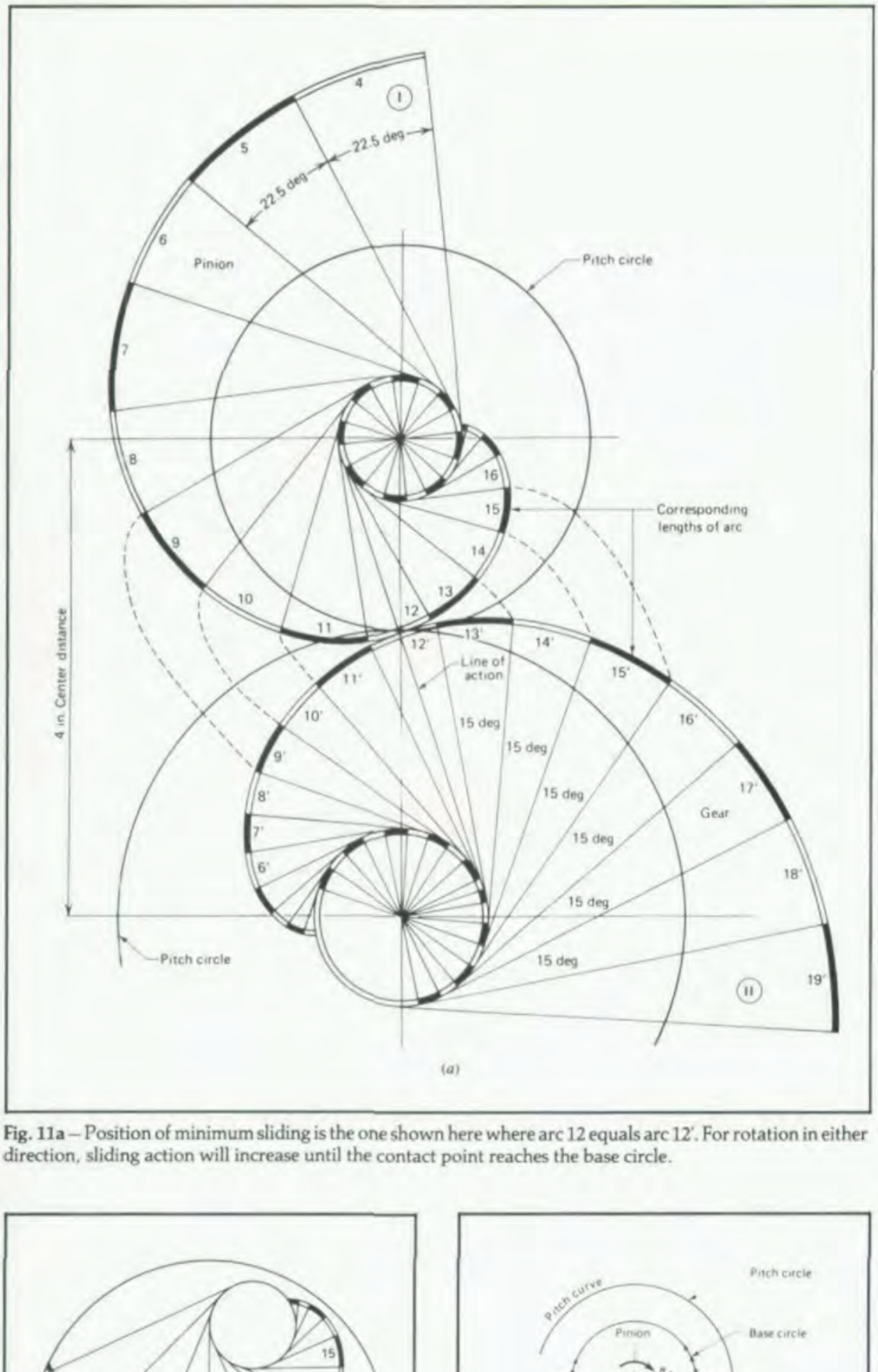

Fig. 11a – Position of minimum sliding is the one shown here where arc 12 equals arc 12'. For rotation in either direction, sliding action will increase until the contact point reaches the base circle.

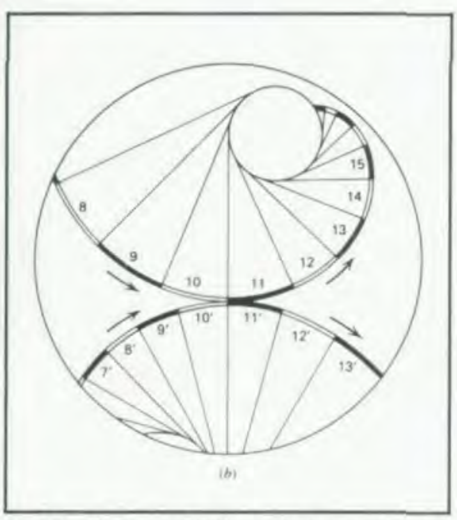

Fig. 11b – Rolling and sliding action between two involutes on fixed centers. Contact between arcs 10 and 10' involves much sliding, since arc 10 is almost one-third longer than arc 10'.

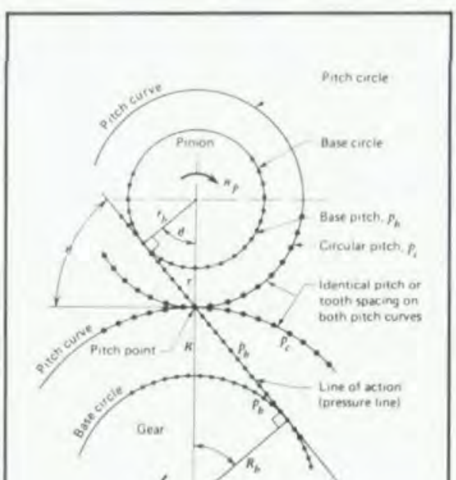

Fig. 12 – Gear geometry and terminology.

nion and the larger base cylinder of the gear. The angular but equal displacements of the gear are, therefore, smaller than those of the pinion by a ratio of 1:1.5.

For clarity, the angular increments of the pinion were chosen at 22.5°, making those of the gear 15° The length of arc corresponding to each pair of increments will be in contact during rotation. However, since each pair varies in length, the rolling motion of one involute on another inevitably must be accompanied by sliding because the time elapsed to cover corresponding but unequal lengths is the same.

For counterclockwise rotation of the pinion, the lengths of arc 11, 10, 9 and so forth, will be in synchronized contact with the arc 11', 10', 9' and so on (Fig. 11b). The former steadily increase in length, but the latter steadily decrease in length, making sliding inevitable. Rotation in opposite direction produces the same effect, but this time gear teeth have the greater surface speed. Maximum sliding takes place when the point of contact is close to either base circle. Thus, in gearing, only a small section of any involute is useful if sliding is to be minimized.

Gear Terminology

Basic Terminology. To make further discussion more meaningful, geometric quantities resulting from involute contact will now be defined, discussed and assigned nomenclature, as shown in Figs. 12-14.

Pinion. A pinion is usually the smaller of two mating gears. The larger is often called the gear.

Center distance (C). The distance between the centers of the pitch or base circles.

$$C = 0.5(D + d) \tag{3}$$

where

D = pitch diameter of gear
d = pitch diameter of pinion

Base circle. The circle from which an involute tooth curve is developed.

Base Pitch. (p_b). The pitch on the base circle (or along the line of action) corresponding to the circular pitch.

Pitch Circle. Since the pitch point is fixed, only two circles, each concentric with a base circle, can be drawn through the pitch point. These two imaginary circles, tangent to each other, are the pitch circles. They are visualized as rolling on each other, without sliding, as the base circles rotate in conjugate motion.

The ratio of pitch diameters is also that of the base diameters (similar triangles). Because the pitch circles are tangent to each other, they are used in preference to the base circles in many of the calculations. Note that pitch circles must respond to any center distance variation for a meshing gear pair by enlarging or contracting. In contrast, the base circles never change size.

Circular Pitch (p_c). The identical tooth spacing on each of the two pitch circles.

Pressure Angle (ϕ). The pressure angle lies between the common tangent to the pitch circles and the common tangent to the base circles, shown exaggerated in Fig. 8. The pressure angle is also the acute angle between the common normal and the direction of motion, when the contact point is on the centerline. Since a pair of meshing gear teeth is, in essence, a pair of cams in contact, the pressure angle of gearing is identical to the one encountered in cam design. The pressure angle of contacting involutes, as opposed to the one on cams, is constant throughout its entire cycle, a feature of great practical importance.

Line of Action. This is the common tangent to the base circles. Contact between the involutes must be on this line to give smooth operation. Force is transmitted between tooth surfaces along the line of action. Thus a constant force generates a constant torque.

Velocity Ratio (m_G). This ratio, also called speed ratio, is the angular velocity of the driver divided by the angular velocity of the driven member. Because the line of action cuts the line of centers into the respective pitch radii, the speed ratio becomes the inverse proportion of those distances and related quantities (e.g., base and pitch diameters).

Because most gears are designed for speed reduction, one generally finds the pinion driving the gear; from now on we will assume that this is the case. Therefore

$$m_G = \frac{n_P}{n_G} = \frac{D}{d} = \frac{N_G}{N_P} \qquad (4)$$

where

m_G = speed ratio (gear ratio)
n_p = speed of pinion; rpm

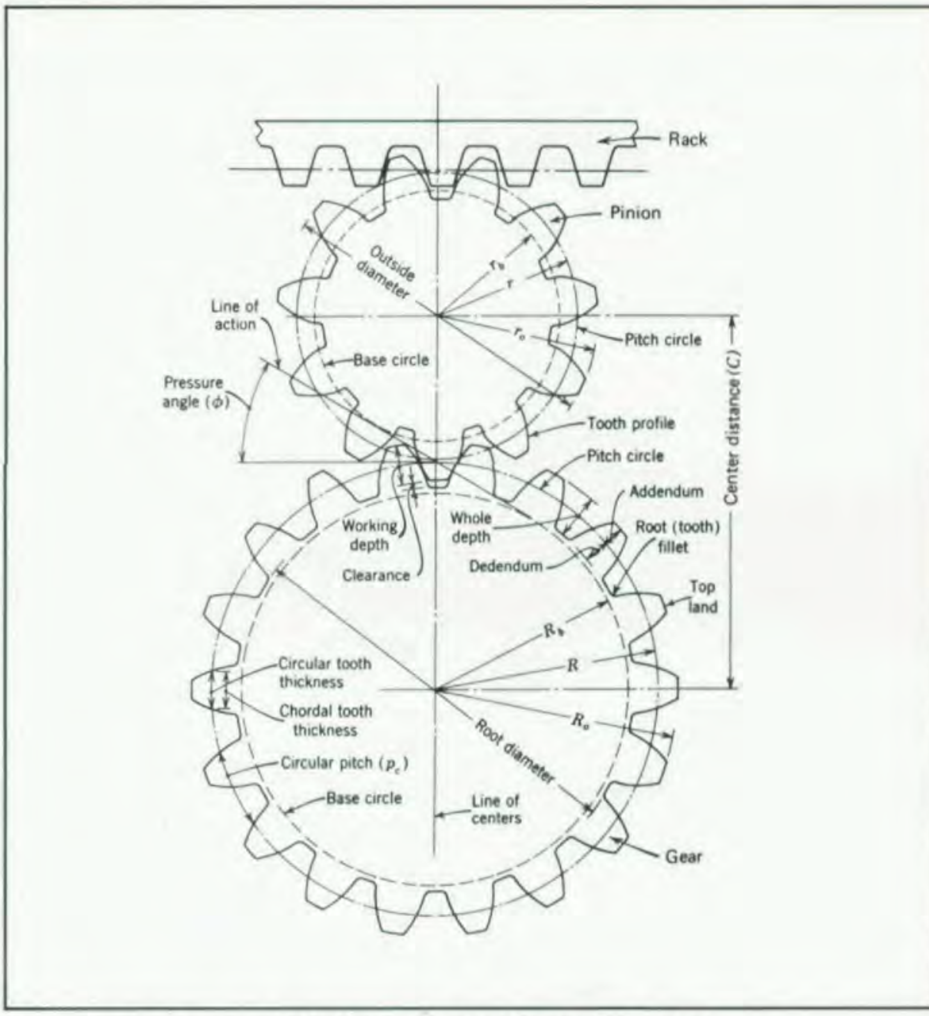

Fig. 13 – Spur gear geometry. (G. W. Michalec, *Precision Gearing*, Wiley, 1966.)

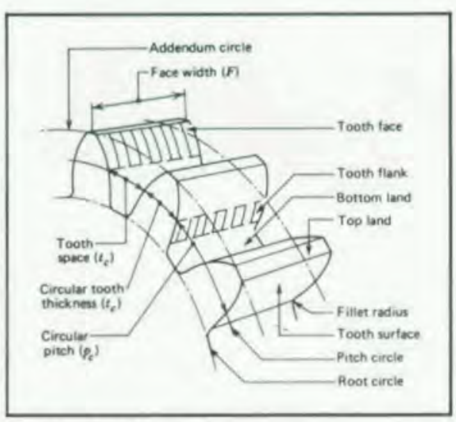

Fig. 14 – Tooth parts of spur gears.

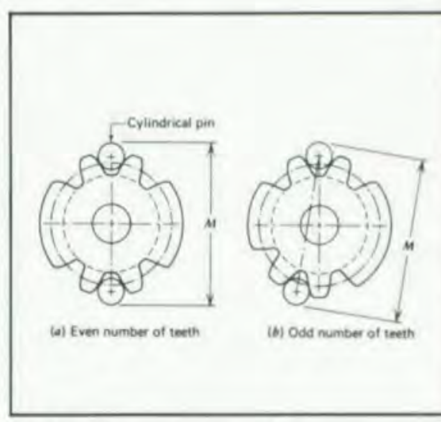

Fig. 15 – Measurement over pins.

n_G = speed of gear; rpm
D = pitch diameter of gear; mm, in.
d = pitch diameter of pinion; mm, in.
N_G = number of teeth in the gear
N_p = number of teeth in the pinion

In practice, speed ratios are determined principally from ratios of tooth numbers because they involve whole numbers only.

Tooth Parts. The following tooth parts are shown in Figs. 13 and 14.

Addendum. Height of tooth above pitch circle (Fig. 13).

Bottom land. The surface of the gear between the flanks of adjacent teeth (Fig. 14).

Dedendum. Depth of tooth below the

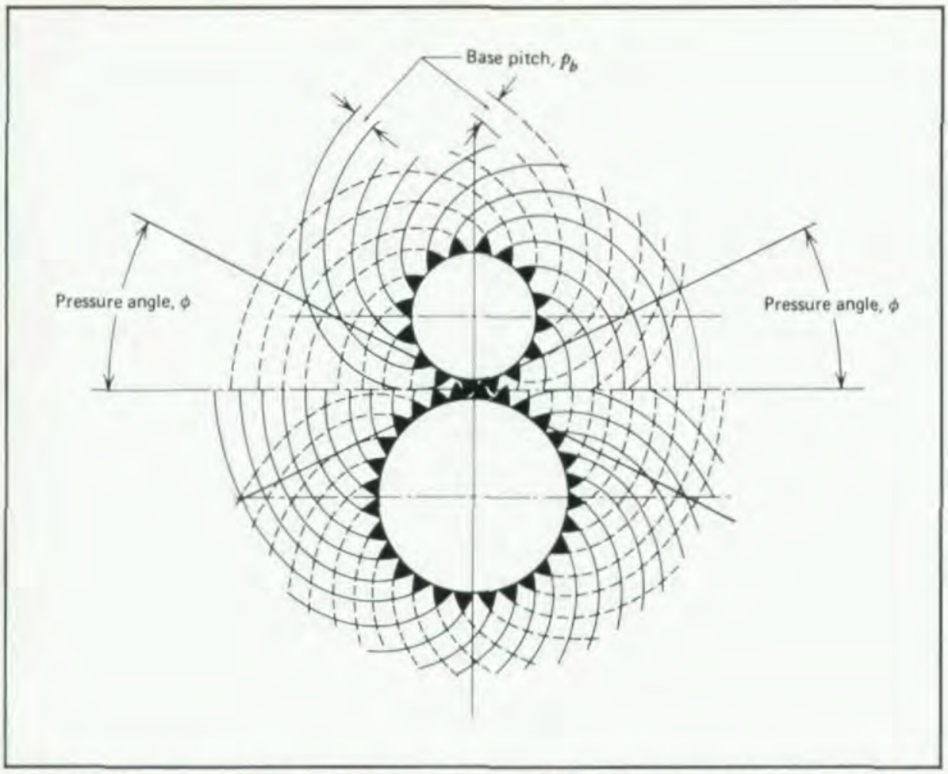

Fig. 16 – Involute gear teeth are generated by a series of symmetrical involutes oriented alternately in a clockwise and counterclockwise direction. For the two gears to mesh properly, they must have the same base pitch.

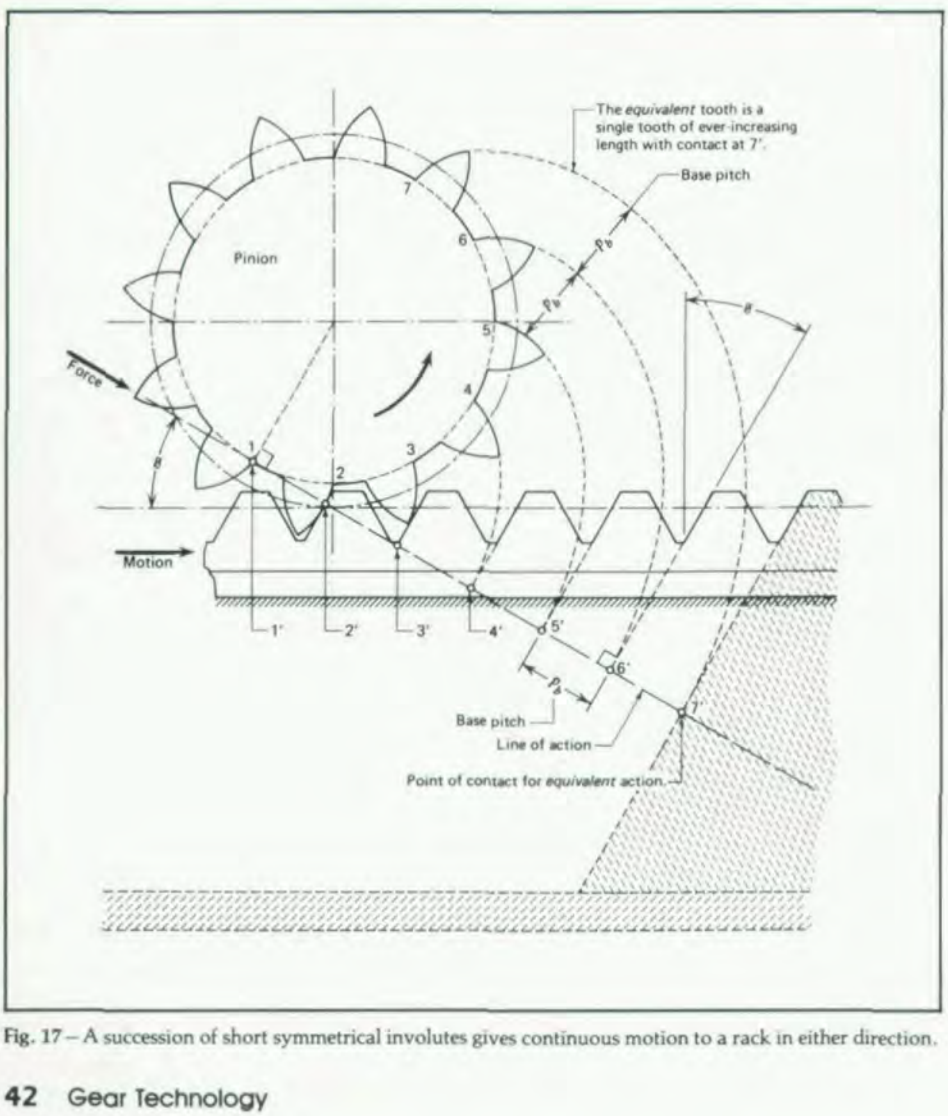

Fig. 17 – A succession of short symmetrical involutes gives continuous motion to a rack in either direction.

pitch circle (Fig. 13).

Face width (F). Length of tooth in axial direction (Fig. 14).

Tooth face. Surface between the pitch line element and top of tooth (Fig. 14).

Tooth fillet. Portion of tooth flank joining it to the bottom land. (Fig. 13).

Tooth flank. The surface between the pitch line element and the bottom land (Fig. 14).

Tooth surface. Tooth face and flank combined (Fig. 14).

Top land. The surface of the top of the tooth (Fig. 14).

Circular tooth thickness (t_c). This dimension is the arc length on the pitch circle subtending a single tooth. For equal addendum gears the theoretical thickness is half the circular pitch (Fig. 14).

Overpins measurements (M). The pitch circle is an imaginary circle; hence, pitch diameters cannot be measured directly. However, indirectly the pitch diameter of spur gears can be measured by the pin method. When spur gear sizes are checked by this method, cylindrical pins of known diameter are placed in diametrically opposite tooth spaces; or, if the gear has an odd number of teeth, the pins are located as nearly opposite one another as possible (Fig 15). The measurement M over these pins is then checked by using any sufficiently accurate method of measurement.

Involute Gear Teeth

So far we have considered only two profiles in contact. However, successive revolutions are merely successive contacts of two profiles. Fig. 16 shows how a series of symmetrical involute profiles, alternately clockwise and counterclockwise and with a tooth space allowed for meshing, will produce a complete set of pointed teeth. By using only the portion near the base circle, mating gear tooth profiles can be formed with two or more teeth in contact at all times, thus permitting continuous rotation in either direction.

Fig. 17 shows in greater detail the development of curved and straight teeth. Continuous motion of a rack necessitates a series of short, symmetrical, equally spaced involute teeth on the base circle circumference. The pitch, in this case, is named base pitch (p_b). Point 1 is the point of tangency for the line of action. Thus the distances 1-2, 2-3 and the like, measured along the base circle, are all equal; by definition, this is the base pitch. From points 2 to 7 involutes have been extended until they intersect the line of action, dividing it into distances equal to the base pitch. From the equidistant points 1′ to 7′, lines have been drawn perpendicular to the line of action. The full line portion represents one side of the rack.

As the gear rotates, the gear teeth will contact successive rack teeth in a continuous, overlapping motion. The force will be exerted along the line of action, causing the rack to move horizontally. The pressure angle, as shown, is the acute angle between the directions of force and motion.

When the gear rotates in the direction shown, the surface of an involute gear tooth contacts the flat-surfaced rack tooth. As rotation continues, the contact points move down the line of action away from the base circle. This continues until the tooth surfaces lose contact at the upper end of the line of action represented by the full line. Before contact is lost, another pair of teeth come into contact, thus providing continuous motion. This tooth action is equivalent to the action of a single tooth of ever-increasing length contacting one ever-increasing flat surface along an ever-increasing line of action. The outward motion of the involute originating at point 7 mirrors the equivalent single tooth action. For the position shown, contact is at point 7′. Rack and pinion, like meshing gears, have two pressure lines and, hence, permit motion in both directions.

Summary of Involute Gears. The simplicity and ingenuity of involute gearing may be summarized as follows.

- Involute profiles fulfill the law of gearing at any center distance.
- All involute gears of a given pitch and pressure angle can be produced from one tool and are completely interchangeable.
- The basic rack has a straight tooth profile and therefore can be made accurately and simply.

Standard Spur Gears

Spur gears can be made with greater precision than other gears because they are the least sophisticated geometrically. All teeth are cut across the faces of the gear blanks parallel to the axis, a procedure that greatly facilitates manufacturing and accounts for the relatively low cost of spur gears compared to other types. Spur gears are therefore the most widely used means of transmitting motion and are found in everything from watches to drawbridges.

Pitches and Modules. The base pitch (p_b) is the distance between successive involutes of the same hand, measured along the base circle. It is the base circle circumference divided by the number of teeth.

$$P_b = \frac{\pi D_b}{N} \qquad (5)$$

Mating teeth must have the same base pitch (Figs. 16 and 17).

The circular pitch (P_c) is the distance along the pitch circle between corresponding points of adjacent teeth. Meshing teeth must have the same circular pitch (Fig 13). The pitch circle circumference is thus the circular pitch times the number of teeth.

$$p_c N = \pi D$$

$$p_c = \frac{\pi D}{N} \qquad (6)$$

Module:
$$m = \frac{D}{N} \frac{\text{mm}}{\text{tooth}} \text{ (definition)} \qquad (7)$$

Diametral pitch:
$$P_d = \frac{N}{D} \frac{\text{teeth}}{\text{in.}} \text{ (definition)} \qquad (8)$$

By substituting $D_b = D \cos \phi$ into Equation 2, we obtain

$$p_b = p_c \cos \phi \qquad (9)$$

Diametral pitch is related to the module as follows.

$$mP_d = 25.4 \qquad (10)$$

Module, the amount of pitch diameter per tooth, is an index of tooth size. A higher module number denotes a larger tooth, and vice versa. Because module is proportional to circular pitch, meshing gears must have the same module.

$$p_c = \pi m \qquad (11)$$

Diametral pitch, the number of teeth per inch of pitch diameter, is also an index of tooth size. A large diametral pitch number denotes a small tooth, and vice versa. Because diametral pitch is inversely proportional to circular pitch, meshing gears must have the same diametral pitch.

$$P_d p_c = \pi \qquad (12)$$

The diametral pitch is the number of teeth per inch of pitch diameter and is not a pitch. A misnomer, it is easily confused with base and circular pitch. To avoid confusion, the word "pitch," when used alone from now on, refers solely to diametral pitch.

Standard Tooth Proportions of Spur Gears

Gears are standardized to serve those who want the convenience of *stock gears* or standard tools for cutting their own gears. To meet these needs, however, gear standards must provide users with sufficient latitude to cover their requirements. Optimum design requires a wide range of pitches and modules, but only a few pressure angles. There should also be an extensive choice in the number of teeth available. A practical range of stock gears is from 16 to 120 teeth with suitable incremental steps. The corresponding ratios vary from 1:1 to 7.5:1.

Pressure Angle. The preferred pressure angle in both systems – module and pitch – is 20°, followed by 25°, 22.5°, and 14.5°. The 20° angle is a good compromise for most power and precision gearing. Increasing the pressure angle, for instance, would improve tooth strength but shorten the duration of contact. Decreasing the pressure angle on standard gears requires more teeth in the pinion to avoid undercutting of the teeth.

Diametral Pitch System. This system applies to most gears made in the United States and is covered by AGMA standards. These standards are outlined in 65 technical publications available from AGMA. For gear systems we have 201.02-1968: Tooth Proportions for Coarse-Pitch Involute Spur Gears.

Despite the rapid transition to SI by the mechanical industries, the change to the module system will probably be slower. The reasons are:

- AGMA has yet to complete its SI standards.
- Many existing gear hobs (tools for making gears), for reasons of economy, will be kept in service and not be replaced until worn out.
- The need for repair of older gears will continue for several decades.

Thus, future gear reduction units may be all metric except for the pitch system.

Selection of pitch is related to load and gear size. Optimum design is achieved by varying the pitch, but rarely the pressure angle; hence, there is a wide selection of "preferred values" (Table 1). Small pitch values yield large teeth; large pitch values yield small teeth. Table 2 gives involute tooth dimensions based on pitch.

Module System. Tooth proportions for metric gears are specified by the International Standards Organizations (ISO). They are based on the ISO basic rack (not shown) and the module m. A wide variety of modules is available to cover every tooth size required from instrument gears to gears for steel mills. Table 3 shows only the preferred values ranging from 0.2 to 50 mm. Specific tooth dimensions are obtained by multiplying the dimension of the rack by the module (Table 4).

Because of the simple relationship between pitch and module ($mP_d = 25.4$), metrication of gearing does not seem overly difficult. However, *the transition from pitch to module rarely yields standard values.* Thus module gears are *not interchangeable* with pitch gears. Herein lies the difficulty of metric conversion in gearing.

Limitations on Spur Gears

Two spur gears will mesh properly, within wide limits, provided they have the same pressure angle and the same diametral pitch or module. Limitations are set by many factors, but two in particular are important: contact ratio and interference. To obtain the contact ratio, the length of action must first be introduced. The length of action (Z) or length of contact is the distance on an involute line of action through which the point of contact moves during the action of the tooth profiles. It is the part of the line of action located between the two addendum circles or outside diameters (Fig. 18).

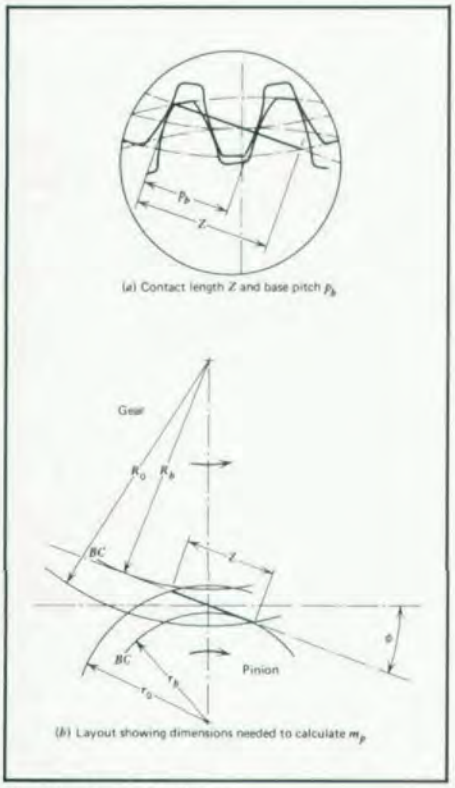

Fig. 18 — Contact ratio, m_p.

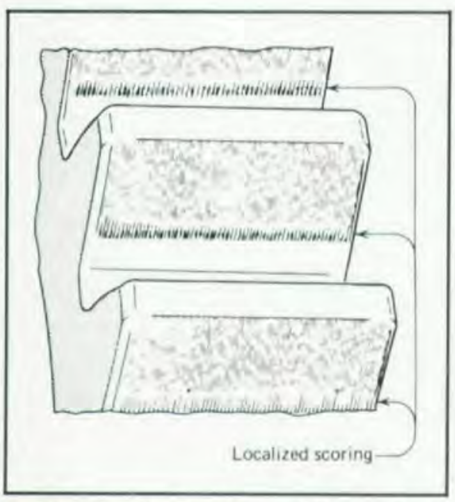

Fig. 19 — Tip and root interference. This gear shows clear evidence that the tip of its mating gear has produced an interfence condition in the root section. Localized scoring has taken place, causing rapid removal in the root section. Generally, an interference of this nature causes considerable damage if not corrected. (Extracted from AGMA Standard Nomenclature of Gear Tooth Failure Modes (AGMA 110.04), with permission of the publisher, the American Gear Manufacturers Association.)

TABLE 1 National Pitch System

					Coarse Pitch					
0.5	0.75	1	1.5	2	2.5	3	3.5	4	5	6
7	8	9	10	11	12	13	14	15	16	18
					Fine Pitch					
20	22	24	28	30	32	36	40	44	48	
50	64	72	80	96	120	125	150	180	200	

TABLE 2 Involute Gear Tooth Dimensions Based on Pitch-Coarse

	Stub	Full Depth	Stub	Full Depth
Pressure angle, 0 deg	20	20	25	25
Addendum, a	$0.80/P$	$1/P$	$0.80/P$	$1/P$
Dedendum, b	$1.00/P$	$1.25/P$	$1.00/P$	$1.25/P$
Tooth thickness, t_c (theoretical)	$\pi/2P$	$\pi/2P$	$\pi/2P$	$\pi/2P$

TABLE 3 Preferred Values for Module m (mm)

0.2	0.6	0.9	1.75	2.75	3.75	5	7	14	24	42
0.3	0.7	1.0	2.00	3	4	5.5	8	16	30	50
0.4	0.75	1.25	2.25	3.25	4.50	6	10	18	36	
0.5	0.80	1.50	2.50	3.50	4.75	6.5	12	20		

TABLE 4 Involute Gear Tooth Dimensions Based on Module m (mm)

	Stub	Full Depth	Stub	Full Depth
Pressure angle, 0°	20	20	25	25
Addendum, a	$0.8m$	m	$0.8m$	m
Dedendum, b	$1.25m$	$1.25m$	$1.25m$	$1.25m$
Tooth thickness, t_c (theoretical)	$0.5\pi m$	$0.5\pi m$	$0.5\pi m$	$0.5\pi m$
Circular pitch, P_c	πm	πm	πm	πm

Contact ratio (m_p). As two gears rotate, smooth, continous transfer of motion from one pair of meshing teeth to the following pair is achieved when contact of the first pair continues until the following pair has established initial contact. In fact, considerable overlapping is necessary to compensate for contact delays caused by tooth deflection, errors in tooth spacing, and center distance tolerances.

To assure a smooth transfer of motion, overlapping should not be less than 20%. In power gearing it is often 60 to 70%. Contact ratio, m_p, is another, more common means of expressing overlapping tooth contact. On a time basis, it is the number of pairs of teeth simultaneously engaged. If two pairs of teeth were in contact all the time, the ratio would be 2.0, corresponding to 100% overlapping.

Contact ratio is calculated as length of contact Z divided by the base pitch P_b (Fig. 13-18).

$$m_p = \frac{Z}{p_b} = \frac{\sqrt{R_0^2 - R_b^2} + \sqrt{r_0^2 - r_b^2} - C \sin\phi}{p_c \cos\phi} \qquad (13)$$

where

p_c = circular pitch; mm, in.
R_0 = outside radius, gear; mm, in.
R_b = base circle radius, gear; mm, in.
r_0 = outside radius, pinion; mm, in.
r_b = base radius, pinion; mm, in.
C = center distance; mm, in.
ϕ = pressure angle; deg

Note that base pitch p_b equals the theoretical minumum path of contact because $m_p = 1.0$ for $Z = p_b$.

Contact ratios should always be calculated to avoid intermittent contact. Increasing the number of teeth and decreasing the pressure angle are both beneficial, but each has an adverse side effect such as increasing the probability of interference.

Interference. Under certain conditions, tooth profiles overlap or cut into each other. This situation, termed interference, should be avoided because of excess wear, vibration or jamming. Generally, it involves contact between involute surfaces of one gear and noninvolute surfaces of the mating gears (Fig. 19).

Fig. 20 shows maximum length of contact being limited to the full length of the common tangent. Any tooth addendum extended beyond the tangent points T and Q, termed interference points, is useless and interferes with the root fillet area of the mating tooth. To operate without profile overlapping would require undercut teeth. But undercutting weakens a tooth (in bending) and may also remove part of the useful involute profile near the base circle (Fig. 21).

Interference is first encountered during "approach," when the tip of each gear tooth digs into the root section of its mating pinion tooth. During "recess" this sequence is reversed. Thus we have both tip and root interference as shown in Fig. 19. Because addenda are standardized ($a = m$), the interference condition intensifies as the number of teeth on the pinion decreases. The pinion in Fig. 21 has less than 10 teeth. The minimum number of teeth N_c in a pinion meshing with a rack to avoid undercut is given by the expression

$$N_c = \frac{2}{\sin^2\phi} \qquad (14)$$

The minimum number of teeth varies inversely with the pressure angle. By increasing the pressure angle from 14.5° to 20°, the limiting number drops from 32 to 17. The corresponding increase in the maximum speed ratio potential indicates one of several reasons why the 20° pressure angle is preferred in power gearing.

Interference can be avoided if:

$$R_0 \leq \sqrt{R_b^2 + C^2 \sin^2\phi} \qquad (15)$$

$$r_0 \leq \sqrt{r_b^2 + C^2 \sin^2\phi} \qquad (16)$$

For a given center distance, an increase in pressure angle, with the resulting decrease in base radius, lengthens the involute curve between the base and pitch circles, thereby diminishing interference (Fig. 22).

When stock gears to suit a specific ratio are selected, it may not be sufficient to provide gears of the same module, pressure angle and width. A pair must also have an acceptable contact ratio and mesh without interference.

Other limitations on spur gears are set by speed and noise level. When standard spur gears mesh, overlapping is less than 100%. The transmitted load is therefore briefly carried by one tooth on each gear. The sudden increase in load causes deflection of both meshing teeth and thus affects gear geometry adversely. The ideal constant velocity is no longer achieved. At low speed, this is not a serious factor but, as speed and load increase, deformation and impact may cause noise and shock beyond acceptable limits. Consequently, spur gears are seldom used for pitch line velocities exceeding 50 m/s (10,000 fpm).

Modifications of Spur Gears (Nonstandard)

The teeth of a pinion will always be

(continued on page 48)

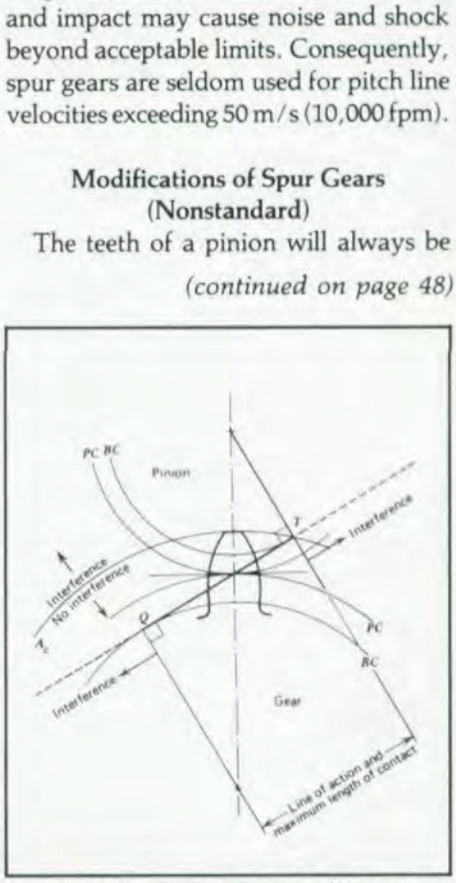

Fig. 20 – Interference sets a geometrical limitation on tooth profiles. For standard tooth forms interference takes place for contact to the right of point T and to the left of point Q.

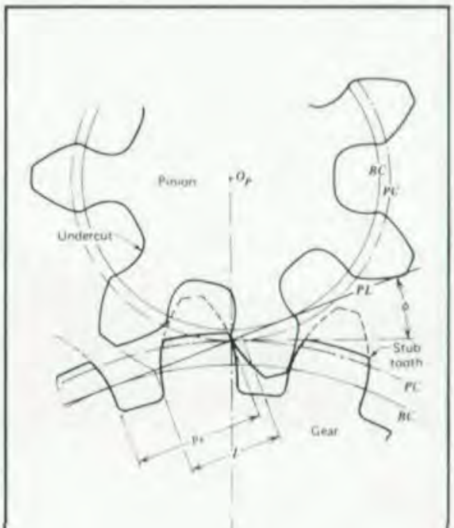

Fig. 21 – To operate without interference, either the pinion must be undercut or the gear must have stub teeth. Although interference is avoided, intermittent contact persists as p_b is greater than Z.

CLASSIFIED

Rates: Classified Display—per inch (minimum 3) **1X**-$130, **3X**-$120, **6X**-$110. Type will be set to advertiser's layout or *Gear Technology* will set type at no extra charge. **Word Count:** 35 characters per line, 7 lines per inch.

Payment: Full payment must accompany classified ads. Mail copy to *Gear Technology*, P.O. Box 1426, Elk Grove Village, IL 60009. **Agency Commission:** No agency commission on classifieds.

Material Deadline: Ads must be received by the 25th of the month, two months prior to publication. **Acceptance:** Publisher reserves the right to accept or reject classified advertisements at his discretion.

COMPUTER AIDS

GEAR

DESIGN ANALYSIS
IBM COMPATIBLE COMPUTERS
WORM • SPUR • HELICAL • INTERNAL

- Source Code Provided (Basic)
- Self Prompting
- Complete Instruction Manuals
- Non-Standard Center Distances
- Recess Designs
- Non-Standard Tooth Depths
- Contact Diagram for Worm Drives
- Tolerances per AGMA 390.03

LOAD ANALYSIS per

- Buckingham Equations
- AGMA 218.01 or 440.04 for WORMS
- Buckingham Gear Books Available

BUCKINGHAM ASSOCIATES INC.
Springfield, VT 05156

CIRCLE A-18 ON READER REPLY CARD

GEAR ESTIMATING

The COSTIMATOR® computer aided cost estimating system insures speed and consistency in the difficult task of estimating the costs of all types of gears.

Used by small shops and Fortune 500 companies throughout the country.

For complete information contact us today.

Manufacturers Technologies, Inc.
59G Interstate Dr.
West Springfield, MA 01089
(413) 733-1972

CIRCLE A-19 ON READER REPLY CARD

GEARTECH
Software, Inc.

GEAR DESIGN/ANALYSIS for IBM PC & compatibles. GEARCALC ($995): design optimum spur & helical gearsets from application data. AGMA218 ($1495): calculate pitting and bending fatigue lives per AGMA Std. 218.01. SCORING+ ($495): analyze/plot scoring & wear probabilities. Fast, menu-driven programs work as one system (combined price $2495), do extensive error-checking. Comprehensive manuals (theory, operation, examples) included. Demo available. GEARTECH Software, Inc., 1017 Pomona Ave., Albany, CA 94706 (415) 524-0668.

CIRCLE A-20 ON READER REPLY CARD

SERVICE

GEAR TESTING AND DESIGN FACILITIES

- GEAR DESIGN (NOISE — STRENGTH)
- ROTATING GEAR (TORQUE — SPEED CONTROL) TEST MACHINES.
- SINGLE TOOTH BENDING FATIGUE TESTING.
- STATISTICAL PLANNING — ANALYSIS.
- WROUGHT STEELS, SINTERED METALS, NON-METALLIC MAT'LS.
- CAD FACILITIES FOR LOW COST SET-UP.
- CUSTOM TEST MACHINE DESIGN
- EXPERIENCED PERSONNEL.

PACKER ENGINEERING
312/355-5722, ext. 214
BOX 353, NAPERVILLE, IL 60566

CIRCLE A-21 ON READER REPLY CARD

GEAR TOOTH GRINDING SERVICE

Open Capacity On Our

REISHAUER GEAR TOOTH GRINDERS

We are capable of grinding your gears to AGMA standards for salvage or as a planned operation in prototype or production quantities.

CERTIFIED GEAR INSPECTION

For immediate service phone:
716-892-0400

Or send inquiries to:
PRO-GEAR COMPANY
400 Kennedy Road
Buffalo, N.Y. 14227

CIRCLE A-22 ON READER REPLY CARD

PRECISION GEAR TOOTH GRINDING & HONING

- Production and Prototype Quantities
- 3/4" P.D. to 27.5" P.D.
  3.5 D.P. and 11" Face
- Specialists in Gear Tooth Grinding
- Finishing Spur & Helical Gears to all AGMA Quality Standards
- Able to match delivery to your needs

Call or Fax Inquiries to:

ALLEGHENY GEAR CORP.
23 Dick Road
Depew, NY 14043
716-684-3811
FAX (716) 684-7717

MEMBER OF AGMA

CIRCLE A-23 ON READER REPLY CARD

Bring in new customers for your business by advertising in *GEAR TECHNOLOGY*, The Journal of Gear Manufacturing.
Call (312) 437-6604

FILLET GEOMETRY OF GROUND . . .
(continued from page 35)

and the calculation proceeds based on formulae similar to Equations 20 to 29 except that ν_t lim $= \alpha_{tG}$ for non-underground teeth, and the parameters β, α_t, h_{a0}, ϱ_{a0}, α_n, m_n, x_{g0}, u_n, w and r are replaced by β_G, α_{tG}, h_{aG}, ϱ_{aG}, α_{nG}, m_{nG}, x_{gG}, u_{nG}, w_G and r_G respectively.

Fillet analysis after heat treatment. Let us consider a gear which is deformed because of heat treatment after cutting. The x value of the addendum modification coefficient does not change, as it is "nominal," and the prescribed final thickness must be attained, so the i_{bn} value of the normal base thickness reduction has to be maintained.

The following procedure can be adopted:

- Measure the actual root diameter d_f, hence r_f
- Assess the necessary grinding stock u_s
- Imagine that the gear has been cut by a fictitious tool: rate i_{bn0} from Equation 11 inversely, and x_{g0} from Equation 12 and deduce a fictitious tool addendum, h_{a0}, from Equation 16.

The general computer program can be applied to analyze fillets.

If the gear deformations have been irregular, the analyses must be repeated for various tooth zones by maintaining the same positioning of the grinding wheel; i.e., the same value of r_{fG0}.

ACKNOWLEDGEMENT: *This article was originally printed by the American Society of Mechanical Engineers as their Paper No. 84-DET-181.*

SPUR GEAR FUNDAMENTALS . . .
(continued from page 45)

weaker than those of the gear when standard proportions are used. They are narrower at the root and are loaded more often. If the speed ratio is three, each pinion tooth will be loaded three times as often as any gear tooth. Furthermore, if the number of teeth is less than the theoretical minimum, undercutting – with its resulting loss of strength – cannot be avoided. These adverse conditions can be circumvented by specifying nonstandard addenda and dedenda.

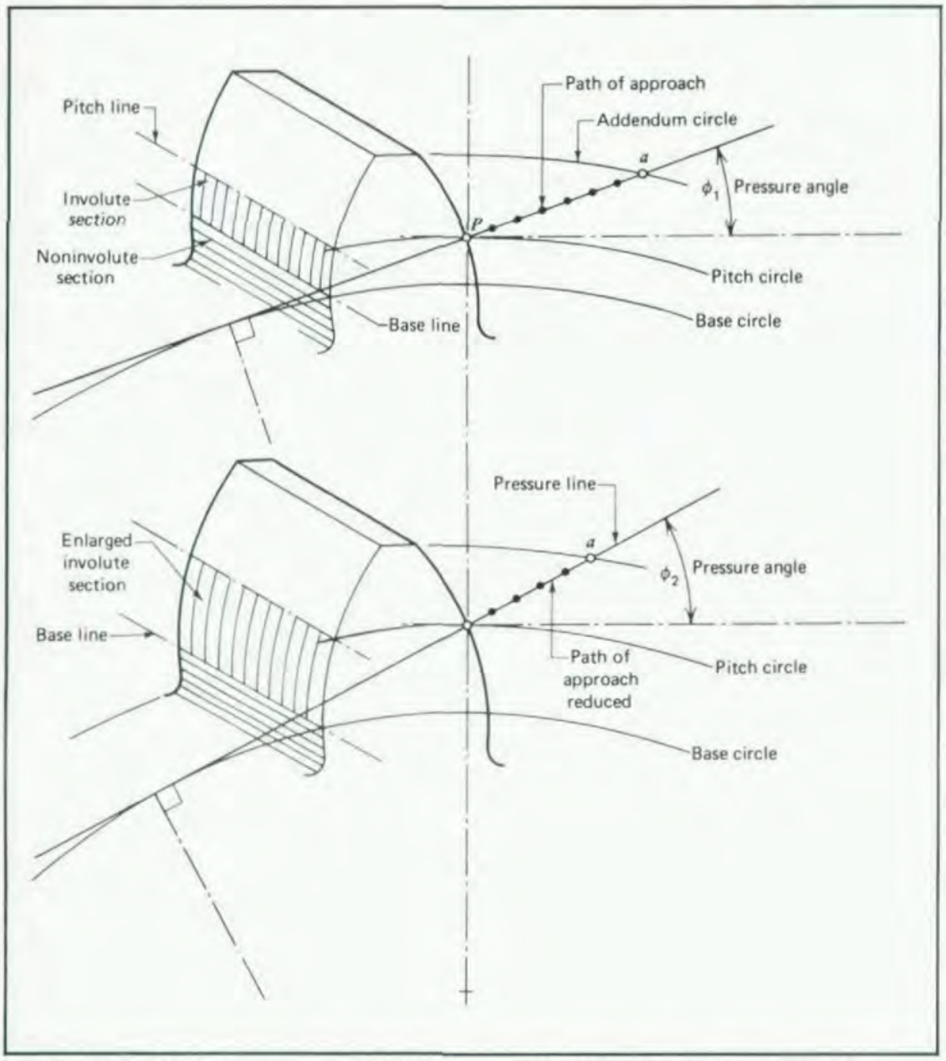

Fig. 22 – Effect of changing the pressure angle. Interference and contact ratio vary inversely with the pressure angle. When the pressure angle increases from $\emptyset_1$ to $\emptyset_2$, the involute section between the pitch line and the base line lengthens, tending to alleviate interference. The path of contact, however, shortens, thereby effectively lowering the contact ratio. (Only the path of approach is shown.)

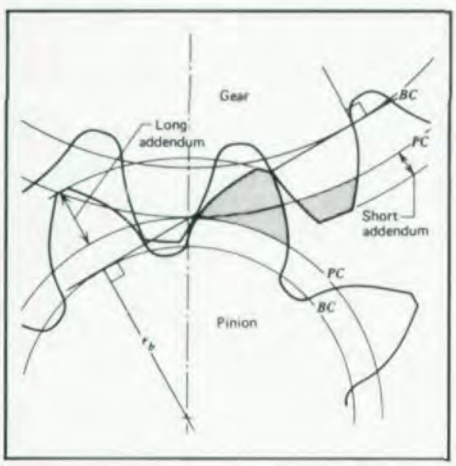

Fig. 23 – Long and short addenda.

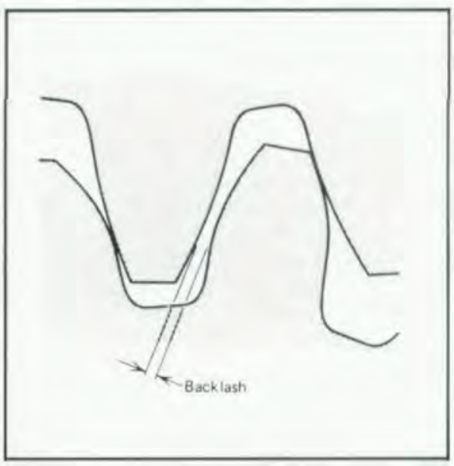

Fig. 24 – Backlash.

Long and Short Addenda or Profile Shift Gears. In order to strengthen the pinion tooth, avoid undercutting and improve the tooth action, its dedendum may be decreased and the addendum increased correspondingly. In practice, this is done by retracting the gear cutter a predetermined distance from its standard setting prior to cutting. Each pinion tooth becomes thicker and, therefore, stronger (Fig. 23). For such pinions to mesh properly with the driven gear, on the same center distance, the addendum of each driven tooth is correspondingly decreased and its dedendum increased. Although the gear teeth have thus become weaker, the net effect has been one of equalizing tooth strengths. The increased outer diameter of the pinion and decreased outer diameter of the gear have been achieved without changing the pitch diameters.

Extended Center Distance. In this arrangement a modified pinion is meshed with a standard gear. Pinions with decreased dedenda and increased addenda have thicker teeth than equivalent standard gear teeth. They also provide less space for any mating gear tooth. Consequently, proper mesh requires a larger center distance.

Both modifications are widely used because they can be achieved by means of standard cutters. A different setting of the generating tool is all that is required.

Backlash (B) (tooth thinning), in general, is play between mating teeth (Fig. 24). It occurs only when gears are in mesh. In order to measure and calculate backlash, it is defined as the amount by which a tooth space exceeds the thickness of an engaging tooth. The general purpose of backlash is to prevent gears from jamming together (making contact on both sides of their teeth simultaneously). Backlash also compensates for machining errors and heat expansion. It is obtained by decreasing the tooth thickness and thereby increasing the tooth space or by increasing the center distance between mating gears.

These modifications will improve primarily the kinematics of spur gears.

Acknowledgement:
Reprinted from Hindhede/Zimmerman/Hopkins/Ersman/Hull/Lang, *Machine Design Fundamentals: A Practical Approach*, c 1983. Excerpted by permission of Prentice-Hall, Inc., Englewood Cliffs, NJ.